BANGLADESH-INDIA FRIENDSHIP POWER COMPANY (PVT.) LIMITED

2x660MW MAITREE SUPER THERMAL POWER PROJECT RAMPAL, BANGLADESH

OWNER'S CONSULTANT:

FICHTNER

M/s FICHTNER GmbH & Co KG.
STUTTGART, GERMANY

SITE SPECIFIC SEISMIC STUDY REPORT

DOC. NO. : Maitree-00-UTX-ED-421602C002PEM
REV-1

Maharatna Company

BHARAT HEAVY ELECTRICALS LIMITED
PROJECT ENGINEERING MANAGEMENT
NOIDA-201301

Seismic Hazard Estimation for BIFPCL, Maitree STPP Project site, located at Bagerhat, Bangladesh

Submitted To

Project Engineering Management,
Bharath Heavy Electricals Limited,
Noida, UP-201301

Prepared by

Principal Investigator: **Dr. S. T. G. Raghukanth**
Research Associate: Dhanya J

PROJECT No: IC1617CIE155BHELSTGR
REPORT- February 2017

DEPARTMENT OF CIVIL ENGINEERING
INDIAN INSTITUTE OF TECHNOLOGY MADRAS
CHENNAI - 600036

CONTENTS

LIST OF TABLES

LIST OF FIGURES

Department of Civil Engineering
Indian Institute of Technology Madras
Chennai-600 036
Tel: 22574296/22576296
FAX: 22575286
Email: raghukanth@iitm.ac.in

Dr.STG RAGHUKANTH
Associate Professor

Seismic Hazard Estimation for BIFPCL, Maitree STPP Project site, BHEL, located at Bagerhat, Bangladesh

1. Introduction

BHEL has requested I I T Madras to carry out seismic hazard analysis for the proposed BIFPCL, Maitree STPP project site located in Bagerhat, Bangladesh. The proposed site lies in the zone I as per the seismic zoning map of Bangladesh National Building Code (2012).

The importance of estimating seismic hazard at constructions sites needs no special emphasis. In this exercise, one has to be not only scientific but also adopt state-of-art international methodologies to validate the procedures of estimating hazard parameters such as peak ground acceleration (PGA) and design basis response spectrum. Engineering design of a new structure has to assure safety in future. Thus, the design has to be based on future scenarios and not on a few past observations. The subject of Engineering Seismology is sufficiently advanced, so as to include the future uncertainty in hazard estimation. The seismic hazard can be estimated deterministically by considering only a particular scenario which can cause maximum ground motion or probabilistically, in which uncertainities involved in earthquake size, location and ground motion is taken into account. The uncertainties of the seismic phenomenon cannot be overlooked in arriving at a design basis spectrum. Thus probabilistic seismic hazard assessment (PSHA) has become the norm even for normal buildings in USA(IBC-2009, DOE 2024, USNRC-RG1.165). Engineering design and construction cannot be viewed in isolation from socio-economic considerations. Since the economic lifetime of a structure can be envisioned, the uncertain seismic scenario has to be tailored to match

with the design life of the structure. In the case of engineering structures, apart from a safe economic life period one can easily see the need for defining a safe social life period also. Thus, the traditional seismic coefficients have to be interpreted in terms of the future hazard that is foreseen for safety of engineering structures. This hazard in turn has to be scientifically expressed in terms of return periods.

The objective of the report is to estimate design response spectra for the BIFPCL, Maitree site, by DSHA and PSHA methodologies. This involves collection of seismicity data and seismotectonics details around the site. The uncertainities in magnitude and site to source distance are quantified from using the past data. The uncertainities in ground motion are obtained using ground motion predictions equation (GMPE). The three uncertainities are integrated to obtain the uniform hazard response spectra.

1.1 Return Period

The frequency of occurrence of a rare event is expressed in terms of return periods. This is the average time between consecutive occurrences of the specified rare event. For example, this rare event can be the ground acceleration exceeding 0.1g due to an earthquake anywhere in a control region of 500 km radius around the site. Return period is the average duration between consecutive occurrence of the desired event and is not the actual inter-arrival time, which is a random variable. Since the occurrence of an earthquake is unpredictable, the target event is equally likely to occur in any year during its return period T_R. Let us consider the ground acceleration at the site as the random variable and the rare event as ($Y>a_g$) that is the PGA exceeding a value a_g in any year. It follows the annual probability of exceedance

$$P(Y>a_g) = P_a=1/T_R \qquad (1)$$

Hence, a 1000-year earthquake would mean that magnitude which has a return period of 1000 years ocurring in a catchment region of 500 km radius around the site. This is same as that magnitude which has annual probability of exceedance P_a of 0.001. In engineering problems it is more appropriate to characterize the future earthquake in terms of its PGA and S_a. In this case the above probability can be related to the

exceedance levels of the above strong motion parameters during the economic and/or social lifetime of the facility. Let the design life of the STPP be N years. For an event ($Y>a_g$) with return period T_R and annual probability of exceedance P_a , the exceedance probability over N years is

$$P(Y>a_g \text{ in N years}) = 1-(1-P_a)^N \cong [1-e^{(-N/TR)}] \cong N/T_R \quad (2)$$

The approximations are valid for small Pa and large N. Hence, if the design period is 100 years and a PGA value of a_g is chosen with a1000-year return period (P_a=0.001), the exceedance probability is still 0.1 or 10 percent. As per BNBC code, MCE corresponds to 2 % prob of exceedance in 50 years, which means N= 50 years and Pa = 0.02. The corresponding return period (TR) can be estimated from Equation 2 as 2500 yrs. Hence the site specific spectra should be obtained for 2500 yr return period.

1.2 Geology and Seismic Status of the Region

Estimation of seismic hazard requires identification of geological and tectonic zones in the 500 km region around the site. A brief review on seismotectonic setting and geology is presented in this section. The geological map of Indian subcontinent is reported in GSI (2000) is shown in Figure 1. The project site is located in the Bengal basin tectonic unit. it can be observed from Figure 1 that the Bengal basin is predominantly of alluvial deposits. Further the basement contour map of the region is given in Figure 2. It can be noticed that the contours trend N-S and are parallel to the Indian shield margin and basement occurs at as depth of around 4.0km just west of Bharampur. Along Culcutta-Krishnanagar line the basement depth varies between 7-10km. Thus the basin depth is observed to increase from 4km to 7km. In Bangladesh the basement trent NE. It can be seen from the Figure 2. that the basement depth at the project site is around 15km. This high basement depth is attributed to the enormous amount of sediments flown down by the Ganga-Brahmaputra drainage system building the world's largest submarine fan-Bengal fan.

The broad and detailed geological map of Bangladesh published by Geological Survey of Bangladesh (GSB) is shown in Figure 3 and Figure 4 respectively. The three major

geological formations in Bangladesh are (i) Teritinary hill segment in the north-eastern hills, (ii) the Madhupur clay from Madhupur Barind Tract and (iii) the recent alluvium in the flood plain and esturine areas occupying the remainder country (Brammer (1996)). Physiographically Bangladesh can be divided into 7 divisions (Figure 3.). Each of these divisions has distinguished characteristic of its own.

a) Hilly regions (in the eastern and northern frontier): i) Chittagong Hill Tracts, ii) Hill Ranges of northeastern Sylhet, iii) Hills along the narrow northern strip of Sylhet and Mymensingh
b) Pleistocene uplands: i) Barind Tract in the north western part, ii) Madhupur Tract in the central part, iii) Lalmai Hill
c) Tippera Surface
d) Tista Fan (in the northern part)
e) Flood plains: i) Ganges flood plain, ii) Atrai flood plain, iii) Brahmaputra-Jamuna flood plain, iii) Old Brahmaputra flood plain, iv) Meghna flood plain
f) Deltaic plain of the Ganges-Brahmaputra-Meghna Delta Complex: i) Inactive delta, ii) Active delta, iii) Tidal delta
g) Sylhet Depression and Inland marshes (Scattered all over Bangladesh)

The Bengal delta is a combination of three deltas namely the Ganges delta, the old Brahmaputra-Meghna delta and the Ganges-Jamuna (the present Brahmaputra)-Meghna delta. In some recent literature the name, "Ganges-Brahmaputra-Meghna Delta Complex" has been used. Holocene or Holocene sediments from a few hundred to thousands of meters cover the Flood plains and the Delta.

Geologic evolution of the Bengal Basin starting from Upper Paleozoic time is directly related with the break up of eastern Gondwanaland and collision of the Indian plate with the Asian plate, it can be divided into four major stages: I. Permo-carboniferous pre-breakup stage, II. Early Cretaceous Rift stage, III. Late Cretaceous-Eocene Plate or drift stage, and IV. Oligocene-Holocene Orogenic stage. The sedimentary cover of the basin with a maximum thickness of 20 km includes three major lithostratigraphic units separated by three major unconformities. The western part of Bangladesh is the platform shelf, whereas the eastern part of the country is represented by the folded belt. The central part representing the most subsided part of the basin comprises two major

depressions at the north (Sylhet Trough) and south (Patuakhali Depression). The transition zone from the shelf to basin is represented by the hinge zone-a Eocene shelf/slope break. The western and Northern foreland shelves, which were source areas earlier, the rising chains of the Himalayas and the Indo-Burman Ranges were increasingly subjected to erosion and supplied much of the sediments since the Mid-Miocene in the basinal area (Shamsuddin and Abdullah, 1997).

Bangladesh contain thick sediment (up to 20 km in the southern part) sequences of Permian to Holocene. The sediment thickness is shallowest in northern Bangladesh (114 m). Recently, Singh *et al.* (2016) determined the sedimentary and crustal depth at the Bengal Basin at 11 stations by inversion of high quality receiver functions. The results from their study are presented in Figure 5. It is clear that the thickness of the sediments increases dramatically across the Hinge Zone of the Early Cretaceous passive margin from 3 to 17 km. The Moho depth shallows across the region. This reflects thinning of the crystalline crust from 38 km in the Indian Craton to 34 km at the Hinge Zone to <16 km in the Bengal Basin. This variation in the crust thickness is depicted in Figure 6 for NS and EW sections through the region (Alam *et al.* (2003)). The thickness of the sediments increases dramatically from 3 to 17 km south of Madhupur tract which reflects the regions of highest influx of clastic sediments from the Himalayan collision zone. Major part of the sediment is deposited by the Ganges-Brahmaputra-Meghna river systems during Miocene to Holocene time. In Bangladesh the oldest sediment is the Permian Gondwana rock that lies over the Pre-Cambrian Basement complex. Over the Gondwana rock successively lies the Cretaceous Rajmal Trap, Paleocene Tura Sandstone, Eocene Sylhet limestone and Kopili, Oligocene Barail, Miocene Bhuban, Bokabil and Tipam Sandstone, Pliocene Dihing and Dupi Tila Sandstone, Pleistocene Madhupur Clay and Holocene Alluvium sediments (Islam and Uddin (2002)). This generalized sequence is not common in all parts of the country and in some places many formations are missing due to depositional, non-depositional, and post depositional erosion. The stratigraphic sequence is also variable between the Fore Deep area and the Shelf areas. The Holocene alluvium sediments mainly constitute of sand silt and clay. In the Ganges-Brahmaputra-Meghna Delta complex, vertical and horizontal variations of the lithofacies in the Holocene are very high. It is difficult to

correlate them from one place to another even at short distances. Inter fingering of the sediments are common. We must keep in mind that the Bengal Basin is one of the fastest subsiding regions of the world. The high rate of subsidence along with similar high rate of sediment deposition makes mapping of these units quite difficult. Thus, From Figure 2, 3, 4 and 5 it is clear that in the project site lies on the tidal deltaic deposit. The basement depth at the site is around 15 km.

The fault map of Bangladesh prepared from the Bangladesh Meteorological Department (BMD) and GSI (2000) is shown in Figure 5. The collision between the Indian subcontinent and the Eurasian continent, which started in Paleogene time and continues today, produced the Himalaya and the Tibetan Plateau. The region under consderation is in close proximity to West Bengal. Tectonically Bangladesh is divided broadly into the following divisions

1. Indian Platform and Shelf (a) Dinajpur slope (Himalayan Fore Deep); b) Rangpur Saddle, c) Bogra Slope
2. Hinge Zone (Eocene slope break)
3. Bengal Fore Deep: a)Folded flank, b) Basinal area; i) Sylhet Trough, ii) Chandpur-Barisal High, v) Patuakhali Depression (Hatia Trough)

The area around BIFPCL, Maitree site, comprises part of two major tectonic domains- the outer molasse basin of Tripura Chittagong and the Bengal basin. The Bengal basin has three structural domains; the western scrap zone architectured by badin marginal fault, middle shelf zone and eastern deeper basinal part. The major structures of the area are the regional antiforms and synforms with N-S trending axes and NE and NW trending conjugate fault/ lineament system developed as a result of E-W compression. The Tripura Chittagong domain , comprises the Tripura-Mizoram Hills, the Chittagong hill tracts and Coastal Burma, represent a large Neogene basin formed west of Paleogene Arakan-Yoma Fold belt and is broadly confined within the Naga Thrust and Dauki Fault to the north and Sylhet Fault and Barisal Chandpur High to the west and northwest. The Bengal basin tectonic domain of the area comprises enormous sediments flown down by the Ganga--Brahmaputra drainage system, building the world's largest submarine fan- the Bengal fan, to the south. Incidently, the Bengal fan conceals the northern extension of the Ninety East Ridge and the bathymetric trench,

related to subduction of Indian Plate. Teritary sequence in the shelf zone dips homoclinically towards southwest with a sudden flexure along the Ecocene Hinge Zone. The Garhamoyna-Khandaghosh fault (GKF) is quite extensive along the basin margin that joins the Rajmahal Fault in the north. The NE trending Jangipu- Gaibhandha Fault (JGF) branches from GKF that separates Rangpur-malada saddle from the Bogra shelf. The seismicity near the region is mostly of shallow focus. It is mostly of moderate magnitude earthquakes.

The plate boundary fault from Myanmarto to Chittagong is the northern extension of the rupture area which has caused the 2004 Mw 9.2 Sumatra earthquake. The 1762 earthquake has occurred in this region and accompanied the tsunami in the river near Dhaka (Steckler et al., 2008). The Madhupur blind fault is inferred on the western margin of the Madhupur Tract, northwest of Dhaka. The fault is considered as an important structure for the seismic hazard assessment of Dhaka, the capital of Bangladesh, although there is no definitive evidence for its presence (ADPC (2013)). tilted to the east. The straight low scarps with NW-SE direction are recognized on the western margin of the Madhupur Tract.

2 Seismogenic Zones

The seismotectonic map (Figure 7) shows that there are some regions that are more active than the other. This activity is correlated with the number of occurrence of past earthquakes and also with the presence of faults and lineaments. There is a possibility that not all past epicentres can be uniquely identified with particular faults. This gives rise to the postulation of diffuse aerial sources in some places to be the cause of seismic activity. The distribution of faults varies spatially as seen from Figure 7. Some specific patterns can be recognized about the faults and epicentres being dense in some regions. This pattern and the known tectonic disposition can be used to demarcate source zones for further work. The first official seismic hazard-zoning map for Bangladesh wad published in 1979 for the Geological Survey of Bangladesh prepared by a Committee of experts on Earthquake Hazard Minimization. Recently NDMA (2011) document on PSHA map of India divides Indian-subcontinent into 32 homogeneous seismic source zones based on historical seismicity, tectonic features

and geology. These zones along with the faults and seismicity within each zone are shown in Figure 8 and 9. It can be observed that the ground motion at the BIFPCL, Maitree site is influenced by events occurring on faults located in the neighbouring ten zones surrounding the site.

BIFPCL, Maitree site, lies in Source 9 (Bengal Basin) which has the high b-value of 0.75. The other zones that influences the region includes the seismically active Himalayan zones 3 and 4 with N(4)>2.4, which lies in the north part of the site. These sources represent the plate boundary regions where lie the MBT, MCT, Indus-Tsangpo suture and the Tethys suture. Source zone 8 occupies the Shillong plateau and the Assam valley region. This region has active linear structures like the Dauki, Dhubri, and Kopili faults. Source zone 10 is connected with the subduction of the Indian plate below the Burmese plate. Source zone 18 consists of the Mahanadi Graben and the Eastern Craton of the Indian Shield. The Eastern passive margins are represented by source zones 17. Singhbum Craton lie in source 31. Source 32 encloses the new fault identified in Bay of Bengal by ONGC. There are also various other attempts to determine the seismic hazard of the region (ADPC(2009), Al-Hussaini *et al.* (2015))

2.1 Earthquake Catalogue

Bangladesh Meterological Department (BMD)(2016) has reported 431 events that occured in and around Bangladesh from 1918-2016. Out of these 2 are great events (>8), 10 are major events ($7<M_w<8$), 15 are strong events ($6<M_w<7$), 103 moderate events ($5<M_w<6$), 219 light events ($4<M_w<5$), 78 minor events ($3<M_w<4$) and 4 are very minor events (M_w <3). In addition, NDMA (2011) and USGS website (*http://neic.usgs.gov/*) has compiled the earthquakes of magnitude from 825 to 2016 in the vicinity of the region. From the compiled catalogue, a total of almost 2800 events of $M_w>3$ have been collected form the ten seismic zones near to the BIFPCL, Maitree site. Epicenters of these earthquakes are plotted in Figure 8. A list of earthquakes with magnitudes $M_w \geq 6$ in the historical and instrumental period are reported in Table 1.

2.2 Fault Map

Fault maps for BIFPCL, Maitree site have been prepared using the data from Geological

survey of Bangladesh, Bangladesh Meteorological Department (BMD) and Seismo-tectonic Atlas of India (GSI 2000). These drawings have also been digitized using MATLAB. These drawings are prepared such that all the important seismo-tectonic features within seven seismogenic zones are captured. The causative fault map for the site is shown in Figure 8 along with all known epicenters. This figure immeadiately provides a synoptic view of the spatial pattern of the seismicty in the controlling region. It can be observed that most of seismic activity is concentrated along the Himlalayan region. The major faults and seismogenic zones which influence seismic hazard at the BIFPCL, Maitree site, Bagerhat have been identified from Figure 8 and 9 respectively. Small faults which are at far off distances and which are not seismically active are not considered. Based on past activity and data the maximum potential magnitude of each fault has been estimated. Whenever past events occurred near a fault, the magnitude of the largest of such events has been increased by 0.5 units to fix up M_{max}.

Regional Recurrence

The seismic activity of a region is characterized in terms of Gutenberg-Richter recurrence (frequency-magnitude) relationship. This is represented as

$$\text{Log}_{10} N = a - bM \qquad (3)$$

where N is number of earthquakes greater than a particular magnitude M and (a , b) are the parameters representing the seismicity of the region. The simplest way to obtain (a,b) is through least square regression, but due to the incompleteness of the database, this approach is known to lead to erroneous results. To circumvent this difficulty, Kijko and Sellvoll (1998) proposed a new method where the data is organized into two parts called the extreme and the complete part. Extreme part refers to the time period where information on large historical events are only available and complete part represents the time period in which information on both large as well as small magnitude earthquakes are available. Their method assumes a doubly truncated Gutenberg-Richter relationship and a poisson model for earthquake occurrences. The uncertainty in the estimation of magnitudes is also incorporated in deriving the unknowns. In the

present study, 1958-2016 is considered as complete part and before 1958 is taken as extreme part to find the recurrence parameters. The a-value and b-value for the seven tectonic regions around BIFPCL, Maitree site, obtained from the procedure of Kijko and Sellvoll (1998) are shown in Table 2. The recurrence relation for these ten regions is plotted in Figure 10.

2.3 Fault Deaggregation

The recurrence relation derived above is for the entire source region and is not specific to any particular fault. Now, the recurrence relation has to be found individually for each of these faults, which is a difficult task. With no reliable information on the slip rate of the faults, further analysis has to be heuristically handled. A simple principle based on conservation of seismic activity which states that the regional seismicity value quantified as $N(m_0)$ (number of earthquakes per year with $m > m_0$) should be equal to the sum of individual fault value $N_k(m_0)$ (k=1,2,..23), is invoked for estimating the recurrence relation. Let the number of earthquakes per year with $m > m_0$ in a given source zone consisting of n number of faults be denoted as $N(m_0)$. Since all these events are associated with the faults within the zone, it follows $N(m_0) = \sum N_k(m_0)$ where $N_k(m_0)$ stands for the annual frequency of event $(m > m_0)$ on the kth fault (k=1,2,3,…n). This conservation property ca be heuristically used to develop G-R relations for each fault in the source zone. Here we take (m_0 = 4) for further work. The number of events $N_s(m_0)$ that can occur on a given fault depends on a variety of factors, the most important being the potential of the fault to break depending on its length and known past activity. This argument just reiterates that a long fault is capable of breaking into more number of smaller sections. At the same time a shorter fault might be more active contributing to more small magnitude events in the catalogue. Thus two parameters namely the fault length L_k and the number of past events n_k associated with the sth fault have to be used as weights for finding $N_k(m_0)$. If N_z number of events is available in the zonal catalogue we get two weights for each fault within the zone as,

$$\alpha_k = L_k / \sum L_k \text{ and } \delta_k = n_k / N_k \qquad (4)$$

Taking the mean of the above two factors as indicating the seismic activity of the sth

fault in the zone we get

$$N_k(m_0) = 0.5\ (\alpha_k + \delta_k)\ N(m_0) \tag{5}$$

as the *a*-value in the G-R relation of the kth fault. The *b*-value for all the faults is taken to be constant equal to the zonal *b*-value already computed in Table 2. A further constraint appears in the form of the maximum possible magnitude m_u that can be foreseen on a given fault, depending on its length. This has to be less than the zonal potential but can be higher than the past magnitudes associated with the particular fault. Here it is taken to be half unit more than the past maximum magnitude. In the absence of past activity m_u is estimated depending on the length of the fault using the empirical relation proposed by Wells and Coppersmith (1994).

3. Generation of earthquake ground motion

After determining the recurrence relation for each of the faults, attenuation relation valid for the region under consideration has to be derived. Attenuation equation is a key component in PSHA. This equation describes the average or other moments of the hazard parameter in terms of the magnitude and distance. The instrumental database for Bangladesh is sparse and hence not useful to derive instrument based attenuation relationships. Thus, due to lack of ground motion data during strong earthquakes, no such relation is available for Bangladesh. Hence a global relation derived by Abrahamson et al. (2014), Boore et al. (2014), Campbell and Bozorgnia (2014) and Chiou and Youngs (2014) is used for the region (will be refered as ASK-2014, BSSA-2014, CB-2014 and CY-2014 respectively further in this report).

3.1 BSSA-2014

The functional form of GMPE is given as

$$\begin{aligned}\ln Y = {} & F_E(\mathbf{M}, mech) + F_P(R_{JB}, \mathbf{M}, region) + F_S(V_{S30}, R_{JB}, \mathbf{M}, region, z_1) \\ & + \varepsilon_n \sigma(\mathbf{M}, R_{JB}, V_{S30})\end{aligned} \tag{6}$$

where ln *Y* represents the natural logarithm of a ground motion (PGA, PGV, or PSA); F_E, F_P, and F_S represent functions for source (“E” for “event”), path (“P”), and site (“S”)

effects, respectively; ε_n is the fractional number of standard deviations of a single predicted value of ln $\underline{Y}$ away from the mean (e.g., ε_n = -1.5 is 1.5 standard deviations smaller than the mean); and σ is the total standard deviation of the model. The predictor variables are M, *mech*, R_{JB} (in km), *region*; V_{S30} (in m⁄s), and z_1 (in km). Parameter mech = 0, 1, 2, and 3 for unspecified, SS, NS, and RS, respectively. Parameter region is 0 if no regional correction is to be made (default value); 1 for California, New Zealand, and Taiwan (this also provides no correction); 2 for China and Turkey; and 3 for Italy and Japan. The units of PGA and PSA are g; the units of PGV are cm/s.

The source (event) function is given by:

$$F_E(\mathbf{M}, mech) = \begin{cases} e_0U + e_1SS + e_2NS + e_3RS + e_4(\mathbf{M} - \mathbf{M}_h) + e_5(\mathbf{M} - \mathbf{M}_h)^2 & \mathbf{M} \le \mathbf{M}_h \\ e_0U + e_1SS + e_2NS + e_3RS + e_6(\mathbf{M} - \mathbf{M}_h) & \mathbf{M} > \mathbf{M}_h \end{cases} \quad (7)$$

where *U*, *SS*, *NS*, and *RS* are dummy variables, with a value of 1 to specify strikeslip, normal-slip, and reverse-slip fault types, respectively, and 0 if the fault type is unspecified; the hinge magnitude M_h is period-dependent, and e_0 to e_6 are model coefficients.

The path function is given by:

$$F_P(R_{JB}, \mathbf{M}, region) = [c_1 + c_2(\mathbf{M} - \mathbf{M}_{ref})]\ln(R/R_{ref}) + (c_3 + \Delta c_3)(R - R_{ref}) \quad (8)$$

where, $R = \sqrt{R_{JB}^2 + h^2}$, c_1, c_2, c_3, Δc_3, M_{ref} , R_{ref} and h are model coefficients. Parameter Δc_3 depends on the geographic region,

The site function is given by:

$$F_S(V_{S30}, R_{JB}, \mathbf{M}, region, z_1) = \ln(F_{lin}) + \ln(F_{nl}) + F_{\delta z_1}(\delta z_1) \quad (9)$$

where F_{lin} represents the linear component of site amplification, F_{nl} represents the nonlinear component of site amplification, and $F_{\delta z1}$ represents the effects of basin depth. Terms F_{nl} and $F_{\delta z1}$ are region-dependent. The corresponding expression for each is explained in detail in Boore et al (2014) and the coefficients of the same in Table 3(d)

The Aleatoric uncertainity is represented through the total standard deviation σ, partitioned into components that represent between-event variability (τ) and within-

event variability (ϕ) as follows:

$$\sigma(\mathbf{M}, R_{JB}, V_{S30}) = \sqrt{\phi^2(\mathbf{M}, R_{JB}, V_{S30}) + \tau^2(\mathbf{M})} \tag{10}$$

The **M**-dependent between-event standard deviation τ is given by

$$\tau(\mathbf{M}) = \begin{cases} \tau_1 & \mathbf{M} \leq 4.5 \\ \tau_1 + (\tau_2 - \tau_1)(\mathbf{M} - 4.5) & 4.5 < \mathbf{M} < 5.5 \\ \tau_2 & \mathbf{M} \geq 5.5 \end{cases} \tag{11}$$

and the **M**-, R_{JB}-, and V_{S30}-dependent within-event standard deviation ϕ is given by

$$\phi(\mathbf{M}, R_{JB}, V_{S30}) = \begin{cases} \phi(\mathbf{M}, R_{JB}) & V_{S30} \geq V_2 \\ \phi(\mathbf{M}, R_{JB}) - \Delta\phi_V \left(\frac{\ln(V_2/V_{S30})}{\ln(V_2/V_1)}\right) & V_1 \leq V_{S30} \leq V_2 \\ \phi(\mathbf{M}, R_{JB}) - \Delta\phi_V & V_{S30} \leq V_1 \end{cases} \tag{12}$$

where (13)

$$\phi(\mathbf{M}, R_{JB}) = \begin{cases} \phi(\mathbf{M}) & R_{JB} \leq R_1 \\ \phi(\mathbf{M}) + \Delta\phi_R \left(\frac{\ln(R_{JB}/R_1)}{\ln(R_2/R_1)}\right) & R_1 < R_{JB} \leq R_2 \\ \phi(\mathbf{M}) + \Delta\phi_R & R_{JB} > R_2 \end{cases}$$

and where the M-dependent ϕ is given by:

$$\phi(\mathbf{M}) = \begin{cases} \phi_1 & \mathbf{M} \leq 4.5 \\ \phi_1 + (\phi_2 - \phi_1)(\mathbf{M} - 4.5) & 4.5 < \mathbf{M} < 5.5 \\ \phi_2 & \mathbf{M} \geq 5.5 \end{cases} \tag{14}$$

The coefficients of the GMPE is provided in Table 3. For the present study for developing the attenuation relation the Magnitude is taken from 4-9, distance till 500km, reverse mechanism, applied global parameters and V_{s30}=170m/s (average value obtained at site). The attenuation relation for V_{s30}=170m/s is given in Figure 11 a.

3.2 CB-2014

The median ground motion relation developed by Cambell and Bozorgnia(2014) can be expressed as

$$\ln(Y) = \begin{cases} \ln PGA; & PSA < PGA \quad and \quad T < 0.25s \\ f_{mag} + f_{dis} + f_{flt} + f_{hng} + f_{site} + f_{sed} + f_{hyp} + f_{dip} + f_{atn} & otherwise \end{cases} \tag{15}$$

where *Y* is the intensity measure of interest and *f*-term represents the scaling of ground motion with respect to earthquake magnitude, geometric attenuation, style of faulting, hanging wall geometry, shallow site response, basin response, hypocentral depth, fault dip, and anelastic attenuation, respectively. The terms in the above equation are described further:

Magnitude Term

$$f_{mag} = \begin{cases} c_0 + c_1\mathbf{M}; & \mathbf{M} \le 4.5 \\ c_0 + c_1\mathbf{M} + c_2(\mathbf{M} - 4.5); & 4.5 < \mathbf{M} \le 5.5 \\ c_0 + c_1\mathbf{M} + c_2(\mathbf{M} - 4.5) + c_3(\mathbf{M} - 5.5); & 5.5 < \mathbf{M} \le 6.5 \\ c_0 + c_1\mathbf{M} + c_2(\mathbf{M} - 4.5) + c_3(\mathbf{M} - 5.5) + c_4(\mathbf{M} - 6.5); & \mathbf{M} > 6.5 \end{cases} \tag{16}$$

Geometric Attenuation Term

$$f_{dis} = (c_5 + c_6\mathrm{M})\ln(\sqrt{R_{rup}^2 + c_7^2}) \tag{17}$$

Style of Faulting Term

$$\begin{aligned} f_{flt} &= f_{flt,F} f_{flt,M} \\ f_{flt,F} &= c_9 F_{NM} \\ f_{flt,M} &= \begin{cases} 0; & \mathrm{M} \le 4.5 \\ \mathrm{M} - 4.5 & 4.5 \le \mathrm{M} \le 5.5 \\ 1; & M > 5.5 \end{cases} \end{aligned} \tag{18}$$

Hanging Wall Term

$$f_{hng} = c_{10} f_{hng,R_x} f_{hng,R_{RUP}} f_{hng,M} f_{hng,Z} f_{hng,\delta} \tag{19}$$

$$f_{hng,R_x} = \begin{cases} 0; & R_x < 0 \\ f_1(R_x); & 0 \le R_x < R_1 \\ \max\left[f_2(R_x), 0\right]; & R_x \ge R_1 \end{cases} \tag{20}$$

$$f_1(R_x) = h_1 + h_2(R_x / R_1) + h_3(R_x / R_1)^2$$

$$f_2(R_x) = h_4 + h_5\left(\frac{R_x - R_1}{R_2 - R_1}\right) + h_6\left(\frac{R_x - R_1}{R_2 - R_1}\right)^2$$

$$R_1 = W\cos(\delta) \qquad and \qquad R_2 = 62\mathrm{M} - 350$$

$$f_{hng,R_{RUP}} = \begin{cases} 1; & R_{Rup} = 0 \\ (R_{Rup} - R_{JB}) / R_{Rup} & R_{Rup} > 0 \end{cases} \tag{21}$$

$$f_{hng,M} = \begin{cases} 0; & \mathrm{M} \le 5.5 \\ (\mathrm{M} - 5.5)\left[1 + a_2(\mathrm{M} - 6.5)\right] & 5.5 \le \mathrm{M} \le 6.5 \\ 1 + a_2(\mathrm{M} - 6.5); & M > 6.5 \end{cases} \tag{22}$$

$$f_{hng,Z} = \begin{cases} 1 - 0.06Z_{TOR}; & Z_{TOR} \le 16.66 \\ 0; & Z_{TOR} > 16.66 \end{cases} \tag{23}$$

$$f_{hng,\delta} = (90 - \delta) / 45 \tag{24}$$

Shallow Site Response Term

$$f_{site} = f_{site,G} + S_J f_{site,J} \tag{25}$$

$$f_{site,G} = \begin{cases} c_{11}\ln\left(\frac{V_{s30}}{k_1}\right) + k_2\left\{\ln\left[A_{1100} + c\left(\frac{V_{s30}}{k_1}\right)^n\right] - \ln\left(\frac{200}{k_1}\right)\right\}; & V_{s30} \le k_1 \\ (c_{11} + k_2 n)\ln\left(\frac{V_{s30}}{k_1}\right); & V_{s30} > k_1 \end{cases} \tag{26}$$

$$f_{site,J} = \begin{cases} (c_{12} + k_2 n)\left[\ln\left(\frac{V_{s30}}{k_1}\right) - \ln\left(\frac{200}{k_1}\right)\right]; & V_{s30} \le 200 \\ (c_{13} + k_2 n)\ln\left(\frac{V_{s30}}{k_1}\right); & All\ \ V_{s30} \end{cases} \tag{27}$$

Basin Response Term

$$f_{sed} = \begin{cases} (c_{14} + c_{15} S_J)(Z_{2.5} - 1); & Z_{2.5} \le 1 \\ 0; & 1 \le Z_{2.5} \le 3 \\ c_{16} k_3 e^{-0.75} \left[1 - \exp(-0.25(Z_{2.5} - 3))\right]; & Z_{2.5} > 3 \end{cases} \tag{28}$$

Hypocentral Depth Term

$$f_{hyp} = f_{hyp,H} f_{hyp,M} \tag{29}$$

$$f_{hyp,H} = \begin{cases} 0; & Z_{HYP} \le 1 \\ Z_{HYP} - 7; & 7 \le Z_{HYP} \le 20 \\ 13; & Z_{HYP} > 20 \end{cases} \tag{30}$$

$$f_{hyp,M} = \begin{cases} c_{17}; & \mathrm{M} \le 5.5 \\ \left[c_{17} + (c_{18} - c_{17})(\mathrm{M} - 6.5)\right] & 5.5 \le \mathrm{M} \le 6.5 \\ c_{18}; & M > 6.5 \end{cases} \tag{31}$$

Fault Dip Term

$$f_{dip} = \begin{cases} c_{19}\delta; & \mathrm{M} \le 4.5 \\ c_{19}(5.5 - \mathrm{M})\delta & 4.5 \le \mathrm{M} \le 5.5 \\ 0; & M > 5.5 \end{cases} \tag{32}$$

Anelastic Attenuation Term

$$f_{atn} = \begin{cases} (c_{20} + \Delta c_{20})(R_{Rup} - 80); & R_{Rup} > 80 \\ 0 & R_{Rup} \le 80 \end{cases} \tag{33}$$

The corresponding coefficients obtained after regression is summarized in Table 4

Definitions of Predictor Variables

The definitions of the predictor variables appearing in the equations given in the previous sections are defined as follows:

• **M** is moment magnitude. (4-9)

• R_{RUP} (km) is closest distance to the coseismic fault rupture plane (a.k.a. rupture distance).(0-500km)

• R_{JB} (km) is closest distance to the surface projection of the coseismic fault

ruptureplane (a.k.a. Joyner-Boore distance). (0-500km)

• R_X (km) is closest distance to the surface projection of the top edge of the coseismic fault rupture plane measured perpendicular to its average strike (0-500km)

• W (km) is the down-dip width of the fault rupture plane. (calculated using Wills and coppersmith equation)

• λ (°) is rake angle defined as the average angle of slip measured in the plane of rupture between the strike direction and the slip vector (90^0).

• F_{RV} is an indicator variable representing reverse and reverse-oblique faulting, where F_{RV} = 1 for 30° < λ < 150° and F_{RV} = 0 otherwise.

• F_{NM} is an indicator variable representing normal and normal-oblique faulting, where F_{NM} = 1 for -150° < λ < -30° and F_{NM} = 0 otherwise.

• Z_{TOR} (km) is the depth to the top of the fault rupture plane.

• δ (°) is the average dip angle (45^0) of the fault rupture plane measured from horizontal.

• V_{S30} (m⁄s) is the time-averaged shear wave velocity in the top 30 m of the site (a.k.a. 30 m shear wave velocity). (170km/s)

• A_{1100} (g) is the median estimated value of PGA on rock with V_{S30} = 1100m⁄s (a.k.a. rock PGA).

• S_J is an indicator variable representing regional site effects, where S_J = 1 for sites located in Japan and S_J = 0 otherwise.

• $Z_{2.5}$ (km) is the depth to the 2.5 km⁄s shear wave velocity horizon beneath the site (a.k.a. sediment depth).

• Z_{HYP} (km) is the hypocentral depth of the earthquake measured from sea level.

The attenuation relation for V_{s30}=170m/s is given in Figure 11 b.

3.3 ASK-2014

The function for of the GMPE of Abrahamson *et al.* (2014) is expressed as:

$$
\begin{aligned}
ln\ Sa(g) = & f_1(\mathbf{M}, R_{RUP}) + F_{RV} f_7(\mathbf{M}) + F_N f_8(\mathbf{M}) + F_{As} f_{11}(CR_{JB}) \\
& + f_5(\widehat{Sa}_{1180}, V_{S30}) + F_{HW} f_4(R_{JB}, R_{RUP}, R_x, R_{y0}, W, dip, Z_{TOR}, \mathbf{M}) \\
& + f_6(Z_{TOR}) + f_{10}(Z_1, V_{S30}) + Regional(V_{S30}, R_{RUP})
\end{aligned}
\tag{34}
$$

where, M is the moment magnitude, CR_{jb} centroid $R_{jB,}$ Z_{TOR} Depth to the top of rupture, F_{RV} and F_N flag for reverse and normal faulting respectively, F_{AS} flag for aftershocks, R_{RUP} Rupture distance, R_{JB} Joyner-Boore distance, R_x Horizontal distance from top edge of rupture, R_{y0} Horizontal distance off the end of the rupture measured parallel to strike, V_{s30} shear wave velocity over top 3m (m/s), dip- Fault dip, W Width of fault.

the functional forms for f_1, f_4, f_5, f_6, f_7, f_8, f_{10}, f_{11}, and the regional term are given below: (Detailed description of these functional forms can be checked in Abrahamson *et al.* (2014))

$$
f_1 = \begin{cases} a_1 + a_5(\mathbf{M} - M_1) + a_8(8.5 - \mathbf{M})^2 + [a_2 + a_3(\mathbf{M} - M_1)]\ln(R) + a_{17} R_{RUP} & for\ \mathbf{M} > M_1 \\ a_1 + a_4(\mathbf{M} - M_1) + a_8(8.5 - \mathbf{M})^2 + [a_2 + a_3(\mathbf{M} - M_1)]\ln(R) + a_{17} R_{RUP} & for\ M_2 \le \mathbf{M} < M_1 \\ a_1 + a_4(M_2 - M_1) + a_8(8.5 - M_2)^2 + a_6(\mathbf{M} - M_2) & \\ \quad + a_7(\mathbf{M} - M_2)^2 + [a_2 + a_3(M_2 - M_1)]\ln(R) + a_{17} R_{RUP} & for\ \mathbf{M} < M_2 \end{cases}
\tag{35}
$$

where

$$
R = \sqrt{R_{RUP}^2 + c_{4M}^2}
$$

where

$$
c_{4M}(\mathbf{M}) = \begin{cases} c_4 & for\ \mathbf{M} > 5 \\ c_4 - (c_4 - 1)(5 - \mathbf{M}) & for\ 4 < \mathbf{M} \le 5 \\ 1 & for\ \mathbf{M} \le 4 \end{cases}
$$

Style of Faulting (SOF) Model

$$
f_7(\mathbf{M}) = \begin{cases} a_{11} & for\ \mathbf{M} > 5.0 \\ a_{11}(\mathbf{M} - 4) & for\ 4 \le \mathbf{M} \le 5 \\ 0 & for\ \mathbf{M} < 4.0 \end{cases}
$$

$$
f_8(\mathbf{M}) = \begin{cases} a_{12} & for\ \mathbf{M} > 5.0 \\ a_{12}(\mathbf{M} - 4) & for\ 4 \le \mathbf{M} \le 5 \\ 0 & for\ \mathbf{M} < 4.0 \end{cases}
\tag{36}
$$

Note that although their functional form allows for scaling of reverse faults, the final regression results are such that there is no scaling between strike-slip and reverse events (a11= 0)

Site Response Model

$$f_5(\widehat{Sa}_{1180}, V_{S30}) = \begin{cases} (a_{10} + bn)\, ln\left(\frac{V^*_{S30}}{V_{Lin}}\right) & for\ V_{S30} \geq V_{Lin} \\ (a_{10}) ln\left(\frac{V^*_{S30}}{V_{Lin}}\right) - b\ ln(\widehat{Sa}_{1180} + c) + b\ ln\left(\widehat{Sa}_{1180} + c\left(\frac{V^*_{S30}}{V_{Lin}}\right)^n\right) & for\ V_{S30} < V_{Lin} \end{cases} \tag{37}$$

where

$$V^*_{S30} = \begin{cases} V_{S30} & for\ V_{S30} < V_1 \\ V_1 & for\ V_{S30} \geq V_1 \end{cases}$$

$$V_1 = \begin{cases} 1500 & for\ T \leq 0.5\ \text{s} \\ \exp(-0.35\ \ln(\frac{T}{0.5}) + \ln(1500)) & for\ 0.5\ \text{s} < T < 3\ \text{s} \\ 800 & for\ T \geq 3\ \text{s} \end{cases}$$

Hanging wall model

$$\begin{aligned} & f_4(R_{JB}, R_{RUP}, R_x, R_{y0}, W, dip, Z_{TOR}, \mathbf{M}) \\ & \quad = a_{13} T_1(dip) T_2(\mathbf{M}) T_3(R_x, W, dip) T_4(Z_{TOR}) T_5(R_x, R_{y0}\ \text{OR}\ R_{JB}) \end{aligned} \tag{38}$$

Depth-to-Top of Rupture Model

$$f_6(Z_{TOR}) = \begin{cases} a_{15} \frac{Z_{TOR}}{20} & for\ Z_{TOR} < 20\ \text{km} \\ a_{15} & for\ Z_{TOR} \geq 20\ \text{km} \end{cases} \tag{39}$$

Soil Depth Model

$$f_{10}(Z_1, V_{S30}) = \begin{cases} a_{43}\ ln\left(\frac{Z_1 + 0.01}{Z_{1,ref} + 0.01}\right) & for\ V_{S30} \leq 200 \\ a_{44}\ ln\left(\frac{Z_1 + 0.01}{Z_{1,ref} + 0.01}\right) & for\ 200 < V_{S30} \leq 300 \\ a_{45}\ ln\left(\frac{Z_1 + 0.01}{Z_{1,ref} + 0.01}\right) & for\ 300 < V_{S30} \leq 500 \\ a_{46}\ ln\left(\frac{Z_1 + 0.01}{Z_{1,ref} + 0.01}\right) & for\ 500 < V_{S30} \end{cases} \tag{40}$$

Aftershock Scaling

$$f_{11}(CR_{JB}) = \begin{cases} a_{14} & for\ CR_{JB} \leq 5 \\ a_{14}\left[1 - \frac{CR_{JB} - 5}{10}\right] & for\ 5 < CR_{JB} < 15 \\ 0 & for\ CR_{JB} \geq 15 \end{cases} \tag{41}$$

Regionalization

$$Regional(V_{S30}, R_{RUP}) = F_{TW}(f_{12}(V_{S30}) + a_{25}R_{RUP}) + F_{CN}(a_{28}R_{RUP}) + F_{JP}(f_{13}(V_{S30}) + a_{29}R_{RUP}) \tag{42}$$

The coefficients F_{TW}, F_{CN} and F_{JP} is taken as 0 except for Taiwan, China and Japan. The coefficients in the expression above is given in Table 5. For the present study for developing the attenuation relation the Magnitude is taken from 4-9, distance till 500km, reverse mechanism, applied global parameters and V_{s30}=170m/s (average value obtained at site). The attenuation relation for V_{s30}=170m/s is given in Figure 11 c.

3.4 CY-2014

The revised GMPE given by CY-2014 is explianed as further

$$\begin{aligned}
\ln(y_{refij}) = c_1 &+ \left\{c_{1a} + \frac{c_{1c}}{\cosh(2 \cdot \max(\mathbf{M}_i - 4.5, 0))}\right\} F_{RVi} \\
&+ \left\{c_{1b} + \frac{c_{1d}}{\cosh(2 \cdot \max(\mathbf{M}_i - 4.5, 0))}\right\} F_{NMi} \\
&+ \left\{c_7 + \frac{c_{7b}}{\cosh(2 \cdot \max(\mathbf{M}_i - 4.5, 0))}\right\} \Delta Z_{TORi} \\
&+ \left\{c_{11} + \frac{c_{11b}}{\cosh(2 \cdot \max(\mathbf{M}_i - 4.5, 0))}\right\} (\cos\delta_i)^2 \\
&+ c_2(\mathbf{M}_i - 6) + \frac{c_2 - c_3}{c_n} \ln(1 + e^{c_n(c_M - \mathbf{M}_i)}) \\
&+ c_4 \ \ln(R_{RUPij} + c_5 \ \cosh(c_6 \cdot \max(\mathbf{M}_i - c_{HM}, 0))) \\
&+ (c_{4a} - c_4) \ \ln\left(\sqrt{R_{RUPij}^2 + c_{RB}^2}\right) \\
&+ \left\{c_{\gamma 1} + \frac{c_{\gamma 2}}{\cosh(\max(\mathbf{M}_i - c_{\gamma 3}, 0))}\right\} R_{RUPij} \\
&+ c_8 \max\left(1 - \frac{\max(R_{RUPij} - 40, 0)}{30}, 0\right) \\
&\times \min\left(\frac{\max(\mathbf{M}_i - 5.5, 0)}{0.8}, 1\right) e^{-c_{8a}(\mathbf{M}_i - c_{8b})^2} \Delta DPP_{ij} \\
&+ c_9 F_{HWij} \cos\delta_i \left\{c_{9a} + (1 - c_{9a}) \ \tanh\left(\frac{R_{Xij}}{c_{9b}}\right)\right\} \left\{1 - \frac{\sqrt{R_{JBij}^2 + Z_{TORi}^2}}{R_{RUPij} + 1}\right\}
\end{aligned} \tag{43}$$

$$
\begin{aligned}
\ln(y_{ij}) = \ln(y_{ref_{ij}}) &+ \eta_i \\
&+ \phi_1 \cdot \min\left(\ln\left(\frac{V_{S30j}}{1130}\right), 0\right) \\
&+ \phi_2\left(e^{\phi_3(\min(V_{S30j},1130)-360)} - e^{\phi_3(1130-360)}\right)\ln\left(\frac{y_{ref_{ij}}e^{\eta_i} + \phi_4}{\phi_4}\right) \\
&+ \phi_5\left(1 - e^{-\Delta Z_{1.0j}/\phi_6}\right) \\
&+ \varepsilon_{ij}
\end{aligned}
\tag{44}
$$

Dependent variable y_{ij} is the ground motion amplitude for earthquake i at station j. Variable y_{refij} is the population median for the reference condition V_{s30} = 1130 m/s. Random variables η_i and ε_i represent the two modeling errors that contribute to the aleatory variability of predicted motion. The predictor variables in equations above are

M	=	Moment magnitude.
R_{RUP}	=	Closest distance (km) to the ruptured plane
R_{JB}	=	Closest distance (km) to the surface projection of ruptured plane.
R_X	=	Site coordinate (km) measured perpendicular to the fault strike from the fault line, with the down-dip direction being positive.
F_{HW}	=	Hanging-wall flag: 1 for $R_X \geq 0$ and 0 for $R_X < 0$.
δ	=	Fault dip angle
Z_{TOR}	=	Depth (km) to the top of ruptured plane.
ΔZ_{TOR}	=	Z_{TOR} centered on the M-dependent average Z_{TOR} (km).
F_{RV}	=	Reverse-faulting flag: 1 for 30° ≤ λ ≤ 150° (combined reverse and reverse-oblique), 0 otherwise; λ is the rake angle.
F_{NM}	=	Normal faulting flag: 1 for −120° ≤ λ ≤ −60° (excludes normal-oblique), 0 otherwise.
V_{S30}	=	Travel-time averaged shear-wave velocity (m⁄s) of the top 30 m of soil.
$Z_{1.0}$	=	Depth (m) to shear-wave velocity of 1.0 km⁄s.
$\Delta Z_{1.0}$	=	$Z_{1.0}$ centered on the V_{S30}-dependent average $Z_{1.0}$ (m).
DPP	=	Direct point parameter for directivity effect.
ΔDPP	=	*DPP* centered on the site- and earthquake-specific average *DPP*.

For the present study for developing the attenuation relation the Magnitude is taken from 4-9, distance till 500km, reverse mechanism, applied global parameters and

V_{s30}=170m/s (average value obtained at site). The coefficients of the equations are given in Table 6 and 7. The attenuation relation V_{s30}=170m/s for is given in Figure 11 d.

4. Site Classification

To identify the soil condition at the BIFPCL, Maitree site of interest, the cross hole surveys at site by BHEL is used. This test is usually performed by generating horizontally traveling P and S waves at a particular level in one borehole (Source Hole) and recording their arrivals at same level in two nearby boreholes (Receiver Holes). Using this data the site can be classified based on the average shear wave velocity of the top 30 meters of the subsoil. This technique is popular among engineers as a quick way of understanding how ground motion during an earthquake differs on rock sites and soil sites. Standard documents such as Bangladesh National Building Code (BNBC-2012) can be referred for classifying sites based on borehole data or velocity profiling of the region. This standard site classification definition is shown in Table 8. For the present region soil properties is determined using values reported form the 5 cross hole test. The shear wave velocities, which, is obtained at an interval of every 2 m depth from each of these crossholes are summarized in Figure 12. The average shear wave velocity ($\overline{V}_s$) at a given borehole can be obtained using the following expression as suggested by BNBC-2012.

$$\overline{V_s} = \frac{\sum_{i=1}^{n} d_i}{\sum_{i=1}^{n} \frac{d_i}{V_{s\,i}}} \tag{45}$$

where, d_i is the thickness of a given soil layer and n is the total number of layers. Here, the $\overline{V}_s$ values are obatined for soil upto a depth of 30m from the surface for the five cross hole tests as 169.52m/s, 167.24m/s, 168.08m/s, 171.94m/s and 173.25m/s respectively at each cross holes. It is clear from Table 4 that the all the sites belong to SD- Type soil condition ($\overline{V}_s$ *<180m/s*). In addition, if the $\overline{V}_s$ values are estimated from 5.00m below the ground, then the corresponding values for the five cross holes will be 179.62 m/s, 177.07 m/s, 178.03 m/s, 182.72 m/s, 184.26 m/s. It is clear that the site still

belongs to SD- Type soil condition ($\overline{V}_s$ *<180m/s*).

Further, to accertain the dynamic characteristic of this soil strata, analysis is performed using Equivalent linear Earthquake site Response Analyses (EERA) of layered soil deposits. The simulation is performed with a typical acceleration time history for SC-type soil condition from NGA database as input earthquake ground motion. The tansfer function or the frequency reponse function, which is ratio of the displacement, velocity or accelertion at two different layers, with respect to frequency is obtained and is shown in Figure 13. It is clear from the figure that the predominant period of the soil strata is 0.44sec. Further, the responce spectra following the DSHA, PSHA and according to Bangladesh National Building Code (BNBC (2012)) are generated for SD type (170m/s) soil condition.

5. Response spectra based on National Building Code, Bangladesh

Traditionally design of a building is done based on the response spectra, which is the maximum response of a single degree of freedom system at different frequencies for a given input ground motion. According to BNBC the spectral acceleration for a design earthquake is given by:

$$S_a = \frac{2}{3}\frac{ZI}{R}C_s \tag{46}$$

where S_a is design spectral acceleration, Z is seismic Zone coefficient, I is the importance factor, R is the response reduction factor based on the type of structural system, and C_s is the normalized acceleration response spectrum, which is a function of structure period and soil type as defined by the following equations:

$$
\begin{aligned}
C_s &= S\left(1+\frac{T}{T_B}\left(2.5\eta-1\right)\right) && for \quad 0 \le T \le T_B \\
C_s &= 2.5S\eta && for \quad T_B \le T \le T_C \\
C_s &= 2.5S\eta\left(\frac{T_C}{T}\right) && for \quad T_C \le T \le T_D \\
C_s &= 2.5S\eta\left(\frac{T_C T_D}{T^2}\right) && for \quad T_D \le T \le 4\,\text{sec}
\end{aligned}
\tag{47}
$$

where, S is the soil factor depending on site class and T is the structural period, T_B is the lower limit of the period of the constant spectral acceleration branch, T_C is the upper limit of the period of the constant spectral acceleration branch, T_D is the lower limit of the period of the constant spectral displacement branch. The values of S, T_B, T_C and T_D for different site classes is summarised in Table 5. η is the damping correction factor as a function of damping with a reference value of η=1 for 5% viscous damping. The expression η is

$$
\eta = \sqrt{10/(5+\xi)} \ge 0.55 \tag{48}
$$

where, ξ is the viscous damping ratio of the structure. In the present study, design acceleration response spectra are obtained for the site by taking R and I as unity. As per BNBC (2012), the Z value for Bagerhat is given as 0.12. From the average shear wave velocities obtained from the cross-hole tests (170m/s), the site belongs to 'SD, type soil condition. It is known that the percentage damping to be used depends on the type of structure. Hence response spectra are obtained for 0.8%, 1.0%, 1.6%, 2%, 3%, 5%, 7% and 10% damping according to BNBC (2012) and are summarized in Figure 14 and Table 10. For the particular response spectra I and R are taken as unity. These response spectra will be compared with that obtained from DSHA and PSHA as explained further.

6. Deterministic Seismic Hazard Analysis (DSHA)

The DSHA approach uses the known seismic sources sufficiently near the site and available historical seismic and geological data to generate discrete, single-valued

events or models of ground motion at the site. Typically one or more earthquakes are specified by magnitude and location with respect to the site. Usually the earthquakes are assumed to occur on the portion of the site closest to the site. The site ground motions are estimated deterministically, given the magnitude, source-to-site distance, and site condition. The steps involved in DSHA (Kramer 1996) as expressed through Figure 15 is described in brief as follows

Step 1: Identification of all sources capable of producing significant ground motion at the site such as Large sources at long distances and Small sources at short distances. Characterization includes Definition of source geometry and Establishment of earthquake potential.

Step 2: Selection of source-site distance parameter must be consistent with predictive relationship and should include finite fault effect

Step 3: Selection of Controlling Earthquakes is based on ground motion parameter(s). Consider all sources, assume M_{max} occurs at R_{min} for each source. Compute ground motion parameter(s) based on M_{max} and R_{min}. Then, determine critical value(s) of ground motion parameter(s).

Step 4: Definition of hazard using controlling earthquake involves the use of M and R to determine parameters such as Peak acceleration, spectral acceleration and Duration

The determinstic analysis performed for the region using source characteristics, and the different attenuation relations available in the global database. Here, DSHA is performed by considering the earthquake corresponding to 2% probability of exceedance in 50 years (2500 yrs return period). It is noted that the critical fault according to this analysis is the eocene hinge zone with a magnitude 7.5 at a distance of 106km from site. The corresponding attenuation at the site is illustrated along with response spectra according to BNBC (2012) for 5% damping in Figure 16 and Table 11. It can be seen that the spectral values obtained corresponding to the magnitude with 2% probability of exceedance in 50 years (2500yrs return period, (as per BNBC)) is comparable with BNBC(5% damping). The PGA is obtained as 0.069, 0.074, 0.058 and 0.089 g correspondingly for ASK, BSSA, CB and CY. Similarly for S_a at 0.2 sec is estimated as 0.211, 0.158, 0.114 and 0.199 and for 1 sec the values for corresponding

GMPEs are 0.167, 0.111, 0.115 and 0.160.

The percentage damping considered for the construction of response spectra should depend on the type of the structure. Thus, the flexible structure will have lesser damping percentace, while for rigid structures the damping percentage would be higher. It should be noted that the GMPE's used here is developed based on spectral values correspoinding to 5% damping. Hence, it is nessary to apply suitable damping correction factors to estimate the spectras corresponding to other damping. The commonly used damping correction factors are those given in Newmarks and Halls (1982). There are several other literatures proposing the damping correction factors (Boomer et al. (2000), Priestley (2003), Atkinson and Pierre (2004) etc.). In this report, the more recent damping correction factor (DCF) for deep soil reported by Cameron and Green (2007) is considered. The DCF values is linearly interpolated, for all the required time periods and damping percentages, and is summarized in Table 13. Further, It should be noted that the uncertainities in the source should be accounted in the study and thereby taking just the a single magnitude and distance value will lead to an overconservative estimate of spectral values.

7. Probabilistic Seismic Hazard Analysis (PSHA)

Probabilistic seismic hazard analysis estimates the probability of exceedance of various ground motion levels at a site given all possible earthquakes. The basic formulation for PSHA has been derived by Cornell (1968) assuming point source model for earthquakes. Later PSHA has been improved to include finite source and its uncertainty by Kiureghian and Ang (1977). Now a days, PSHA has become a standard tool for estimating ground motion. The procedure required for PSHA has been discussed in great detail in the literature (Kramer 1996). The same methodology has been followed in the present study also. The basic steps are briefly mentioned here. The uncertainty in the magnitude of a future event is represented as a an exponential random variable

$$p_M(m) = \frac{\beta e^{-\beta(m-m_0)}}{1-\beta e^{-\beta(m_u-m_0)}}; \quad (\mathrm{m}_0 \le \mathrm{m} \le \mathrm{m}_\mathrm{u}),\ \beta = 2.303\mathrm{b} \tag{49}$$

The other unknown factor is the distance *R* of the site to the future hypocenter. The conditional probability distribution function of *R*, given that magnitude *M* = *m* for a rupture segment uniformly distributed along a fault can be numerically computed following the method of Der Kiureghian and Ang (1977) . Referring to Figure 17. we have

$$\begin{aligned}
&P(R < r \mid M = m) = 0 \quad for\ R < \left(D^2 + L_o^2\right)^{1/2} \\
&P(R < r \mid M = m) = \frac{\left(r^2 - D^2\right)^{1/2} - L_o}{L - X(m)} \\
&\qquad for \left(D^2 + L_o^2\right)^{1/2} \le R < \left\{D^2 + \left[L + L_o - X(m)\right]^2\right\}^{1/2} \\
&P(R < r \mid M = m) = 1 \quad for\ R > \left\{D^2 + \left[L + L_o - X(m)\right]^2\right\}^{1/2}
\end{aligned} \tag{50}$$

The rupture length, *X*(*m*), for an event of magnitude *m*, is given by

$$X(m) = MIN\left[10^{(-2.44+0.59m)}, fault\ length\right] \tag{51}$$

Probabilistic seismic hazard analysis estimates the probability of exceedance of spectral acceleration S_a at a site due to all possible future earthquakes as visualized by the previous hazard scenario. Assuming that the number of earthquakes occurring on a fault follows a stationary Poisson process, the probability that the control variable *Y* exceeds level *y**, in a time window of T years is given by

$$P(Y > y^* \text{ in T years }) = 1 - \exp(-\mu_{y^*} T) \tag{52}$$

The rate of exceedance, μ_{y^*} is computed from the expression

$$\mu_{y^*} = \sum_{i=1}^{K} \mathrm{N_i}(\mathrm{m}_0) \int_m \int_r P(Y > y^* \mid m, r)\, p_{R|M}(r \mid m)\, p_M(m) \quad \mathrm{d}r\mathrm{d}m \tag{53}$$

Here, K is the total number of faults in the zone, $p_M(m)$ and $p_{R|M}$ $(r \mid m)$ are the probability density functions of magnitude and hypocentral distance respectively. $P(Y > y^* \mid m, r)$ is the conditional probability of exceedance of the ground motion parameter Y. This is found as a lognormal random variable with mean value given by the attenuation equation conditioned on particular m and r values. The reciprocal of the annual probability of exceedance gives the return period for the corresponding ground motion value. The mean annual rate of exceedance of y^* is obtained by summing over the individual probabilities due to all faults. This is repeated for various ground motion values y^* to obtain the seismic hazard curves. These curves are first obtained individually for all the faults located in the ten tectonic zones and combined to estimate the aggregate hazard at the site.

7.1. Uniform Hazard Response Spectra

The uniform hazard response spectra (UHRS), the spectrum having the same mean recurrence interval at all frequencies, will be developed for BIFPCL, Maitree site, at Bagerhat. These results will be obtained using the appropriate global attenuation ground motion. The site specific UHRS will be obtained for return periods of 2500yrs, which corresponds to 2% probability in 50years or Maximum Considered Earthquake (MCE). According to BNBC (2012), the design basis earthquake is taken as 2/3 of the MCE. Hence, the UHRS for 2/3 of the corresponding value obtained for 2500 return period is given in Table 12 and Figure 18. The PGA is obtained as 0.067, 0.08, 0.056, 0.073 for correspondingly for ASK (2014), BSSA (2014), CB (2014) and CY (2014) for 2/3 of 2500yrs return period. As explained in the previous sections, the GMPE used here is valid for only 5% damping. Hence to generate the UHRS corresponding to other damping, the corresponding values have to be applied with suitable damping correction factor (DCF). In this report the DCF reported by Cameron and Green (2007), given in Table 13, is used to obtain the UHRS for different percentage of damping.

8. Recommended Spectra

The maximum values obtained from the DSHA and the 2/3 of UHRS with 2500yrs return

period is compared with that of BNBC response spectra at 5% damping and is shown in Table 14 and Figure 19. It is clear that the BNBC is higher than the other two spectras up to the time period of 2 seconds. After 2 sec DSHA values are observed to be the highest among the three spectras. Hence it is recommended to consider an envelope encompassing the maximum values of the response spectra for the design of structures at the site (shown as black line in Figure 19). The PGA, S_a (T=0.2s) and S_a (T=1 s) of the envelop are 0.108g 0.272g and 0.216g respectively.

To achieve the recommended response spectra for other damping it is necessary to compare the corresponding value of BNBC (2012) with the DSHA and UHRS values corrected for damping. Thus, the DSHA and UHRS are multiplied with the respective damping correction factors reported in Table 13. Figure 20 (a) and (b) shows the comparison of all the three spectra for 1% and 10% damping respectively. It is clear that for the lower percentage of damping BNBC is lower than that obtained from DSHA and UHRS. Thus it is necessary to increase the BNBC values in the intermediate time period range to obtain the recommended response spectra for the site. The corresponding multiplying factors imposed on BNBC spectra for 0.8%, 1%, 1.6%, 2% and 3% are respectively 1.2823, 1.2589, 1.1776, 1.1147 and 1.1143. The final recommended spectra obtained for different percentage of damping is shown in Table 15 and Figure 21. The PGA value is observed as 0.108g for all the damping ratios. The maximum values of the spectra range between 0.2s to 0.8s and the corresponding values for 0.8%, 1%, 1.6%, 2%, 3%, 5%, 7% and 10% are 0.455g, 0.439g, 0.391g, 0.360g, 0.336g, 0.272g, 0.246g and 0.220g respectively.

9. Spectrum Compatible Acceleration Time History

Acceleration time histories are essential for the non-linear and dynamic analysis of the structure. These acceleration time histories will be desirable if it represent the spectral characteristics of the site under consideration. There are various methods available to generate this synthetic acceleration which is compatible with the site specific response spectra. One such method is that developed by Alexander *et al.* (2014). According to this method, first, the seed time series (any desired time series from the global

database) is re-expressed as a discrete Volterra series. The first-order Volterra kernel is estimated by a multilevel wavelet decomposition using the stationary wavelet transform. Second, the higher-order Volterra kernels are estimated using a complete multinomial mixing of the first-order kernel functions. Finally, the weighting of every term in this Volterra series is optimally adapted using a Levenberg–Marquardt algorithm such that the modified time series matches any target response spectrum.

For the present site this method is applied to generate 5 samples of acceleration time history which are compatible with the response spectra corresponding to the recommended envelope for 5% damping given in Figure 21. The comparison of the response spectras of the sample acceleration time histories with that of the envelope is shown in Figure 22. Further, the generated acceleration time histories are represented in Figure 23 and also provided as '.txt' document along with this report. These samples can be used for the analysis of the structure at site.

10. Summary and Recommendation

The objective of this report is to derive the site specific response spectra for BIFPCL, Maitree STPP project site located in Bagerhat, Bangladesh. The site response spectras are obtained according to deterministic seismic hazard analysis, probabilistic seismic hazard analysis and as per the Bangladesh national building code procedure. Since there are no regional ground motion prediction equations available for Bangladesh, the GMPEs available in the global database which account for various active regions in the world are considered for the study.

A brief review on the geological and tectonic zones surrounding the site is presented in the report. The site is located in tidal delta geological zone. It is observed that the thickness of holocene sediments at the site is around 15 km. In the present study, first, all the faults located within 500km of the site are identified. The faults surrounding the site are grouped into ten homogeneous seismogenic zones to estimate the recurrence parameters. A comprehensive earthquake catalogue consisting of around 2800 events is compiled for the bridge site. To determine the site specific response spectra it is necessary to determine the site condition through field tests. The 5 cross-hole test data

supplied by BHEL for the site is used for this purpose. It is observed that the site belongs to SD type soil (V_{s30}<180m/s) condition, even after removal of top 5m soil, according to BNBC-2012. Further, design response spectra are constructed for the site following BNBC (2012), DSHA and PSHA and are summarized in Figures 14, 16 and 18 and Table 10, 11 and 12. The maximum value obtained from DSHA and 2/3UHRS-2500yrs RP (PSHA) at each time period is compared with BNBC-5% damping as shown Figure 19. It is observed from the figures that the response spectra according to DSHA (M7.5 corresponding to 2500yrs return period) as well as from UHRS (2500yrs return period) is lower than that obtained according to BNBC for 5% damping till 2 seconds. After 2 seconds the DSHA response spectra is observed to be dominant among the three spectras considered. Hence it is recommended to use an envelope of the maximum value shown in Figure 19 for the design of structure at site.

Further it is known that the damping ratio to be considered in design should depend on the type of structure. Typically the damping ratio ranges for different type of structure are 0.1% -1% for aluminum structures, 1%-2% for steel structures, 5%-7% for concrete structures and 10% to 20% for soil structures. Hence in this report response spectras are obtained for 0.8%, 1%, 1.6%, 2%, 3%, 5%, 7% and 10% damping. Since the GMPE's used in the present work corresponded to 5% damping only the DSHA and UHRS values obtained from this case is multiplied with suitable damping correction factors as proposed by Cameron and Green (2007).

The spectral acceleration for design earthquake (refer Clause 2.5.6.3 of BNBC 2012) based upon the site specific seismic study shall be considered as follows (instead of using equation 2.5.4 of BNBC 2012):-

$$S_a = C_{ss} * I/R \tag{54}$$

where,

Sa = Design spectral acceleration (in units of g)

C_{ss} = Site specific acceleration response spectrum. Recommended values are given in Table 15 and Figure 21 for various viscous damping ratios.

I = Structure Importance factor. Shall be considered as per BNBC 2012.
R = Reponse reduction factor. Shall be considered as per BNBC 2012.

Thus final recommended site specific spectra obtained by considering the maximum values from all the cases individually for different percentage of damping, shown in Table 15 and Figure 21, are obtained by considering *I* and *R* as unity.

The features of the final recommended spectra (C_s) are as follows

- The Zero period design acceleration value is observed as 0.108g for all the damping ratios.
- The maximum values of the spectra range between 0.2s to 0.8s time period.
- The maximum value of the spectra for 0.8%, 1%, 1.6%, 2%, 3%, 5%, 7% and 10% are 0.455g, 0.439g, 0.391g, 0.360g, 0.336g, 0.272g, 0.246g and 0.220g respectively.
- It is observed that the soil class at site belongs to 'SD' type according to BNBC-2012 even after removal of top 5m of soil. Hence the spectras reported in Table 15 and Figure 21 is valid for a depth of 5m as well.
- The values given in Table 15 and Figure 21 are for *I*/*R*=1. In order to obtain the spectral acceleration for the design earthquake to be applied for the design of structure at site, these recommended values should be multiplied by suitable *I*/*R* (BNBC (2012)); where *I* is the Structural Importance Factor and *R* is the response reduction factor, considered as per BNBC 2012.

. Further, acceleration time histories compatible with recommended envelope corresponding to 5% damping is provided, which can be used for the analysis of the structure at site.

References

Abrahamson, Norman A., Walter J. Silva, and Ronnie Kamai(2014) Summary of the ASK14 ground motion relation for active crustal regions. *Earthquake Spectra* 30, no. 3: 1025-1055.

Al-Hussaini, Tahmeed M., Ishika N. Chowdhury, and Md NA Noman. (2015) Seismic Hazard Assessment For Bangladesh-Old And New Perspectives. First International Conference on Advances in Civil Infrastructure and Construction Materials MIST, Dhaka, Bangladesh, 14–15 December 2015

Alexander, N. A., A. A. Chanerley, A. J. Crewe, and S. Bhattacharya. (2014) Obtaining Spectrum Matching Time Series Using a Reweighted Volterra Series Algorithm (RVSA). *Bulletin of the Seismological Society of America.*

Alam, M., Alam, M.M., Curray, J.R., Chowdhury, M.L.R. and Gani, M.R., 2003. An overview of the sedimentary geology of the Bengal Basin in relation to the regional tectonic framework and basin-fill history. *Sedimentary Geology*, *155*(3), pp.179-208.

Asian Disaster Preparedness Center- ADPC (2013), Report of active fault mapping in Bangladesh, July 2013.

Atkinson, G. M., and J. R. Pierre (2004). Ground-motion response spectra in eastern North America for different critical damping values, *Seism. Res. Lett.* **75,** no. 4, 541–545.

Bangladesh National Building Code (2012), BNBC, Earthquake load part 6

Banglapedia, en.banglapedia.org/index.php?title=Fault

Bangladesh Meteorological Department, http://www.bmd.gov.bd/?/home/

Brammer, H. (1996). *geography of the soils of Bangladesh*. University Press.

Bommer, J. J., A. S. Elnashai, and A. G. Weir (2000). Compatible acceleration and displacement spectra for seismic design codes, Presented at *Proc. 12th World Conference on Earthquake Engineering*, Auckland, paper no. 207.

Cameron, W.I. and Green, R.A., (2007) Damping correction factors for horizontal ground-motion response spectra. *Bulletin of the Seismological Society of America*, *97*(3), pp.934-960.

David M. Boore, Jonathan P. Stewart, Emel Seyhan, and Gail M. Atkinson (*2014*) NGA-West2 Equations for Predicting PGA, PGV, and 5% Damped PSA for Shallow Crustal Earthquakes. Earthquake Spectra: August 2014, Vol. 30, No. 3, pp. 1057-1085

Campbell, Kenneth W., and Yousef Bozorgnia (2014) NGA-West2 ground motion model for the average horizontal components of PGA, PGV, and 5% damped linear acceleration response spectra." *Earthquake Spectra* 30, no. 3: 1087-1115.

Cornell, C.A. (1968), Engineering seismic risk analysis, *Bulletin of Seismological* Society *of America*, 58, 1583-1606.

Center, Asian Disaster Preparedness. Seismic Hazard Assessment of Dhaka, Chittagong & Sylhet city corporation area. (2009).

Chiou, Brian S-J., and Robert R. Youngs(2014) Update of the Chiou and Youngs NGA model for the average horizontal component of peak ground motion and response spectra. *Earthquake Spectra* 30, no. 3: 1117-1153.

Der Kiureghian, A. and Ang, A. H.-S. (1977), A fault rupture model for seismic risk analysis. *Bull. Seismol. Soc. Am.*, 67:1173–1194.

GSI (2000). Seismotechnic Atlas of India, Geology Society of India, New Delhi.

Geological Survey of Bangladesh (GSB), http://www.gsb.gov.bd/rvedr$/

Islam, M.N. and Uddin, M.N., 2002. Country paper on hydrogeology section. In *Proceedings of International Workshop on Arsenic Issue in Bangladesh*.

Kijko A and Graham G (1998) Parametric-historic procedure for probabilistic seismic hazard analysis, Part I: Estimation of maximum regional magnitude Mmax; *Pure Appl. Geophys*. 152 413–442.

Kramer S L (1996), Geotechnical Earthquake Engineering, Prentice-Hall, Inc.

Newmark, N. M., and W. J. Hall (1982). Earthquake Spectra and Design, EERI Monograph Series. Earthquake Engineering Research Institute, Oakland, California.

NDMA (2011), Development of probabilistic seismic hazard map of India, Technical report of the working comittee of experts National Disaster Management Authority (NDMA), Govt. of India, New Delhi

Persits, F.M., WAndrey, C.J., Milici, R.C. and Manwar, A., 1997. *Digital geologic and geophysical data of Bangladesh* (No. 97-470-H).

Priestley, M.J.N. (2003). *Myths and Fallacies in Earthquake Engineering,Revisited*, The Mallet Milne Lecture, IUSS Press, Istituto Universitario di Studi Superiori di Pavia, Pavia, Italy.

Raghukanth, STG (2011). Seismicity parameters for important urban agglomerations in India, *Bulletin of earthquake Engineering*, 9(5),1361-1386.

Singh, A., Bhushan, K., Singh, C., Steckler, M.S., Akhter, S.H., Seeber, L., Kim, W.Y., Tiwari, A.K. and Biswas, R.,(2016). Crustal structure and tectonics of Bangladesh: New constraints from inversion of receiver functions. *Tectonophysics*, *680*, pp.99-112.

Steckler, M.S., S.H. Akhter, and L. Seeber, (2008), Collision of the Ganges–Brahmaputra Delta with the Burma Arc: implications for earthquake hazard. *Earth planet Sci. Lett.*, **273**, 367–378.

Seismic risk assessment in Bangladesh (2015), Ministry of Disaster management and relief, Bangladesh

Shamsuddin, A.K.M and Abdullah S.K.M, (1997) Geologic Evolution of the Bengal Basin and its implication in Hydrocarbon Exploration in Bangladesh. *Indian Jounal Of Geology, Vol.69, No. 2, p 93-121.*

USNRC (1997). Regulatory guide 1.165: Identification and characterization of seismic sources and determination of safe shutdown earthquake ground motion. Report No. DG- 1032(RG 1.165), USA.

Wells, D.L. and Coppersmith, K.J. (1994), Empirical relationships among magnitude, rupture length, rupture width, rupture area and surface displacements, *Bull. Seismol. Soc. Am.*, 84(4):974-1002.

Table 1. Earthquakes of magnitude Mw ≥ 6 around BIFPCL, Maitree site, Bagerhat, Bangladesh.

Long. (^{0}N)	Lat. (^{0}E)	Year	Month	Date	Magnitude (M_w)	Depth (km)
91.80	26.10	825	1	1	8	0
88.40	22.60	1737	10	11	7.2	0
92.00	22.00	1762	4	2	7.5	0
88.00	24.00	1764	6	4	6	0
89.75	24.50	1787	6	1	7.8	0
91.00	23.50	1822	4	3	6	0
89.40	25.80	1834	7	8	6.3	0
90.00	25.00	1842	11	11	6.5	0
90.40	24.80	1846	10	17	6.3	0
92.70	26.30	1847	1	1	6.3	0
92.50	22.20	1865	12	19	6	0
92.50	24.50	1869	1	10	7.5	0
90.00	24.00	1885	7	14	7	0
91.00	25.90	1897	6	12	8.1	0
91.00	24.50	1918	7	8	7.6	0
93.20	22.20	1920	8	15	6	0
93.40	22.60	1923	8	10	6	0
91.00	25.30	1923	9	9	7.1	0
93.00	25.00	1924	1	30	6	0
90.20	25.80	1930	7	2	7.1	0
93.80	25.30	1930	9	22	6	0
90.00	25.00	1932	3	24	7.4	0
92.00	24.50	1932	3	27	7.4	0
92.00	26.50	1932	11	09	7.4	0
91.00	26.00	1933	3	6	7.6	0
86.80	26.60	1934	1	15	8.3	0
89.50	24.40	1935	3	21	6.2	0
92.00	27.00	1941	1	21	6.8	0
90.90	25.10	1945	5	19	6.1	0
89.00	26.00	1949	12	10	6	0
93.00	25.00	1950	8	15	6	0
92.70	21.60	1955	12	14	6.7	0
91.30	28.30	1954	2	23	6.5	0
90.90	24.80	1956	6	12	6	0
93.95	22.60	1956	7	12	6.3	0

93.76	24.38	1957	7	1	7.2	41
90.30	26.90	1960	7	29	6.5	11
90.50	24.90	1963	6	19	6.2	0
93.58	22.33	1964	1	22	6	60
86.63	26.72	1988	8	20	6.4	65
91.36	27.40	2009	9	21	6.4	
99.49	20.70	2011	3	24	6.8	0
88.17	27.48	2011	9	18	6.8	0
95.55	23.47	2012	11	11	6.6	0
18.80	87.50	2014	5	21	6.1	
84.52	28.5	2015	4	25	7.5	0
86.10	27.60	2015	5	12	7.1	0
86.11	27.48	2015	4	26	6.6	0
94.26	23.21	2016	4	13	7.2	0
93.15	24.50	2016	4	1	6.6	

Table 2. Seismicity parameters for seven seismogenic zones considered in this study

Source No.	Zones	*b*-value	*N(4)*	Max. Potential Magnitude (M_{max})	No. of earthquakes
3	Central Himalaya II	0.8±0.03	2.39±0.31	8.8±0.4	403
4	Eastern Himalaya	0.74±0.03	2.87±0.54	8±0.3	243
8	Shillong Plateau & Assam Valley	0.76±0.03	2±0.34	8.4±0.3	200
9	Bengal Basin	0.75±0.03	2±0.22	8.1±0.5	330
10	Indo Burmese Arc	0.82±0.02	12.04±1.74	7.8±0.3	1126
11	Shan-Sagaing fault	0.68±0.03	5.64±1.11	8.1±0.3	319
17	Eastern Passive Margin	0.8±0.07	0.36±0.07	6.3±0.3	42
18	Mahanandi Garben & Eastern Carton	0.79±0.09	0.3±0.1	5.8±0.5	27
31	Gangetic region	0.89±0.08	0.33±0.08	6.3±0.5	31
32	Bay of Bengal	0.63±0.06	1.07±0.26	6.8±0.3	75

Table 3. (a) Coefficients in the attenuation relation of BSSA-2014 for Magnitude scaling term

Period(sec)	e0	e1	e2	e3	e4	e5	e6	Mh
0	4.47E-01	4.86E-01	2.46E-01	4.54E-01	1.43E+00	5.05E-02	-1.66E-01	5.5
0.01	4.53E-01	4.92E-01	2.52E-01	4.60E-01	1.42E+00	4.93E-02	-1.66E-01	5.5
0.02	4.86E-01	5.24E-01	2.97E-01	4.89E-01	1.43E+00	5.34E-02	-1.66E-01	5.5
0.03	5.69E-01	6.09E-01	4.04E-01	5.58E-01	1.43E+00	6.14E-02	-1.67E-01	5.5
0.05	7.54E-01	7.99E-01	6.07E-01	7.27E-01	1.40E+00	6.74E-02	-1.81E-01	5.5
0.075	9.64E-01	1.01E+00	7.77E-01	9.56E-01	1.42E+00	7.35E-02	-1.97E-01	5.5
0.1	1.13E+00	1.17E+00	8.87E-01	1.15E+00	1.43E+00	5.52E-02	-1.98E-01	5.54
0.15	1.31E+00	1.35E+00	1.06E+00	1.33E+00	1.28E+00	-4.21E-02	-1.82E-01	5.74
0.2	1.33E+00	1.36E+00	1.12E+00	1.34E+00	1.13E+00	-1.11E-01	-1.59E-01	5.92
0.3	1.22E+00	1.24E+00	1.02E+00	1.27E+00	9.57E-01	-1.96E-01	-9.29E-02	6.14
0.4	1.10E+00	1.12E+00	8.98E-01	1.16E+00	9.68E-01	-2.26E-01	-2.32E-02	6.2
0.5	9.70E-01	9.91E-01	7.62E-01	1.01E+00	1.04E+00	-2.35E-01	2.91E-02	6.2
0.75	6.69E-01	6.97E-01	4.75E-01	6.92E-01	1.29E+00	-2.16E-01	1.08E-01	6.2
1	3.93E-01	4.22E-01	2.07E-01	4.12E-01	1.50E+00	-1.90E-01	1.79E-01	6.2
1.5	-1.50E-01	-1.19E-01	-3.14E-01	-1.44E-01	1.76E+00	-1.47E-01	3.39E-01	6.2
2	-5.87E-01	-5.50E-01	-7.15E-01	-6.07E-01	1.92E+00	-1.12E-01	4.48E-01	6.2
3	-1.19E+00	-1.14E+00	-1.23E+00	-1.27E+00	2.13E+00	-4.33E-02	6.27E-01	6.2
4	-1.64E+00	-1.57E+00	-1.67E+00	-1.75E+00	2.20E+00	-1.46E-02	7.63E-01	6.2
5	-1.97E+00	-1.89E+00	-2.02E+00	-2.09E+00	2.23E+00	-1.49E-02	8.73E-01	6.2
7.5	-2.59E+00	-2.49E+00	-2.82E+00	-2.69E+00	2.12E+00	-8.16E-02	1.01E+00	6.2
10	-3.07E+00	-2.95E+00	-3.38E+00	-3.17E+00	1.88E+00	-1.51E-01	1.07E+00	6.2

Table 3(b) Coefficients in the attenuation relation of BSSA-2014 for Distance scaling term

Period(sec)	c1	c2	c3	Mref	Rref (km)	h (km)
0	-1.13	1.92E-01	-8.09E-03	4.5	1	4.5
0.01	-1.13	1.92E-01	-8.09E-03	4.5	1	4.5
0.02	-1.14	1.90E-01	-8.07E-03	4.5	1	4.5
0.03	-1.14	1.88E-01	-8.34E-03	4.5	1	4.49
0.05	-1.12	1.87E-01	-9.82E-03	4.5	1	4.2
0.075	-1.08	1.82E-01	-1.06E-02	4.5	1	4.04
0.1	-1.07	1.72E-01	-1.02E-02	4.5	1	4.13
0.15	-1.05	1.54E-01	-8.98E-03	4.5	1	4.39
0.2	-1.06	1.45E-01	-7.72E-03	4.5	1	4.61
0.3	-1.09	1.34E-01	-5.48E-03	4.5	1	4.93
0.4	-1.12	1.25E-01	-4.05E-03	4.5	1	5.16
0.5	-1.15	1.20E-01	-3.22E-03	4.5	1	5.34
0.75	-1.18	1.11E-01	-1.93E-03	4.5	1	5.6
1	-1.19	1.02E-01	-1.21E-03	4.5	1	5.74
1.5	-1.21	9.64E-02	-3.65E-04	4.5	1	6.18
2	-1.22	9.64E-02	0.00E+00	4.5	1	6.54
3	-1.22	9.76E-02	0.00E+00	4.5	1	6.93
4	-1.22	1.02E-01	-5.20E-05	4.5	1	7.32
5	-1.22	1.04E-01	0.00E+00	4.5	1	7.78
7.5	-1.25	1.25E-01	0.00E+00	4.5	1	9.48
10	-1.33	1.52E-01	0.00E+00	4.5	1	9.66

Table 3 (c) Coefficients in the attenuation relation of BSSA-2014 for Site term

Period (sec)	Linear Site term			Linear Site term			Basin Depth	
	c	Vc (m/s)	Vref (m/s)	f3	f4	f5	f6 (1/km)	f7
0	-6.00E-01	1500	760	0.1	-1.50E-01	-7.01E-03	-9.90E+00	-9.90E+00
0.01	-6.04E-01	1500.2	760	0.1	-1.48E-01	-7.01E-03	-9.90E+00	-9.90E+00
0.02	-5.74E-01	1500.36	760	0.1	-1.47E-01	-7.28E-03	-9.90E+00	-9.90E+00
0.03	-5.34E-01	1502.95	760	0.1	-1.55E-01	-7.35E-03	-9.90E+00	-9.90E+00
0.05	-4.58E-01	1501.42	760	0.1	-1.92E-01	-6.47E-03	-9.90E+00	-9.90E+00
0.075	-4.44E-01	1494	760	0.1	-2.35E-01	-5.73E-03	-9.90E+00	-9.90E+00
0.1	-4.87E-01	1479.12	760	0.1	-2.49E-01	-5.60E-03	-9.90E+00	-9.90E+00
0.15	-5.80E-01	1442.85	760	0.1	-2.57E-01	-5.85E-03	-9.90E+00	-9.90E+00
0.2	-6.88E-01	1392.61	760	0.1	-2.47E-01	-6.14E-03	-9.90E+00	-9.90E+00
0.3	-8.42E-01	1308.47	760	0.1	-2.19E-01	-6.70E-03	-9.90E+00	-9.90E+00
0.4	-9.11E-01	1252.66	760	0.1	-1.96E-01	-7.13E-03	-9.90E+00	-9.90E+00
0.5	-9.69E-01	1203.91	760	0.1	-1.75E-01	-7.44E-03	-9.90E+00	-9.90E+00
0.75	-1.02E+00	1147.59	760	0.1	-1.39E-01	-8.12E-03	9.23E-02	5.90E-02
1	-1.05E+00	1109.95	760	0.1	-1.05E-01	-8.44E-03	3.67E-01	2.08E-01
1.5	-1.05E+00	1072.39	760	0.1	-6.20E-02	-7.71E-03	6.38E-01	3.09E-01
2	-1.04E+00	1009.49	760	0.1	-3.61E-02	-4.79E-03	8.71E-01	3.82E-01
3	-1.01E+00	922.43	760	0.1	-1.36E-02	-1.83E-03	1.13E+00	5.16E-01
4	-9.69E-01	844.48	760	0.1	-3.21E-03	-1.52E-03	1.27E+00	6.29E-01
5	-9.20E-01	793.13	760	0.1	-2.55E-04	-1.44E-03	1.33E+00	7.38E-01
7.5	-7.77E-01	771.01	760	0.1	-5.46E-05	-1.37E-03	1.33E+00	8.09E-01
10	-6.56E-01	775	760	0.1	0.00E+00	-1.36E-03	1.18E+00	7.03E-01

Table 3 (d) Coefficients in the attenuation relation of BSSA-2014 for Aleatory Uncertainity

Period (s)	$R`_1$ (km)	R_2 (km)	DfR	DfV	V_1 (m/s)	V_2 (m/s)	ϕ_1	ϕ_2	τ_1	τ_2
0	110	270	0.1	0.07	225	300	0.695	0.495	0.398	0.348
0.01	111.67	270	0.096	0.07	225	300	0.698	0.499	0.402	0.345
0.02	113.1	270	0.092	0.03	225	300	0.702	0.502	0.409	0.346
0.03	112.13	270	0.081	0.029	225	300	0.721	0.514	0.445	0.364
0.05	97.93	270	0.063	0.03	225	300	0.753	0.532	0.503	0.426
0.075	85.99	270.04	0.064	0.022	225	300	0.745	0.542	0.474	0.466
0.1	79.59	270.09	0.087	0.014	225	300	0.728	0.541	0.415	0.458
0.15	81.33	270.16	0.12	0.015	225	300	0.72	0.537	0.354	0.388
0.2	90.91	270	0.136	0.045	225	300	0.711	0.539	0.344	0.309
0.3	103.15	268.59	0.138	0.05	225	300	0.675	0.561	0.363	0.229
0.4	106.02	266.54	0.122	0.049	225	300	0.643	0.58	0.381	0.21
0.5	105.54	265	0.109	0.06	225	300	0.615	0.599	0.41	0.224
0.75	108.39	266.51	0.1	0.07	225	300	0.581	0.622	0.457	0.266
1	116.39	270	0.098	0.02	225	300	0.553	0.625	0.498	0.298
1.5	125.38	262.41	0.104	0.01	225	300	0.532	0.619	0.525	0.315
2	130.37	240.14	0.105	0.008	225	300	0.526	0.618	0.532	0.329
3	130.36	195	0.088	0	225	300	0.534	0.619	0.537	0.344
4	129.49	199.45	0.07	0	225	300	0.536	0.616	0.543	0.349
5	130.22	230	0.061	0	225	300	0.528	0.622	0.532	0.335
7.5	130.72	250.39	0.058	0	225	300	0.512	0.634	0.511	0.27
10	130	210	0.06	0	225	300	0.51	0.604	0.487	0.239

Table 4. Coefficients of the median horizontal ground motion model (CB-2014)

T (s)	c_0	c_1	c_2	c_3	c_4	c_5	c_6	c_7	c_9
0.01	-4.365	0.97	0.533	-1.485	-0.499	-2.773	0.248	6.753	-0.214
0.02	-4.348	0.97	0.549	-1.488	-0.501	-2.772	0.247	6.502	-0.208
0.03	-4.024	0.93	0.628	-1.494	-0.517	-2.782	0.246	6.291	-0.213
0.05	-3.479	0.88	0.674	-1.388	-0.615	-2.791	0.24	6.317	-0.244
0.075	-3.293	0.90	0.726	-1.469	-0.596	-2.745	0.227	6.861	-0.266
0.1	-3.666	0.99	0.698	-1.572	-0.536	-2.633	0.21	7.294	-0.229
0.15	-4.866	1.26	0.51	-1.669	-0.49	-2.458	0.183	8.031	-0.211
0.2	-5.411	1.36	0.447	-1.75	-0.451	-2.421	0.182	8.385	-0.163
0.25	-5.962	1.45	0.274	-1.711	-0.404	-2.392	0.189	7.534	-0.15
0.3	-6.403	1.52	0.193	-1.77	-0.321	-2.376	0.195	6.99	-0.131
0.4	-7.566	1.73	-0.02	-1.594	-0.426	-2.303	0.185	7.012	-0.159
0.5	-8.379	1.87	-0.121	-1.577	-0.44	-2.296	0.186	6.902	-0.153
0.75	-9.841	2.02	-0.042	-1.757	-0.443	-2.232	0.186	5.522	-0.09
1	-11.011	2.18	-0.069	-1.707	-0.527	-2.158	0.169	5.65	-0.105
1.5	-12.469	2.27	0.047	-1.621	-0.63	-2.063	0.158	5.795	-0.058
2	-12.969	2.27	0.149	-1.512	-0.768	-2.104	0.158	6.632	-0.028
3	-13.306	2.15	0.368	-1.315	-0.89	-2.051	0.148	6.759	0
4	-14.02	2.13	0.726	-1.506	-0.885	-1.986	0.135	7.978	0
5	-14.558	2.11	1.027	-1.721	-0.878	-2.021	0.14	8.538	0
7.5	-15.509	2.22	0.169	-0.756	-1.077	-2.179	0.178	8.468	0
10	-15.975	2.13	0.367	-0.8	-1.282	-2.244	0.194	6.564	0
PGA	-4.416	0.98	0.537	-1.499	-0.496	-2.773	0.248	6.768	-0.212
PGV	-2.895	1.51	0.27	-1.299	-0.453	-2.466	0.204	5.837	-0.168

Table 4. Coefficients of the median horizontal ground motion model (CB-2014) (contd..)

T (s)	c_9	c_{10}	c_{11}	c_{12}	c_{13}	c_{14}	c_{15}	c_{16}	c_{17}
0.01	-0.214	0.72	1.094	2.191	1.416	-0.007	-0.207	0.39	0.0981
0.02	-0.208	0.73	1.149	2.189	1.453	-0.0167	-0.199	0.387	0.1009
0.03	-0.213	0.759	1.29	2.164	1.476	-0.0422	-0.202	0.378	0.1095
0.05	-0.244	0.826	1.449	2.138	1.549	-0.0663	-0.339	0.295	0.1226
0.075	-0.266	0.815	1.535	2.446	1.772	-0.0794	-0.404	0.322	0.1165
0.1	-0.229	0.831	1.615	2.969	1.916	-0.0294	-0.416	0.384	0.0998
0.15	-0.211	0.749	1.877	3.544	2.161	0.0642	-0.407	0.417	0.076
0.2	-0.163	0.764	2.069	3.707	2.465	0.0968	-0.311	0.404	0.0571
0.25	-0.15	0.716	2.205	3.343	2.766	0.1441	-0.172	0.466	0.0437
0.3	-0.131	0.737	2.306	3.334	3.011	0.1597	-0.084	0.528	0.0323
0.4	-0.159	0.738	2.398	3.544	3.203	0.141	0.085	0.54	0.0209
0.5	-0.153	0.718	2.355	3.016	3.333	0.1474	0.233	0.638	0.0092
0.75	-0.09	0.795	1.995	2.616	3.054	0.1764	0.411	0.776	-0.0082
1	-0.105	0.556	1.447	2.47	2.562	0.2593	0.479	0.771	-0.0131
1.5	-0.058	0.48	0.33	2.108	1.453	0.2881	0.566	0.748	-0.0187
2	-0.028	0.401	-0.514	1.327	0.657	0.3112	0.562	0.763	-0.0258
3	0	0.206	-0.848	0.601	0.367	0.3478	0.534	0.686	-0.0311
4	0	0.105	-0.793	0.568	0.306	0.3747	0.522	0.691	-0.0413
5	0	0	-0.748	0.356	0.268	0.3382	0.477	0.67	-0.0281
7.5	0	0	-0.664	0.075	0.374	0.3754	0.321	0.757	-0.0205
10	0	0	-0.576	-0.027	0.297	0.3506	0.174	0.621	0.0009
PGA	-0.212	0.72	1.09	2.186	1.42	-0.0064	-0.202	0.393	0.0977
PGV	-0.168	0.305	1.713	2.602	2.457	0.106	0.332	0.585	0.0517

Table 4. Coefficients of the median horizontal ground motion model (CB-2014) (contd..)

T (s)	c_{18}	c_{19}	c_{20}	$\Delta c_{20,JI}$	$\Delta c_{20,CH}$
0.01	0.0334	0.00755	-0.0055	-0.0035	0.0036
0.02	0.0327	0.00759	-0.0055	-0.0035	0.0036
0.03	0.0331	0.0079	-0.0057	-0.0034	0.0037
0.05	0.027	0.00803	-0.0063	-0.0037	0.004
0.075	0.0288	0.00811	-0.007	-0.0037	0.0039
0.1	0.0325	0.00744	-0.0073	-0.0034	0.0042
0.15	0.0388	0.00716	-0.0069	-0.003	0.0042
0.2	0.0437	0.00688	-0.006	-0.0031	0.0041
0.25	0.0463	0.00556	-0.0055	-0.0033	0.0036
0.3	0.0508	0.00458	-0.0049	-0.0035	0.0031
0.4	0.0432	0.00401	-0.0037	-0.0034	0.0028
0.5	0.0405	0.00388	-0.0027	-0.0034	0.0025
0.75	0.042	0.0042	-0.0016	-0.0032	0.0016
1	0.0426	0.00409	-0.0006	-0.003	0.0006
1.5	0.038	0.00424	0	-0.0019	0
2	0.0252	0.00448	0	-0.0005	0
3	c_{18}	0.00345	0	0	0
4	0.0334	0.00603	0	0	0
5	0.0327	0.00805	0	0	0
7.5	0.0331	0.0028	0	0	0
10	0.027	0.00458	0	0	0
PGA	0.0288	0.00757	-0.0055	-0.0035	0.0036
PGV	0.0325	0.00613	-0.0017	-0.0006	0.0017

Table 4. Coefficients of the median horizontal ground motion model (CB-2014) (contd..)

T (s)	k_1	k_2	k_3	a_1	h_1	h_2	h_3	h_5	h_6
0.01	865	-1.186	1.839	0.168	0.242	1.471	-0.714	-0.336	-0.27
0.02	865	-1.219	1.84	0.166	0.244	1.467	-0.711	-0.339	-0.263
0.03	908	-1.273	1.841	0.167	0.246	1.467	-0.713	-0.338	-0.259
0.05	1054	-1.346	1.843	0.173	0.251	1.449	-0.701	-0.338	-0.263
0.075	1086	-1.471	1.845	0.198	0.26	1.435	-0.695	-0.347	-0.219
0.1	1032	-1.624	1.847	0.174	0.259	1.449	-0.708	-0.391	-0.201
0.15	878	-1.931	1.852	0.198	0.254	1.461	-0.715	-0.449	-0.099
0.2	748	-2.188	1.856	0.204	0.237	1.484	-0.721	-0.393	-0.198
0.25	654	-2.381	1.861	0.185	0.206	1.581	-0.787	-0.339	-0.21
0.3	587	-2.518	1.865	0.164	0.21	1.586	-0.795	-0.447	-0.121
0.4	503	-2.657	1.874	0.16	0.226	1.544	-0.77	-0.525	-0.086
0.5	457	-2.669	1.883	0.184	0.217	1.554	-0.77	-0.407	-0.281
0.75	410	-2.401	1.906	0.216	0.154	1.626	-0.78	-0.371	-0.285
1	400	-1.955	1.929	0.596	0.117	1.616	-0.733	-0.128	-0.756
1.5	400	-1.025	1.974	0.596	0.117	1.616	-0.733	-0.128	-0.756
2	400	-0.299	2.019	0.596	0.117	1.616	-0.733	-0.128	-0.756
3	400	0	2.11	0.596	0.117	1.616	-0.733	-0.128	-0.756
4	400	0	2.2	0.596	0.117	1.616	-0.733	-0.128	-0.756
5	400	0	2.291	0.596	0.117	1.616	-0.733	-0.128	-0.756
7.5	400	0	2.517	0.596	0.117	1.616	-0.733	-0.128	-0.756
10	400	0	2.744	0.596	0.117	1.616	-0.733	-0.128	-0.756
PGA	865	-1.186	1.839	0.167	0.241	1.474	-0.715	-0.337	-0.27
PGV	400	-1.955	1.929	0.596	0.117	1.616	-0.733	-0.128	-0.756

Table 5. (a) Coefficient of median ground motion derived by ASK-2014

T	c_4	M_1	M_2	a_1	a_2	a_3	a_4	a_5	a_6	a_8
0.010	4.500	6.750	5.000	0.587	-0.790	0.275	-0.100	-0.410	2.154	-0.015
0.020	4.500	6.750	5.000	0.598	-0.790	0.275	-0.100	-0.410	2.146	-0.015
0.030	4.500	6.750	5.000	0.602	-0.790	0.275	-0.100	-0.410	2.157	-0.015
0.050	4.500	6.750	5.000	0.707	-0.790	0.275	-0.100	-0.410	2.085	-0.015
0.075	4.500	6.750	5.000	0.973	-0.790	0.275	-0.100	-0.410	2.029	-0.015
0.100	4.500	6.750	5.000	1.169	-0.790	0.275	-0.100	-0.410	2.041	-0.015
0.150	4.500	6.750	5.000	1.442	-0.790	0.275	-0.100	-0.410	2.121	-0.022
0.200	4.500	6.750	5.000	1.637	-0.790	0.275	-0.100	-0.410	2.224	-0.030
0.250	4.500	6.750	5.000	1.701	-0.790	0.275	-0.100	-0.410	2.312	-0.038
0.300	4.500	6.750	5.000	1.712	-0.790	0.275	-0.100	-0.410	2.338	-0.045
0.400	4.500	6.750	5.000	1.662	-0.790	0.275	-0.100	-0.410	2.469	-0.055
0.500	4.500	6.750	5.000	1.571	-0.790	0.275	-0.100	-0.410	2.559	-0.065
0.750	4.500	6.750	5.000	1.299	-0.790	0.275	-0.100	-0.410	2.682	-0.095
1.000	4.500	6.750	5.000	1.043	-0.790	0.275	-0.100	-0.410	2.763	-0.110
1.500	4.500	6.750	5.000	0.665	-0.790	0.275	-0.100	-0.410	2.836	-0.124
2.000	4.500	6.750	5.000	0.329	-0.790	0.275	-0.100	-0.410	2.897	-0.138
3.000	4.500	6.820	5.000	-0.060	-0.790	0.275	-0.100	-0.410	2.906	-0.172
4.000	4.500	6.920	5.000	-0.299	-0.790	0.275	-0.100	-0.410	2.889	-0.197
5.000	4.500	7.000	5.000	-0.562	-0.765	0.275	-0.100	-0.410	2.898	-0.218
6.000	4.500	7.060	5.000	-0.875	-0.711	0.275	-0.100	-0.410	2.896	-0.235
7.500	4.500	7.145	5.000	-1.303	-0.634	0.275	-0.100	-0.410	2.870	-0.255
10.000	4.500	7.250	5.000	-1.928	-0.529	0.275	-0.100	-0.410	2.843	-0.285
PGA	4.500	6.750	5.000	0.587	-0.790	0.275	-0.100	-0.410	2.154	-0.015
PGV	4.500	6.750	5.000	5.975	-0.919	0.275	-0.100	-0.410	2.366	-0.094

Table 5 (b) Coefficient of median ground motion derived by ASK-2014

T	a_{12}	a_{13}	a_{14}	a_{15}	a_{17}
0.01	-0.1	0.6	-0.3	1.1	-0.0072
0.02	-0.1	0.6	-0.3	1.1	-0.0073
0.03	-0.1	0.6	-0.3	1.1	-0.0075
0.05	-0.1	0.6	-0.3	1.1	-0.008
0.075	-0.1	0.6	-0.3	1.1	-0.0089
0.1	-0.1	0.6	-0.3	1.1	-0.0095
0.15	-0.1	0.6	-0.3	1.1	-0.0095
0.2	-0.1	0.6	-0.3	1.1	-0.0086
0.25	-0.1	0.6	-0.24	1.1	-0.0074
0.3	-0.1	0.6	-0.19	1.03	-0.0064
0.4	-0.1	0.58	-0.11	0.92	-0.0043
0.5	-0.1	0.56	-0.04	0.84	-0.0032
0.75	-0.1	0.53	0.07	0.68	-0.0025
1	-0.1	0.5	0.15	0.57	-0.0025
1.5	-0.1	0.42	0.27	0.42	-0.0022
2	-0.1	0.35	0.35	0.31	-0.0019
3	-0.1	0.2	0.46	0.16	-0.0015
4	-0.1	0	0.54	0.05	-0.001
5	-0.1	0	0.61	-0.04	-0.001
6	-0.2	0	0.65	-0.11	-0.001
7.5	-0.2	0	0.72	-0.19	-0.001
10	-0.2	0	0.8	-0.3	-0.001
PGA	-0.1	0.6	-0.3	1.1	-0.0072
PGV	-0.1	0.25	0.22	0.3	-0.0005

Table 5 (c). Coefficient of linear and non-linear soil response - ASK2014

T	a_{10}	V_{Lin}	b	n	c
0.01	1.735	660	-1.47	1.5	2.4
0.02	1.718	680	-1.459	1.5	2.4
0.03	1.615	770	-1.39	1.5	2.4
0.05	1.358	915	-1.219	1.5	2.4
0.075	1.258	960	-1.152	1.5	2.4
0.1	1.31	910	-1.23	1.5	2.4
0.15	1.66	740	-1.587	1.5	2.4
0.2	2.22	590	-2.012	1.5	2.4
0.25	2.77	495	-2.411	1.5	2.4
0.3	3.25	430	-2.757	1.5	2.4
0.4	3.99	360	-3.278	1.5	2.4
0.5	4.45	340	-3.599	1.5	2.4
0.75	4.75	330	-3.8	1.5	2.4
1	4.3	330	-3.5	1.5	2.4
1.5	2.6	330	-2.4	1.5	2.4
2	0.55	330	-1	1.5	2.4
3	-0.95	330	0	1.5	2.4
4	-0.95	330	0	1.5	2.4
5	-0.93	330	0	1.5	2.4
6	-0.91	330	0	1.5	2.4
7.5	-0.87	330	0	1.5	2.4
10	-0.8	330	0	1.5	2.4
0	1.735	660	-1.47	1.5	2.4
PGV	2.36	330	-2.02	1.5	2400

Table 5 (d). Coefficient for Z_1 scaling of the median ground motion- ASK2014

T	a_{43}	a_{44}	a_{45}	a_{46}
0.01	0.1	0.05	0	-0.05
0.02	0.1	0.05	0	-0.05
0.03	0.1	0.05	0	-0.05
0.05	0.1	0.05	0	-0.05
0.075	0.1	0.05	0	-0.05
0.1	0.1	0.05	0	-0.05
0.15	0.1	0.05	0	-0.05
0.2	0.1	0.05	0	-0.03
0.25	0.1	0.05	0	0
0.3	0.1	0.05	0.03	0.03
0.4	0.1	0.07	0.06	0.06
0.5	0.1	0.1	0.1	0.09
0.75	0.14	0.14	0.14	0.13
1	0.17	0.17	0.17	0.14
1.5	0.22	0.21	0.2	0.16
2	0.26	0.25	0.22	0.16
3	0.34	0.3	0.23	0.16
4	0.41	0.32	0.23	0.14
5	0.51	0.32	0.22	0.13
6	0.55	0.32	0.2	0.1
7.5	0.49	0.275	0.17	0.09
10	0.42	0.22	0.14	0.08
0	0.1	0.05	0	-0.05
PGV	0.28	0.15	0.09	0.07

Table 5(e) Coefficient for the median ground motion of other regions- ASK2014

T	a_{25}	a_{28}	a_{29}	a_{31}
0.01	-0.0015	0.0025	-0.0034	-0.1503
0.02	-0.0015	0.0024	-0.0033	-0.1479
0.03	-0.0016	0.0023	-0.0034	-0.1447
0.05	-0.002	0.0027	-0.0033	-0.1326
0.075	-0.0027	0.0032	-0.0029	-0.1353
0.1	-0.0033	0.0036	-0.0025	-0.1128
0.15	-0.0035	0.0033	-0.0025	0.0383
0.2	-0.0033	0.0027	-0.0031	0.0775
0.25	-0.0029	0.0024	-0.0036	0.0741
0.3	-0.0027	0.002	-0.0039	0.2548
0.4	-0.0023	0.001	-0.0048	0.2136
0.5	-0.002	0.0008	-0.005	0.1542
0.75	-0.001	0.0007	-0.0041	0.0787
1	-0.0005	0.0007	-0.0032	0.0476
1.5	-0.0004	0.0006	-0.002	-0.0163
2	-0.0002	0.0003	-0.0017	-0.1203
3	0	0	-0.002	-0.2719
4	0	0	-0.002	-0.2958
5	0	0	-0.002	-0.2718
6	0	0	-0.002	-0.2517
7.5	0	0	-0.002	-0.14
10	0	0	-0.002	-0.0216
0	-0.0015	0.0025	-0.0034	-0.1503
-1	-0.0001	0.0005	-0.0037	-0.1462

Table 6. Period-dependent coefficients of model ln(y_{ref}) (CY-2014)

Period (s)	c_1	c_{1a}	c_{1b}	c_{1c}	c_{1d}	c_n	c_M	c_3
PGA	-1.5065	0.1650	-0.2550	-0.1650	0.255	16.0875	4.9993	1.9636
PGV	2.3549	0.1650	-0.0626	-0.1650	0.0626	3.30240	5.4230	2.3152
0.01	-1.5065	0.1650	-0.2550	-0.1650	0.2550	16.0875	4.9993	1.9636
0.02	-1.4798	0.1650	-0.2550	-0.1650	0.2550	15.7118	4.9993	1.9636
0.03	-1.2972	0.1650	-0.2550	-0.1650	0.2550	15.8819	4.9993	1.9636
0.04	-1.1007	0.1650	-0.2550	-0.1650	0.2550	16.4556	4.9993	1.9636
0.05	-0.9292	0.1650	-0.2550	-0.1650	0.2550	17.6453	4.9993	1.9636
0.075	-0.6580	0.1650	-0.2540	-0.1650	0.2540	20.1772	5.0031	1.9636
0.1	-0.5613	0.1650	-0.2530	-0.1650	0.2530	19.9992	5.0172	1.9636
0.12	-0.5342	0.1650	-0.2520	-0.1650	0.2520	18.7106	5.0315	1.9795
0.15	-0.5462	0.1650	-0.2500	-0.1650	0.2500	16.6246	5.0547	2.0362
0.17	-0.5858	0.1650	-0.2480	-0.1650	0.2480	15.3709	5.0704	2.0823
0.2	-0.6798	0.1650	-0.2449	-0.1650	0.2449	13.7012	5.0939	2.1521
0.25	-0.8663	0.1650	-0.2382	-0.1650	0.2382	11.2667	5.1315	2.2574
0.3	-1.0514	0.1650	-0.2313	-0.1650	0.2313	9.19080	5.1670	2.3440
0.4	-1.3794	0.1650	-0.2146	-0.1650	0.2146	6.54590	5.2317	2.4709
0.5	-1.6508	0.1650	-0.1972	-0.1650	0.1972	5.23050	5.2893	2.5567
0.75	-2.1511	0.1650	-0.1620	-0.1650	0.1620	3.78960	5.4109	2.6812
1	-2.5365	0.1650	-0.1400	-0.1650	0.1400	3.30240	5.5106	2.7474
1.5	-3.0686	0.1650	-0.1184	-0.1650	0.1184	2.84980	5.6705	2.8161
2	-3.4148	0.1645	-0.1100	-0.1645	0.1100	2.54170	5.7981	2.8514
3	-3.9013	0.1168	-0.1040	-0.1168	0.1040	2.14880	5.9983	2.8875
4	-4.2466	0.0732	-0.1020	-0.0732	0.1020	1.89570	6.1552	2.9058
5	-4.5143	0.0484	-0.1010	-0.0484	0.1010	1.72280	6.2856	2.9169
7.5	-5.0009	0.0220	-0.1010	-0.0220	0.1010	1.57370	6.5428	2.9320
10	-5.3461	0.0124	-0.1000	-0.0124	0.1000	1.52650	6.7415	2.9396

Table 6. Period-dependent coefficients of model ln(*yref*) (CY-2014) (contd..)

Period (s)	c_5	c_{HM}	c_6	c_7	c_{7b}	c_8	c_{8b}
PGA	6.4551	3.0956	0.4908	0.0352	0.0462	0.0000	0.4833
PGV	5.8096	3.0514	0.4407	0.0324	0.0097	0.2154	5.0000
0.01	6.4551	3.0956	0.4908	0.0352	0.0462	0.0000	0.4833
0.02	6.4551	3.0963	0.4925	0.0352	0.0472	0.0000	1.2144
0.03	6.4551	3.0974	0.4992	0.0352	0.0533	0.0000	1.6421
0.04	6.4551	3.0988	0.5037	0.0352	0.0596	0.0000	1.9456
0.05	6.4551	3.1011	0.5048	0.0352	0.0639	0.0000	2.1810
0.075	6.4551	3.1094	0.5048	0.0352	0.063	0.0000	2.6087
0.1	6.8305	3.2381	0.5048	0.0352	0.0532	0.0000	2.9122
0.12	7.1333	3.3407	0.5048	0.0352	0.0452	0.0000	3.1045
0.15	7.3621	3.4300	0.5045	0.0352	0.0345	0.0000	3.3399
0.17	7.4365	3.4688	0.5036	0.0352	0.0283	0.0000	3.4719
0.2	7.4972	3.5146	0.5016	0.0352	0.0202	0.0000	3.6434
0.25	7.5416	3.5746	0.4971	0.0352	0.009	0.0000	3.8787
0.3	7.5600	3.6232	0.4919	0.0352	-0.0004	0.0000	4.0711
0.4	7.5735	3.6945	0.4807	0.0352	-0.0155	0.0000	4.3745
0.5	7.5778	3.7401	0.4707	0.0352	-0.0278	0.0991	4.6099
0.75	7.5808	3.7941	0.4575	0.0352	-0.0477	0.1982	5.0376
1	7.5814	3.8144	0.4522	0.0352	-0.0559	0.2154	5.3411
1.5	7.5817	3.8284	0.4501	0.0352	-0.063	0.2154	5.7688
2	7.5818	3.8330	0.4500	0.0352	-0.0665	0.2154	6.0723
3	7.5818	3.8361	0.4500	0.0160	-0.0516	0.2154	6.5000
4	7.5818	3.8369	0.4500	0.0062	-0.0448	0.2154	6.8035
5	7.5818	3.8376	0.4500	0.0029	-0.0424	0.2154	7.0389
7.5	7.5818	3.8380	0.4500	0.0007	-0.0348	0.2154	7.4666
10	7.5818	3.8380	0.4500	0.0003	-0.0253	0.2154	7.7700

Table 6. Period-dependent coefficients of model ln(*yref*) (CY-2014) (contd..)

Period(s)	c_9	c_{9a}	c_{9b}	c_{11b}	c_{g1}	c_{g2}	c_{g3}
PGA	0.9228	0.1202	6.8607	-0.4536	-0.00715	-0.00676	4.2542
PGV	0.3079	0.1000	6.5000	-0.3834	-0.00185	-0.00740	4.3439
0.01	0.9228	0.1202	6.8607	-0.4536	-0.00715	-0.00676	4.2542
0.02	0.9296	0.1217	6.8697	-0.4536	-0.00725	-0.00676	4.2386
0.03	0.9396	0.1194	6.9113	-0.4536	-0.00787	-0.00676	4.2519
0.04	0.9661	0.1166	7.0271	-0.4536	-0.00832	-0.00676	4.2960
0.05	0.9794	0.1176	7.0959	-0.4536	-0.00874	-0.00676	4.3578
0.075	1.0260	0.1171	7.3298	-0.4536	-0.00954	-0.00619	4.5455
0.1	1.0177	0.1146	7.2588	-0.4536	-0.00983	-0.00533	4.7603
0.12	1.0008	0.1128	7.2372	-0.4536	-0.00991	-0.00473	4.8963
0.15	0.9801	0.1106	7.2109	-0.4536	-0.00990	-0.00381	5.0644
0.17	0.9652	0.1150	7.2491	-0.4536	-0.00979	-0.00328	5.1371
0.2	0.9459	0.1208	7.2988	-0.4440	-0.00951	-0.00269	5.1880
0.25	0.9196	0.1208	7.3691	-0.3539	-0.00892	-0.00213	5.2164
0.3	0.8829	0.1175	6.8789	-0.2688	-0.00825	-0.00181	5.1954
0.4	0.8302	0.1060	6.5334	-0.1793	-0.00727	-0.00127	5.0899
0.5	0.7884	0.1061	6.5260	-0.1428	-0.00649	-0.00107	4.7854
0.75	0.6754	0.1000	6.5000	-0.1138	-0.00515	-0.00112	4.3304
1	0.6196	0.1000	6.5000	-0.1062	-0.00428	-0.00120	4.1667
1.5	0.5101	0.1000	6.5000	-0.102	-0.00298	-0.00168	4.0029
2	0.3917	0.1000	6.5000	-0.1009	-0.00230	-0.00235	3.8949
3	0.1244	0.1000	6.5000	-0.1003	-0.00134	-0.00331	3.7928
4	0.0086	0.1000	6.5000	-0.1001	-0.00108	-0.00357	3.7443
5	0.0000	0.1000	6.5000	-0.1001	-0.00101	-0.00364	3.7090
7.5	0.0000	0.1000	6.5000	-0.1000	-0.00096	-0.00369	3.6632
10	0.0000	0.1000	6.5000	-0.1000	-0.00095	-0.00370	3.6230

Table 7. Coefficients of site response model for ln(y) CY-2014

Period(s)	ϕ_1	ϕ_2	ϕ_3	ϕ_4	ϕ_5	ϕ_6
PGA	-0.5210	-0.1417	-0.00701	0.102151	0	300
PGV	-0.7936	-0.0699	-0.00844	5.410000	0.0202	300
0.01	-0.5210	-0.1417	-0.00701	0.102151	0.0000	300
0.02	-0.5055	-0.1364	-0.00728	0.108360	0.0000	300
0.03	-0.4368	-0.1403	-0.00735	0.119888	0.0000	300
0.04	-0.3752	-0.1591	-0.00698	0.133641	0.0000	300
0.05	-0.3469	-0.1862	-0.00647	0.148927	0.0000	300
0.075	-0.3747	-0.2538	-0.00573	0.190596	0.0000	300
0.1	-0.4440	-0.2943	-0.00560	0.230662	0.0000	300
0.12	-0.4895	-0.3077	-0.00570	0.253169	0.0000	300
0.15	-0.5477	-0.3113	-0.00585	0.266468	0.0000	300
0.17	-0.5922	-0.3062	-0.00596	0.265060	0.0000	300
0.2	-0.6693	-0.2927	-0.00614	0.255253	0.0000	300
0.25	-0.7766	-0.2662	-0.00644	0.231541	0.0000	300
0.3	-0.8501	-0.2405	-0.00670	0.207277	0.0010	300
0.4	-0.9431	-0.1975	-0.00713	0.165464	0.0040	300
0.5	-1.0044	-0.1633	-0.00744	0.133828	0.0100	300
0.75	-1.0602	-0.1028	-0.00812	0.085153	0.0340	300
1	-1.0941	-0.0699	-0.00844	0.058595	0.0670	300
1.5	-1.1142	-0.0425	-0.00771	0.031787	0.1430	300
2	-1.1154	-0.0302	-0.00479	0.019716	0.2030	300
3	-1.1081	-0.0129	-0.00183	0.009643	0.2770	300
4	-1.0603	-0.0016	-0.00152	0.005379	0.3090	300
5	-0.9872	0.0000	-0.00144	0.003223	0.3210	300
7.5	-0.8274	0.0000	-0.00137	0.001134	0.3290	300
10	-0.7053	0.0000	-0.00136	0.000515	0.3300	300

Table 8. Site classification based on soil properties, BNBC-2012

Site Class	Description of soil profile upto 30 meters depth	Average Soil Properties in top 30 meters		
		Shear wave velocity, $\bar{V}s$ (m/s)	SPT Value, $\bar{N}$ (blows/30cm)	Undrained shear strength, $\bar{S}_u$ (kPa)
SA	Rock or other rock-like geological formation, including at most 5 m of weaker material at the surface	>800	--	--
SB	Deposits of very dense sand, gravel, or very stiff clay, at least several tens of meters in thickness, characterised by a gradual increase of mechanical properties with depth	360-800	>50	>250
SC	Deep deposits of dense or medium dense sand, gravel or stiff clay with thickness from several tens to many hundreds of meters	180-360	15-50	70-250
SD	Deposits of loose-to-medium cohesionless soil (with or without some soft cohesive layers), or of predominantly soft-to firm cohesive soil.	<180	<15	<70
SE	A soil profile consisting of a surface alluvium layer with V_s values of type SC or SD and thickness varying between about 5m and 20m, underlain by stiffer material with V_s>800m/s	--	--	--
S_1	Deposits consisting, or containing a layer at laeast 10 m thick, of soft clays/silts with a high plasticity index (PI>40) aand high water content	<100 (indicative)	--	10-20
S_2	Deposits of liquifiable soils of sensitive clays, or any other soil profile not included in types SA to SE or S_1	--	--	--

Table 9. **Site dependent soil factor and other parameters defining eleastic response spectrum, BNBC-2012**

Soil Type	S	T_B	T_C	T_D
SA	1.00	0.15	0.40	2.00
SB	1.20	0.15	0.50	2.00
SC	1.15	0.20	0.60	2.00
SD	1.35	0.20	0.80	2.00
SE	1.40	0.15	0.50	2.00

Table 10. Response spectra according to Bangladesh National Building code (BNBC) for different percentage damping, with Z=0.12, 'SD' type soil class and I and R considered as 1, at BIFPCL, Maitree site, Bagerhat

Natural period (sec)	BNBC different percentage of damping							
	0.8%	1%	1.6%	2%	3%	5%	7%	10%
0.000	0.108	0.108	0.108	0.108	0.108	0.108	0.108	0.108
0.010	0.120	0.120	0.119	0.119	0.118	0.116	0.115	0.114
0.015	0.126	0.126	0.125	0.124	0.123	0.120	0.118	0.116
0.020	0.133	0.132	0.130	0.129	0.127	0.124	0.122	0.119
0.030	0.145	0.144	0.142	0.140	0.137	0.132	0.129	0.125
0.040	0.157	0.156	0.153	0.151	0.147	0.140	0.136	0.130
0.050	0.170	0.168	0.164	0.162	0.156	0.149	0.143	0.136
0.060	0.182	0.180	0.175	0.172	0.166	0.157	0.150	0.142
0.075	0.200	0.198	0.192	0.189	0.181	0.169	0.160	0.150
0.090	0.219	0.216	0.209	0.205	0.195	0.181	0.170	0.159
0.100	0.231	0.228	0.220	0.215	0.205	0.189	0.177	0.164
0.150	0.293	0.288	0.276	0.269	0.253	0.230	0.212	0.192
0.200	0.355	0.349	0.332	0.323	0.302	0.270	0.246	0.220
0.300	0.355	0.349	0.332	0.323	0.302	0.270	0.246	0.220
0.400	0.355	0.349	0.332	0.323	0.302	0.270	0.246	0.220
0.500	0.355	0.349	0.332	0.323	0.302	0.270	0.246	0.220
0.600	0.355	0.349	0.332	0.323	0.302	0.270	0.246	0.220
0.700	0.355	0.349	0.332	0.323	0.302	0.270	0.246	0.220
0.750	0.355	0.349	0.332	0.323	0.302	0.270	0.246	0.220
0.800	0.355	0.349	0.332	0.323	0.302	0.270	0.246	0.220
0.900	0.315	0.310	0.295	0.287	0.268	0.240	0.219	0.196
1.000	0.284	0.279	0.266	0.258	0.241	0.216	0.197	0.176
1.200	0.236	0.232	0.222	0.215	0.201	0.180	0.164	0.147
1.500	0.189	0.186	0.177	0.172	0.161	0.144	0.131	0.118
2.000	0.142	0.139	0.133	0.129	0.121	0.108	0.099	0.088
2.500	0.091	0.089	0.085	0.083	0.077	0.069	0.063	0.056
3.000	0.063	0.062	0.059	0.057	0.054	0.048	0.044	0.039
4.000	0.035	0.035	0.033	0.032	0.030	0.027	0.025	0.022

Table 11. Response spectra according to Bangladesh National Building code (BNBC) for 5% damping, with Z=0.12, 'SD' type soil class and I and R considered as 1, and according to Deterministic Seismic Hazard Analysis at BIFPCL, Maitree site, Bagerhat

Natural period (sec)	BNBC (g) 5% damping	DSHA (Mw 7.5, R= 106 km)			
		ASK (2014)	BSSA (2014)	CB (2014)	CY (2014)
0.000	0.108	0.069	0.074	0.058	0.089
0.010	0.116	0.069	0.075	0.059	0.089
0.015	0.120	0.069	0.072	0.058	0.089
0.020	0.124	0.069	0.069	0.058	0.089
0.030	0.132	0.070	0.065	0.058	0.089
0.040	0.140	0.074	0.064	0.058	0.089
0.050	0.149	0.077	0.063	0.059	0.090
0.060	0.157	0.082	0.068	0.063	0.099
0.075	0.169	0.089	0.075	0.069	0.111
0.090	0.181	0.101	0.087	0.077	0.125
0.100	0.189	0.109	0.095	0.082	0.135
0.150	0.229	0.167	0.129	0.096	0.167
0.200	0.270	0.211	0.158	0.114	0.199
0.300	0.270	0.253	0.193	0.165	0.236
0.400	0.270	0.272	0.191	0.172	0.239
0.500	0.270	0.269	0.181	0.172	0.232
0.600	0.270	0.242	0.159	0.161	0.214
0.700	0.270	0.222	0.143	0.152	0.199
0.750	0.270	0.214	0.136	0.148	0.193
0.800	0.270	0.202	0.130	0.140	0.185
0.900	0.240	0.183	0.120	0.126	0.171
1.000	0.216	0.167	0.111	0.115	0.160
1.200	0.180	0.146	0.095	0.103	0.139
1.500	0.144	0.124	0.079	0.089	0.117
2.000	0.108	0.089	0.060	0.066	0.092
2.500	0.069	0.070	0.047	0.052	0.072
3.000	0.048	0.058	0.039	0.043	0.059
4.000	0.027	0.043	0.029	0.029	0.036

Table 12. Response spectra according to Bangladesh National Building code (BNBC) for 5% damping, with Z=0.12, 'SD' type soil class and I and R considered as 1, and (2/3) of UHRS (from PSHA analysis) corresponding to 2500yrs RP at BIFPCL, Maitree site, Bagerhat

Natural period (sec)	BNBC (g) 5% damping	UHRS			
		ASK (2014) (2/3)×2500yrs RP (g)	BSSA (2014) (2/3)×2500yrs RP (g)	CB (2014) (2/3)×2500yrs RP (g)	CY (2014) (2/3)×2500yrs RP (g)
0.000	0.108	0.067	0.080	0.056	0.073
0.010	0.116	0.067	0.080	0.056	0.073
0.015	0.120	0.068	0.080	0.056	0.073
0.020	0.124	0.068	0.080	0.056	0.073
0.030	0.132	0.069	0.078	0.057	0.074
0.040	0.140	0.074	0.079	0.059	0.076
0.050	0.149	0.078	0.081	0.062	0.078
0.060	0.157	0.084	0.092	0.069	0.086
0.075	0.169	0.092	0.109	0.080	0.098
0.090	0.181	0.106	0.133	0.093	0.110
0.100	0.189	0.115	0.150	0.102	0.119
0.150	0.229	0.176	0.206	0.126	0.151
0.200	0.270	0.218	0.230	0.145	0.184
0.300	0.270	0.250	0.262	0.195	0.225
0.400	0.270	0.259	0.248	0.197	0.230
0.500	0.270	0.249	0.229	0.196	0.226
0.600	0.270	0.225	0.207	0.188	0.210
0.700	0.270	0.201	0.184	0.180	0.194
0.750	0.270	0.189	0.173	0.176	0.186
0.800	0.270	0.180	0.168	0.168	0.179
0.900	0.240	0.164	0.158	0.152	0.166
1.000	0.216	0.147	0.148	0.137	0.152
1.200	0.180	0.131	0.128	0.120	0.135
1.500	0.144	0.108	0.097	0.096	0.109
2.000	0.108	0.078	0.068	0.066	0.084
2.500	0.069	0.063	0.053	0.053	0.068
3.000	0.048	0.048	0.039	0.040	0.051
4.000	0.027	0.034	0.026	0.025	0.030

Table 13. The Damping correction factor applied on the 2/3 UHRS(2500yrs RP) and DSHA values(Cameron and Green (2007))

Damping / Time period	0.8%	1%	1.6%	2%	3%	5%	7%	10%
0	1	1	1	1	1	1	1	1
0.01	1.006	1.006	1.007	1.008	1.006	1	0.998	0.995
0.015	1.008	1.009	1.011	1.012	1.009	1	0.997	0.993
0.02	1.011	1.012	1.014	1.016	1.012	1	0.996	0.991
0.03	1.017	1.018	1.022	1.024	1.018	1	0.993	0.986
0.04	1.022	1.024	1.029	1.032	1.024	1	0.991	0.982
0.05	1.028	1.030	1.036	1.040	1.030	1	0.989	0.977
0.06	1.082	1.080	1.071	1.065	1.049	1	0.982	0.964
0.075	1.164	1.154	1.124	1.104	1.077	1	0.973	0.946
0.09	1.246	1.228	1.176	1.142	1.106	1	0.963	0.927
0.1	1.300	1.278	1.211	1.167	1.125	1	0.956	0.914
0.15	1.457	1.420	1.308	1.233	1.173	1	0.932	0.867
0.2	1.615	1.562	1.404	1.299	1.221	1	0.908	0.819
0.3	1.674	1.615	1.439	1.322	1.237	1	0.897	0.800
0.4	1.673	1.615	1.440	1.324	1.238	1	0.894	0.791
0.5	1.673	1.615	1.442	1.326	1.239	1	0.891	0.782
0.6	1.705	1.643	1.456	1.331	1.243	1	0.889	0.778
0.7	1.738	1.671	1.470	1.337	1.247	1	0.886	0.773
0.75	1.754	1.685	1.478	1.339	1.249	1	0.885	0.771
0.8	1.770	1.699	1.485	1.342	1.250	1	0.884	0.769
0.9	1.725	1.659	1.459	1.327	1.238	1	0.886	0.769
1	1.679	1.618	1.434	1.311	1.226	1	0.888	0.769
1.2	1.619	1.565	1.402	1.294	1.213	1	0.887	0.770
1.5	1.598	1.547	1.395	1.294	1.214	1	0.893	0.782
2	1.531	1.487	1.354	1.266	1.192	1	0.897	0.791
2.5	1.515	1.474	1.350	1.268	1.194	1	0.900	0.797
3	1.498	1.460	1.346	1.270	1.197	1	0.903	0.803
4	1.430	1.394	1.287	1.216	1.155	1	0.910	0.811

Table 14 Comparison of response spectra according to Bangladesh National Building code (BNBC) for 5% damping, with Z=0.12, 'SD' type soil class and I and R considered as 1, with maximum values obtained from DSHA and (2/3) of UHRS (PSHA analysis) corresponding to 2500yrs RP at BIFPCL, Maitree site, Bagerhat

Natural period (sec)	BNBC (g) 5% damping	DSHA (g)	(2/3)UHRS×2500yrs RP (g)
0.000	0.108	0.089	0.080
0.010	0.116	0.089	0.080
0.015	0.120	0.089	0.080
0.020	0.124	0.089	0.080
0.030	0.132	0.089	0.078
0.040	0.140	0.089	0.079
0.050	0.149	0.090	0.081
0.060	0.157	0.099	0.092
0.075	0.169	0.111	0.109
0.090	0.181	0.125	0.133
0.100	0.189	0.135	0.150
0.150	0.229	0.167	0.206
0.200	0.270	0.211	0.230
0.300	0.270	0.253	0.262
0.400	0.270	0.272	0.259
0.500	0.270	0.269	0.249
0.600	0.270	0.242	0.225
0.700	0.270	0.222	0.201
0.750	0.270	0.214	0.189
0.800	0.270	0.202	0.180
0.900	0.240	0.183	0.166
1.000	0.216	0.167	0.152
1.200	0.180	0.146	0.135
1.500	0.144	0.124	0.109
2.000	0.108	0.092	0.084
2.500	0.069	0.072	0.068
3.000	0.048	0.059	0.051
4.000	0.027	0.043	0.034

Table 15. Recommended values of response spectra for different damping percentage, at BIFPCL, Maitree site, Bagerhat

Natural period (sec)	viscous damping ratios							
	0.8%	**1%**	**1.6%**	**2%**	**3%**	**5%**	**7%**	**10%**
0.000	**0.108**	**0.108**	**0.108**	**0.108**	**0.108**	**0.108**	**0.108**	**0.108**
0.010	**0.125**	**0.125**	**0.122**	**0.121**	**0.119**	**0.116**	**0.115**	**0.114**
0.015	**0.134**	**0.133**	**0.129**	**0.127**	**0.125**	**0.120**	**0.118**	**0.116**
0.020	**0.143**	**0.141**	**0.136**	**0.133**	**0.131**	**0.124**	**0.122**	**0.119**
0.030	**0.160**	**0.158**	**0.151**	**0.146**	**0.142**	**0.133**	**0.129**	**0.125**
0.040	**0.177**	**0.174**	**0.165**	**0.158**	**0.154**	**0.141**	**0.136**	**0.130**
0.050	**0.195**	**0.191**	**0.179**	**0.171**	**0.165**	**0.149**	**0.143**	**0.136**
0.060	**0.212**	**0.207**	**0.193**	**0.184**	**0.177**	**0.157**	**0.150**	**0.142**
0.075	**0.238**	**0.232**	**0.214**	**0.202**	**0.194**	**0.169**	**0.160**	**0.150**
0.090	**0.264**	**0.257**	**0.236**	**0.221**	**0.211**	**0.182**	**0.170**	**0.159**
0.100	**0.281**	**0.273**	**0.250**	**0.234**	**0.222**	**0.190**	**0.177**	**0.164**
0.150	**0.368**	**0.356**	**0.321**	**0.297**	**0.279**	**0.231**	**0.212**	**0.192**
0.200	**0.455**	**0.439**	**0.391**	**0.360**	**0.336**	**0.272**	**0.246**	**0.220**
0.300	**0.455**	**0.439**	**0.391**	**0.360**	**0.336**	**0.272**	**0.246**	**0.220**
0.400	**0.455**	**0.439**	**0.391**	**0.360**	**0.336**	**0.272**	**0.246**	**0.220**
0.500	**0.455**	**0.439**	**0.391**	**0.360**	**0.336**	**0.272**	**0.246**	**0.220**
0.600	**0.455**	**0.439**	**0.391**	**0.360**	**0.336**	**0.272**	**0.246**	**0.220**
0.700	**0.455**	**0.439**	**0.391**	**0.360**	**0.336**	**0.272**	**0.246**	**0.220**
0.750	**0.455**	**0.439**	**0.391**	**0.360**	**0.336**	**0.272**	**0.246**	**0.220**
0.800	**0.455**	**0.439**	**0.391**	**0.360**	**0.336**	**0.272**	**0.246**	**0.220**
0.900	**0.378**	**0.372**	**0.355**	**0.316**	**0.295**	**0.240**	**0.219**	**0.196**
1.000	**0.340**	**0.335**	**0.319**	**0.284**	**0.266**	**0.216**	**0.197**	**0.176**
1.200	**0.284**	**0.279**	**0.266**	**0.237**	**0.221**	**0.180**	**0.164**	**0.147**
1.500	**0.227**	**0.223**	**0.213**	**0.189**	**0.177**	**0.144**	**0.131**	**0.118**
2.000	**0.142**	**0.139**	**0.133**	**0.129**	**0.121**	**0.108**	**0.099**	**0.088**
2.500	**0.108**	**0.105**	**0.097**	**0.091**	**0.085**	**0.072**	**0.064**	**0.057**
3.000	**0.088**	**0.085**	**0.079**	**0.074**	**0.070**	**0.059**	**0.053**	**0.047**
4.000	**0.061**	**0.060**	**0.055**	**0.052**	**0.050**	**0.043**	**0.039**	**0.035**

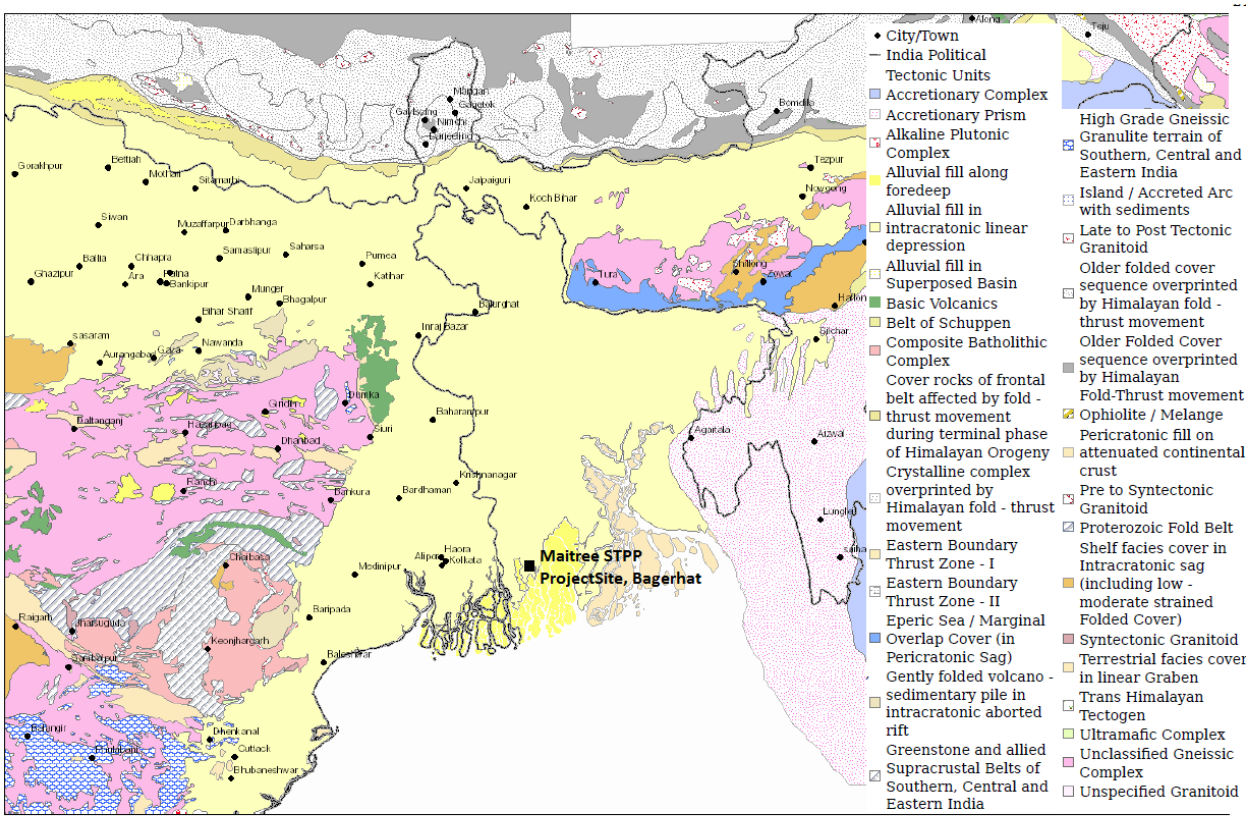

Figure 1. Geological Map of the region (GSI-2000)

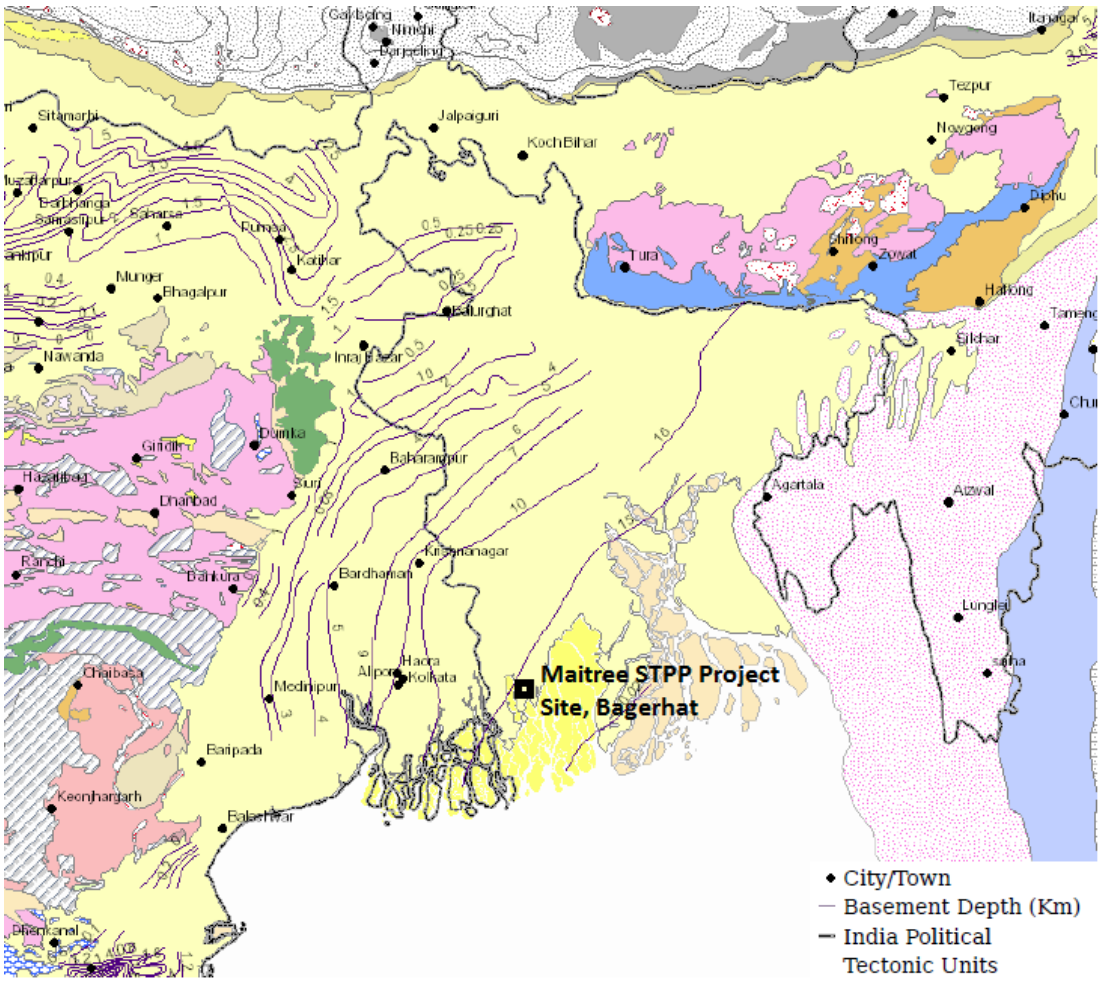

Figure 2. The Geological map of the region along with Basement depth. (GSI 2000)

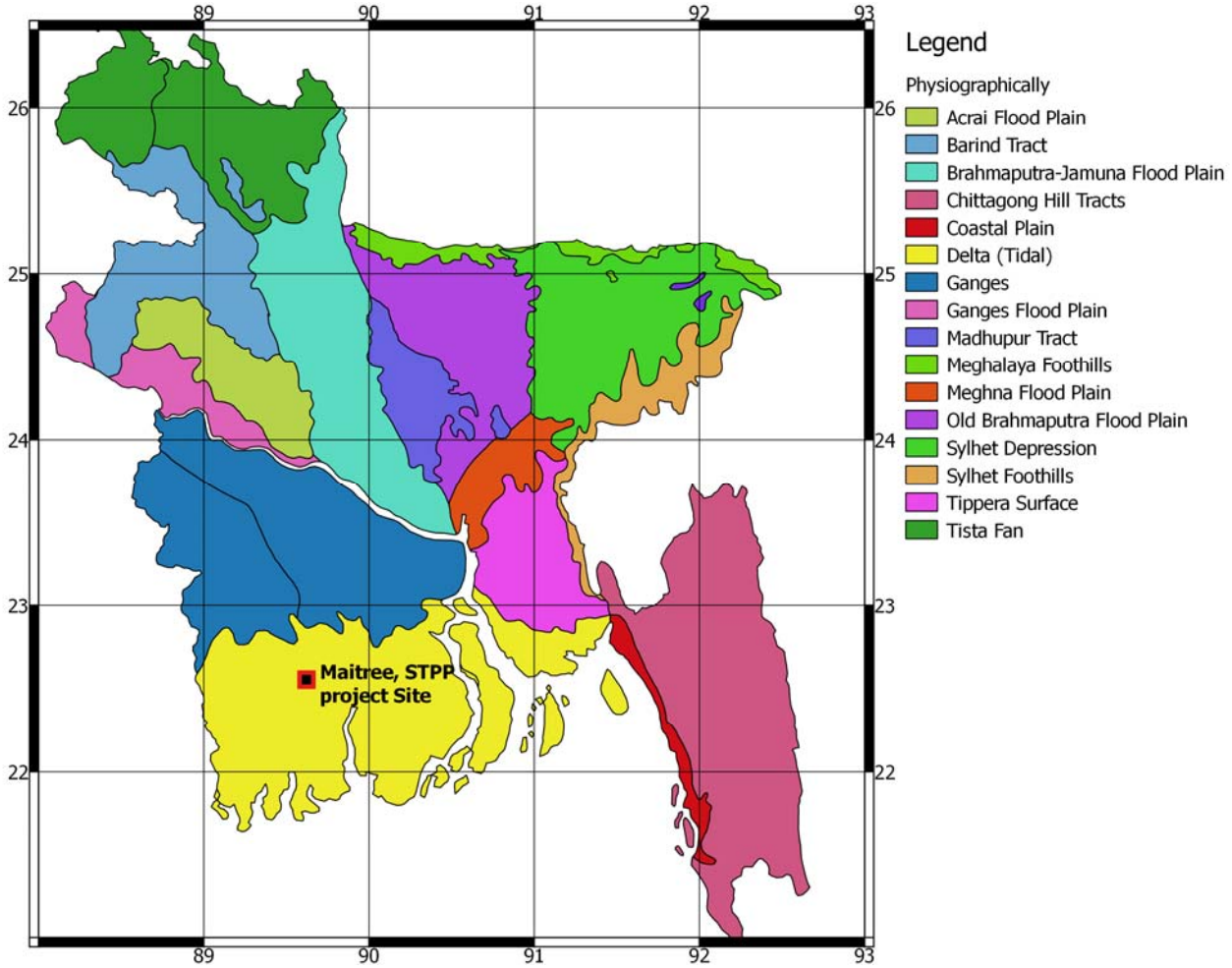

Figure 3. Physiogeographycal description of Bangladesh (Persits *et al.* 1997, updated on 2001(https://pubs.usgs.gov/of/1997/ofr-97-470/OF97-470H/))

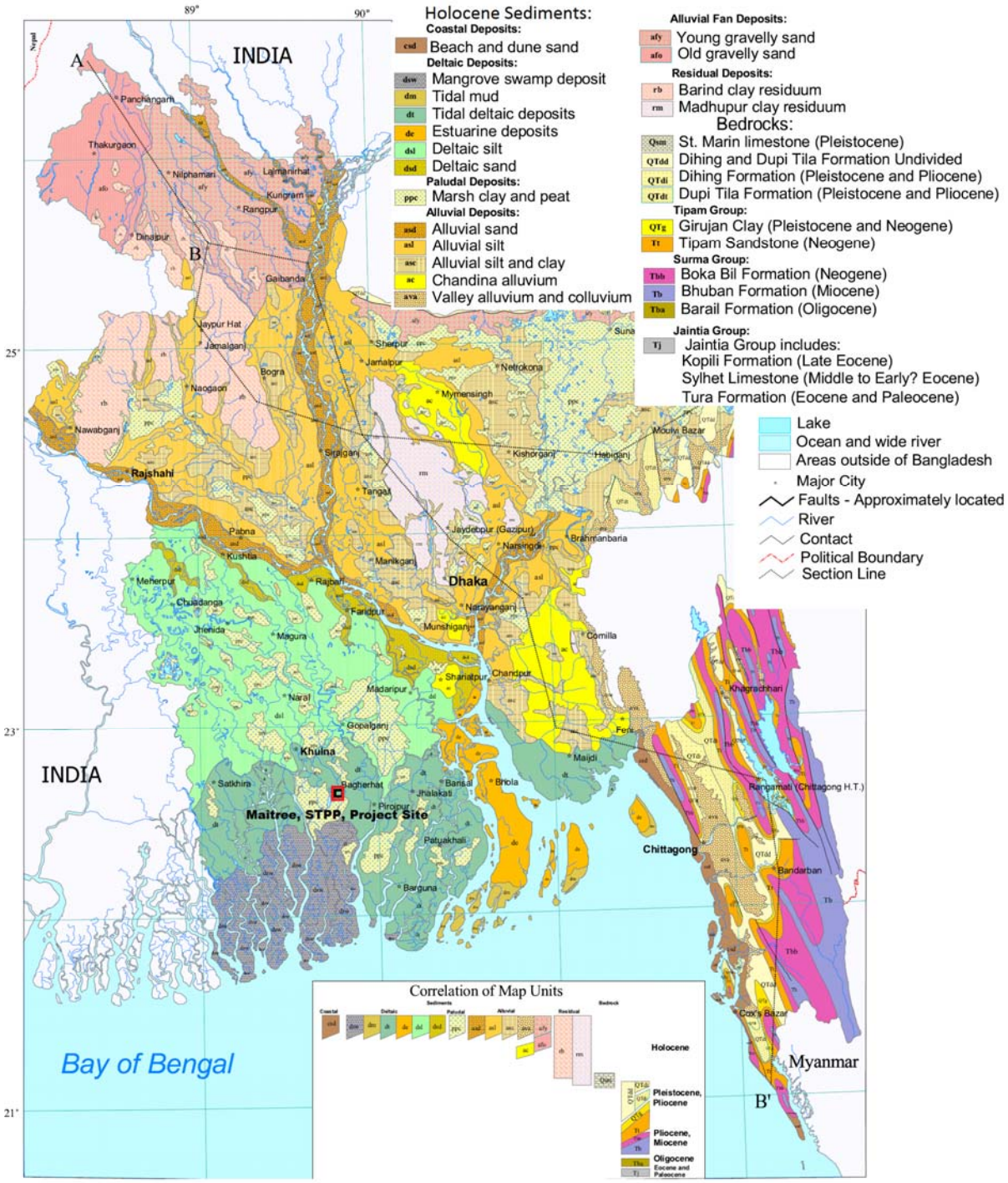

Figure 4. Detailed geological map of Bangladesh (Geological survey of Bangladesh - GSB)

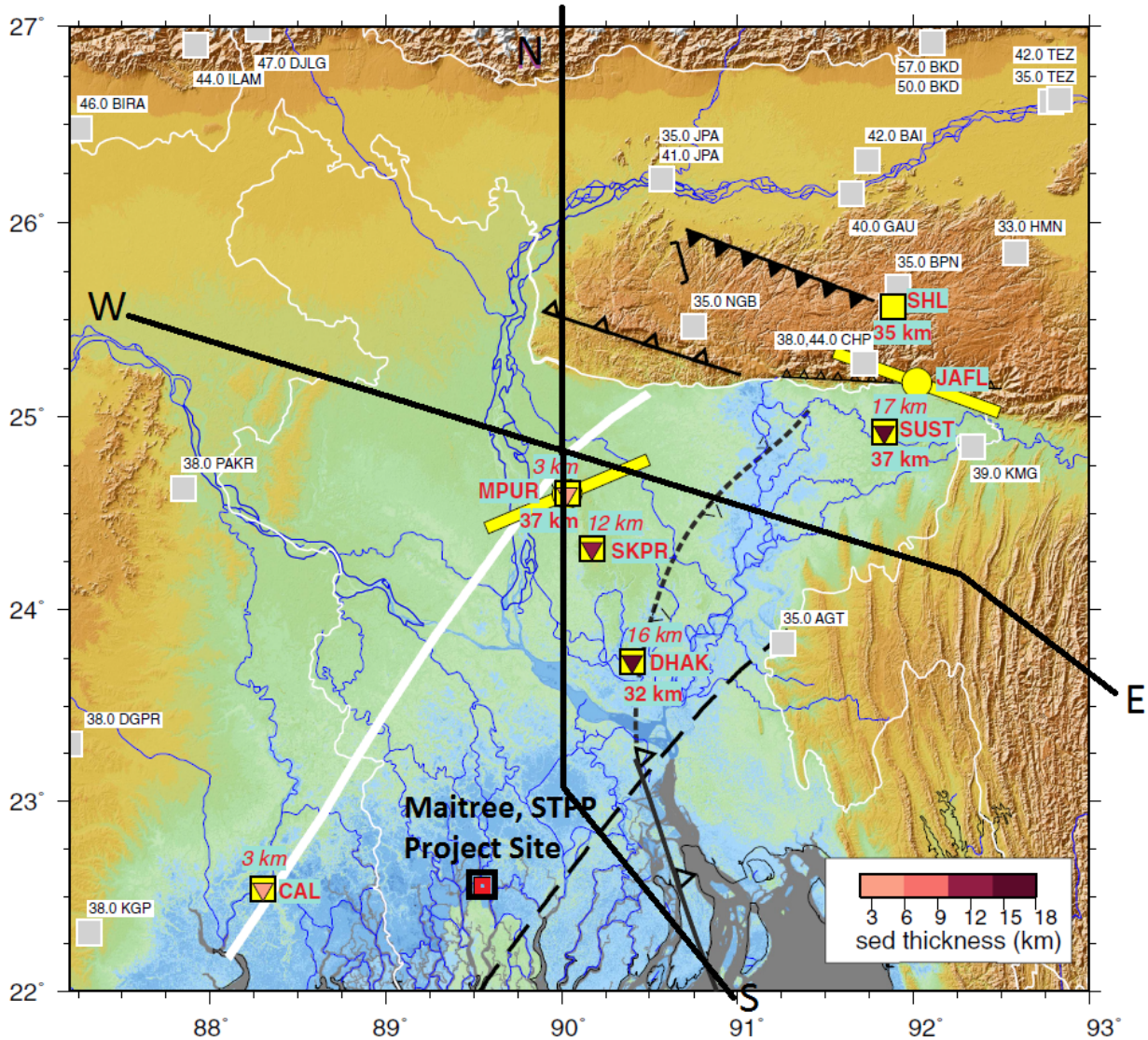

Figure 5. Sedimentary thickness obtained by reversion of receiver functions. (Singh *et al.* (2016)). The inverted triangle are the stations consdered with sediment depth obtained written on top in italics. The crustal thickness obtained are marked on grey squares.

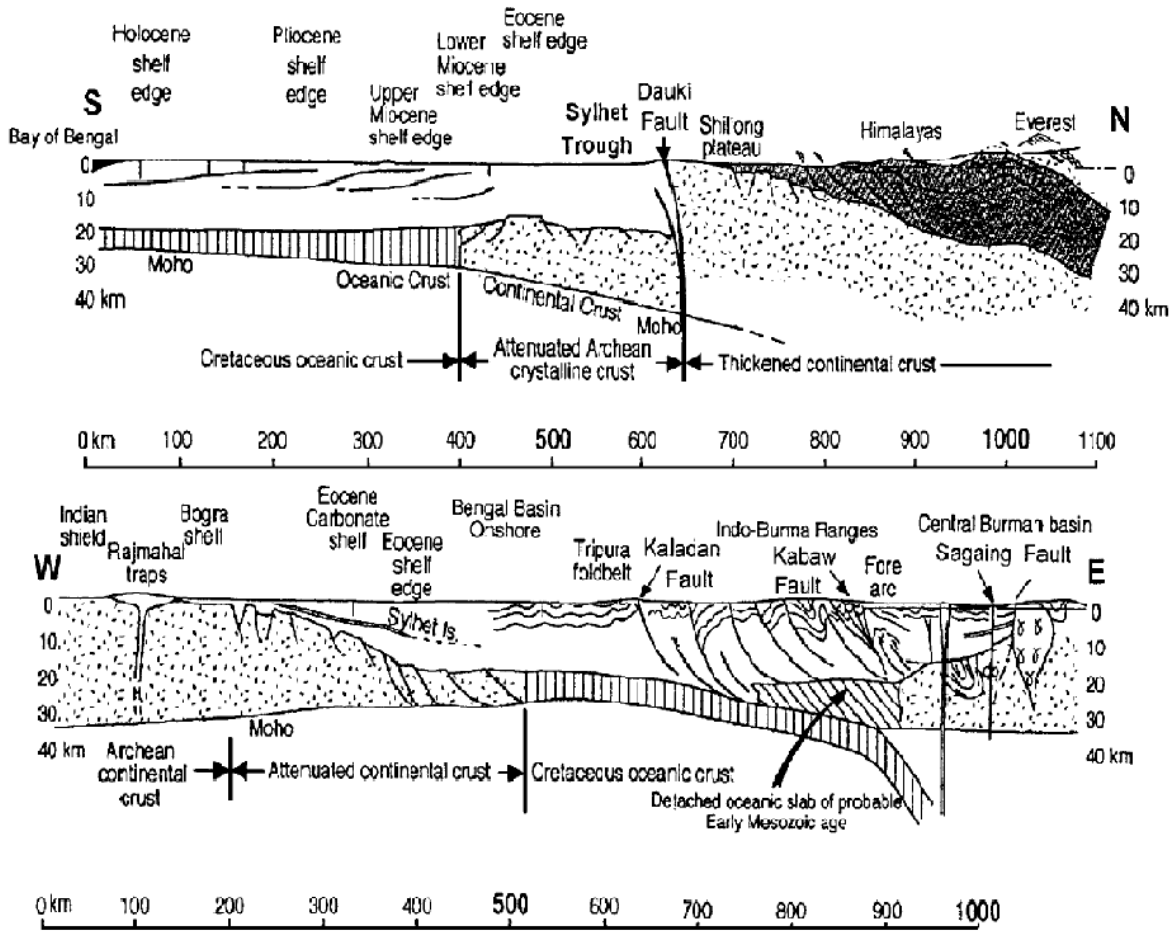

Figure 6. NS and EW sections through the region, indicating the variation of crustal thickness and the soil deposits (Alam et al. (2003))

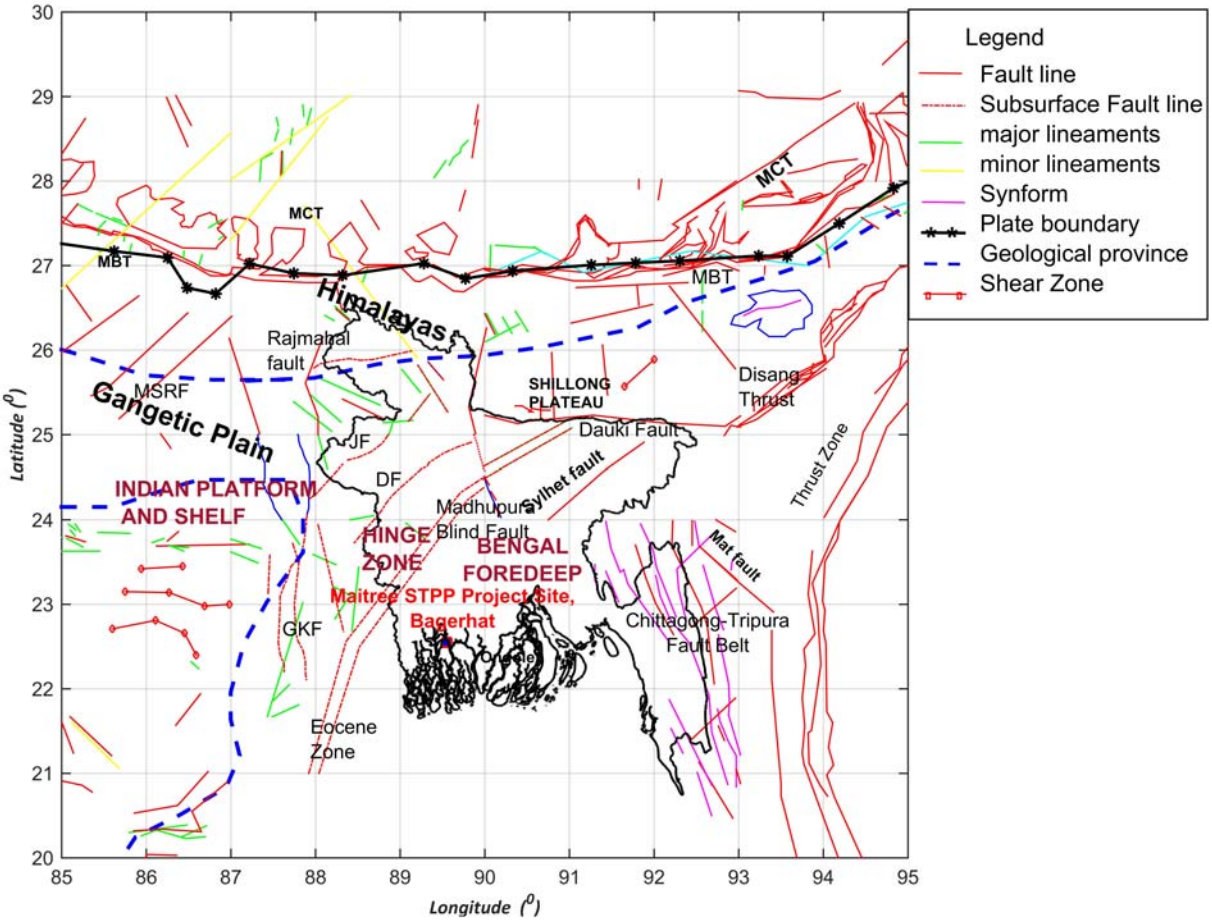

Figure 7. Seismotectonic map Bangladesh (Bangladesh Meteorological Department, Geological survey of Bangladesh, NDMA 2011)

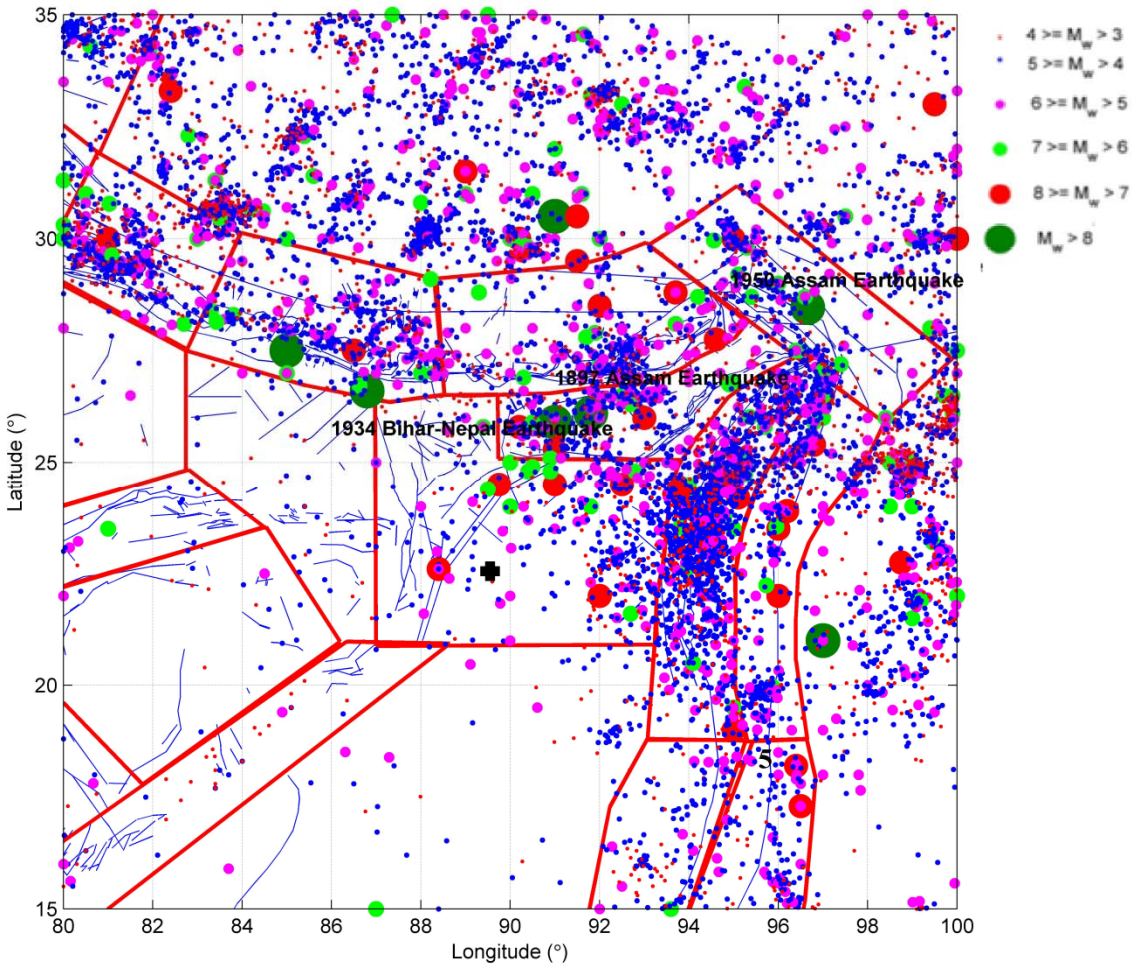

Figure 8. Seismogenic zones of Indian sub continent superimposed with faults (NDMA 2011) Blue lines - Faults, Red lines - Source Zones

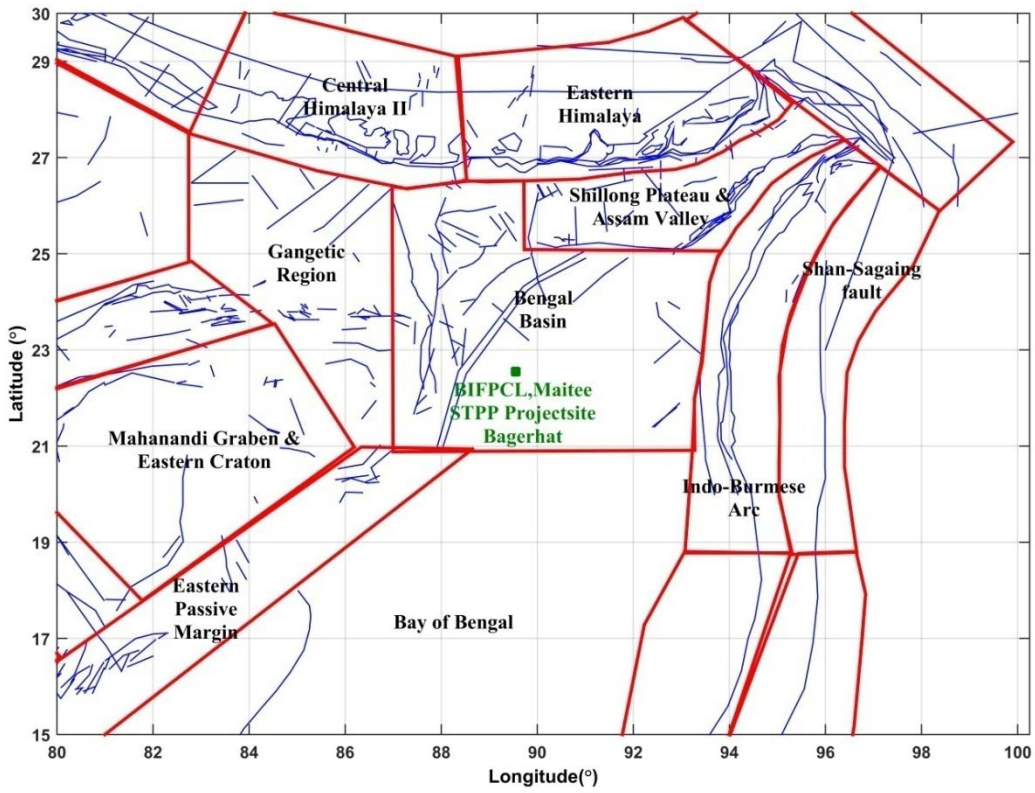

Figure 9 Seismogenic zones according to the 32 Zones identified for the Indian Sub continent as per NDMA (2011) around the BIFPCL, Maitree site, Bagerhat

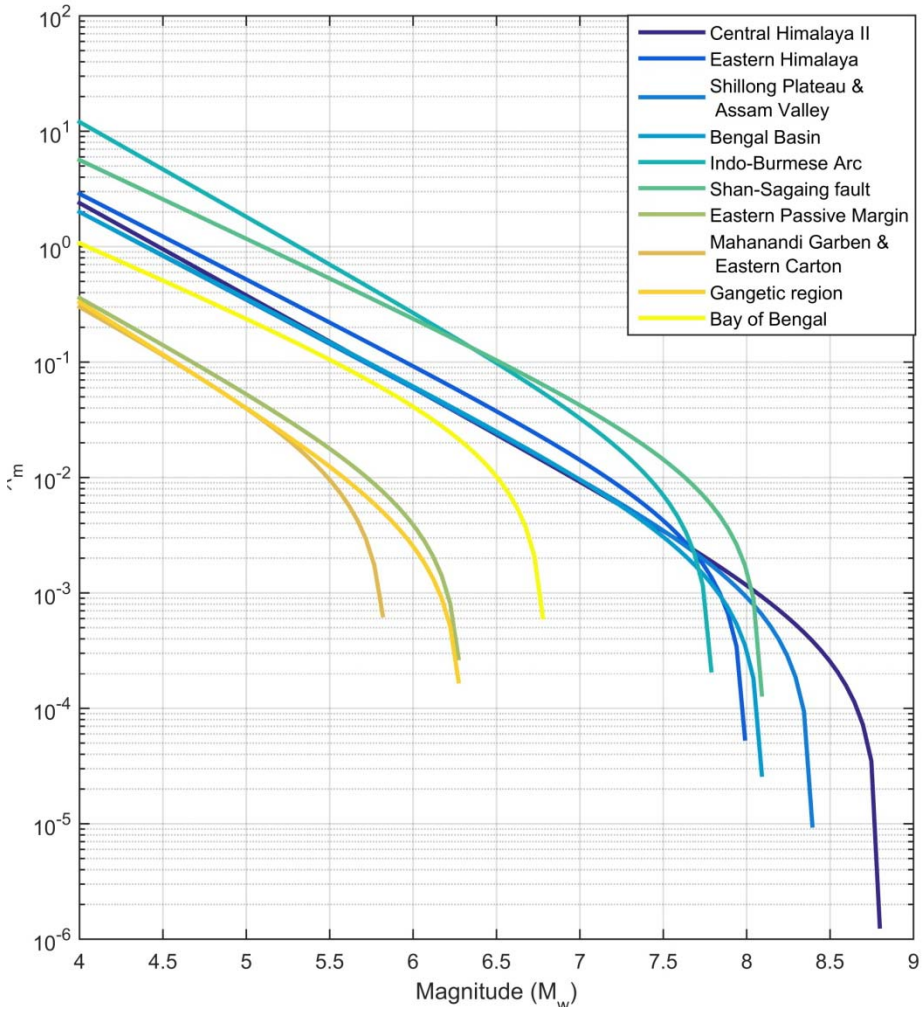

Figure 10. Regional magnitude-frequency relationship

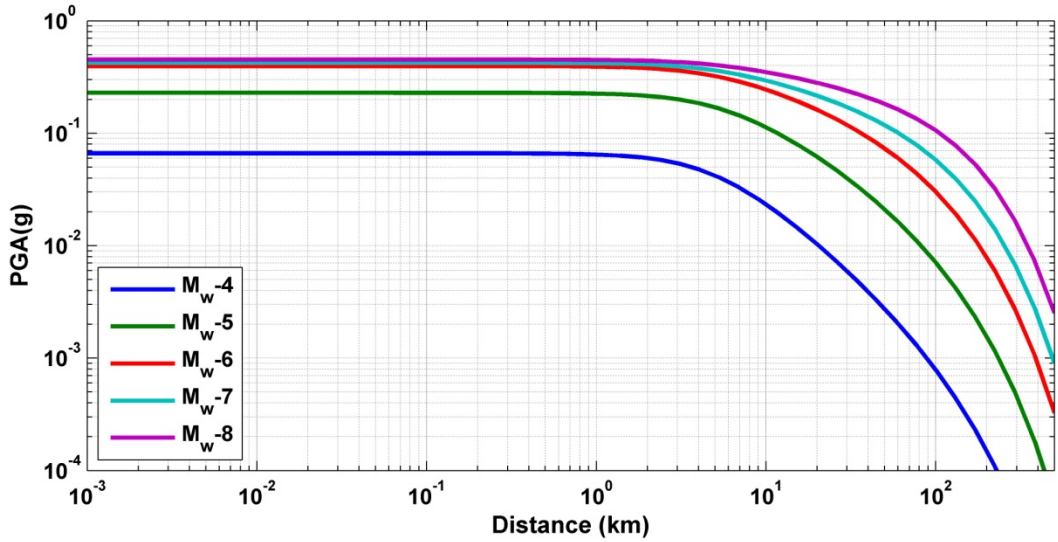
PGA(g)
Distance (km)
M_w-4
M_w-5
M_w-6
M_w-7
M_w-8

(a)

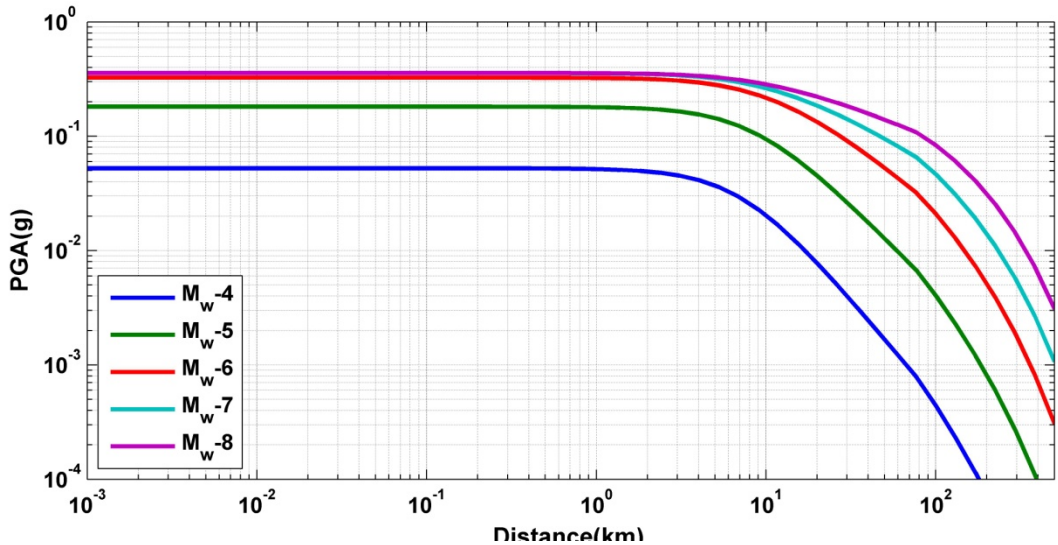
PGA(g)
Distance(km)
M_w-4
M_w-5
M_w-6
M_w-7
M_w-8

(b)

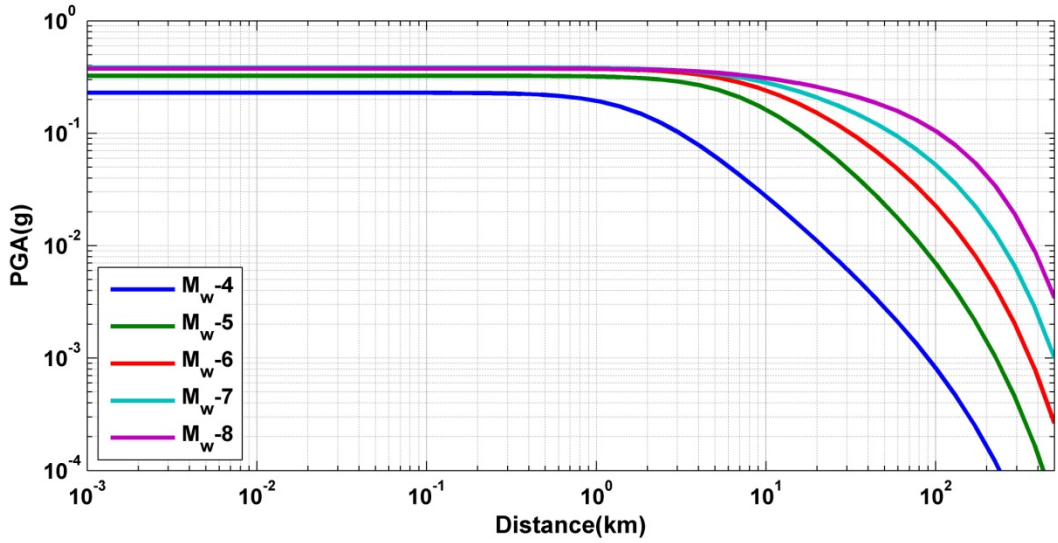

(c)

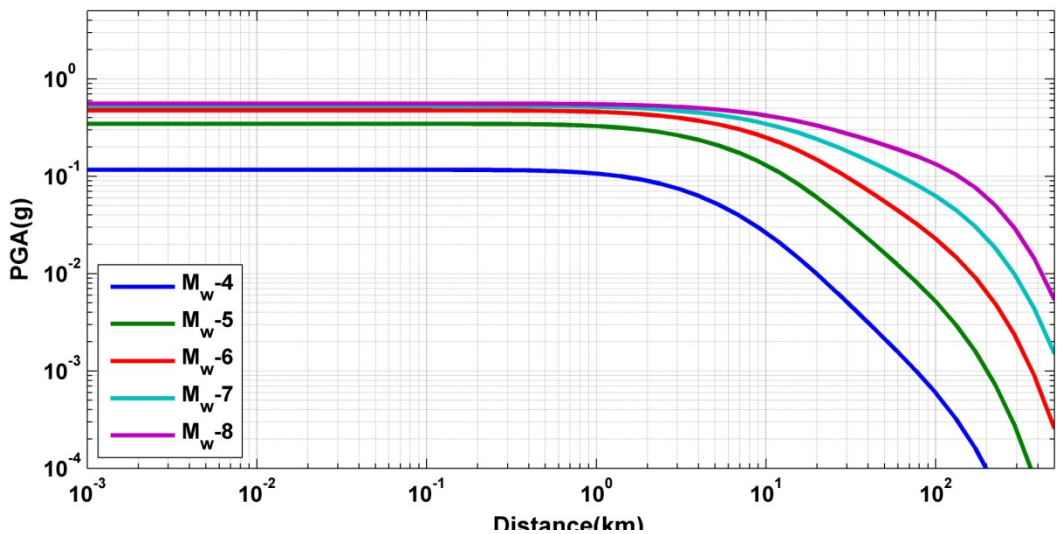

(d)

Figure 11. Attenuation of PGA (in acceleration due to gravity (g)) with hypocentral distance (in km) for SD-Type Soil Condition; (a) Boore et al. (2014), (b) Campbell and Bozorgnia (2014) (c) Atkinson *et al.* (2014) (d) Chiou and Youngs (2014)

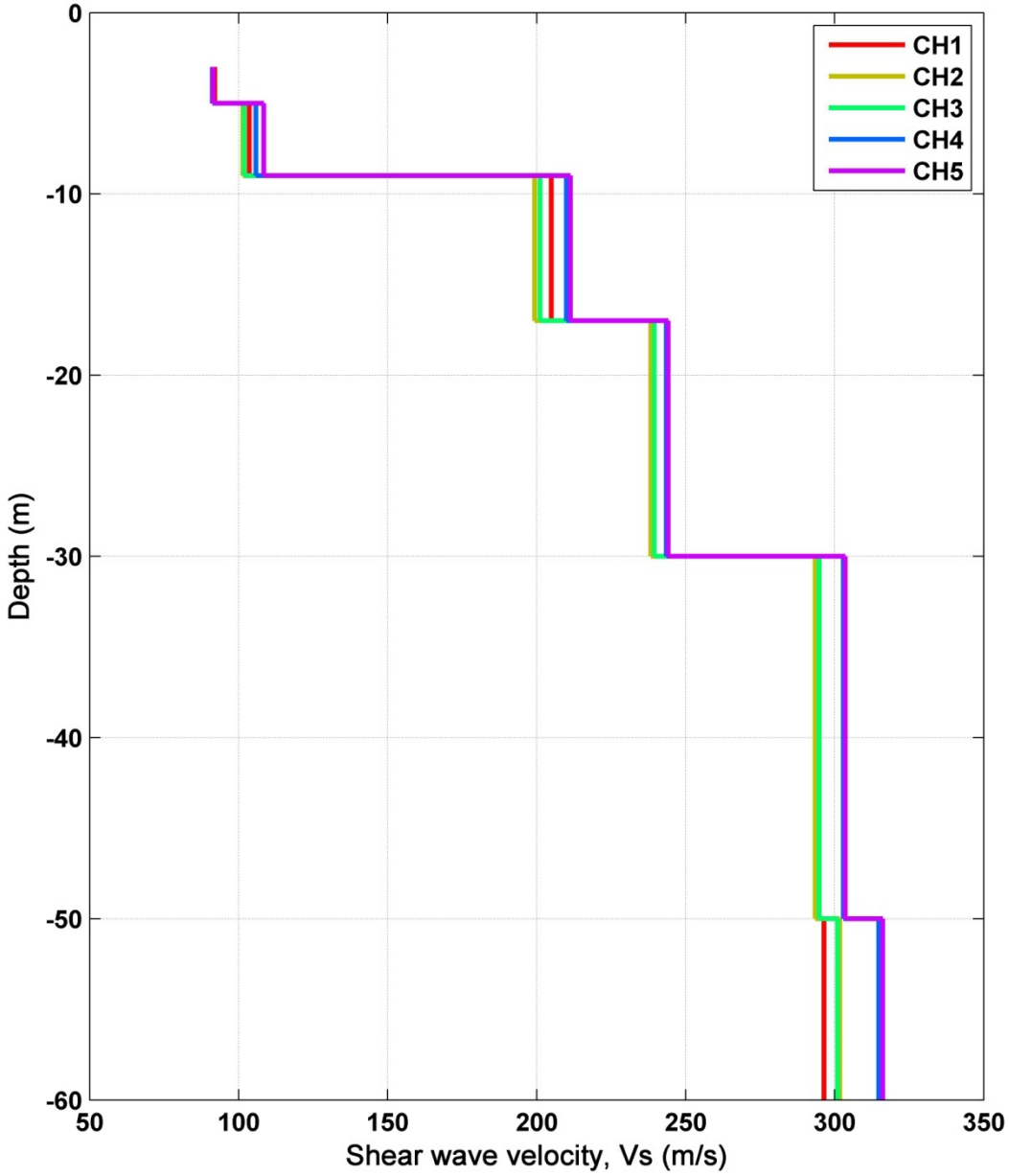

Figure 12. The shear wave velocity profile obtained from Cross Hole test at Rampal, Bagerhat, Bangladesh

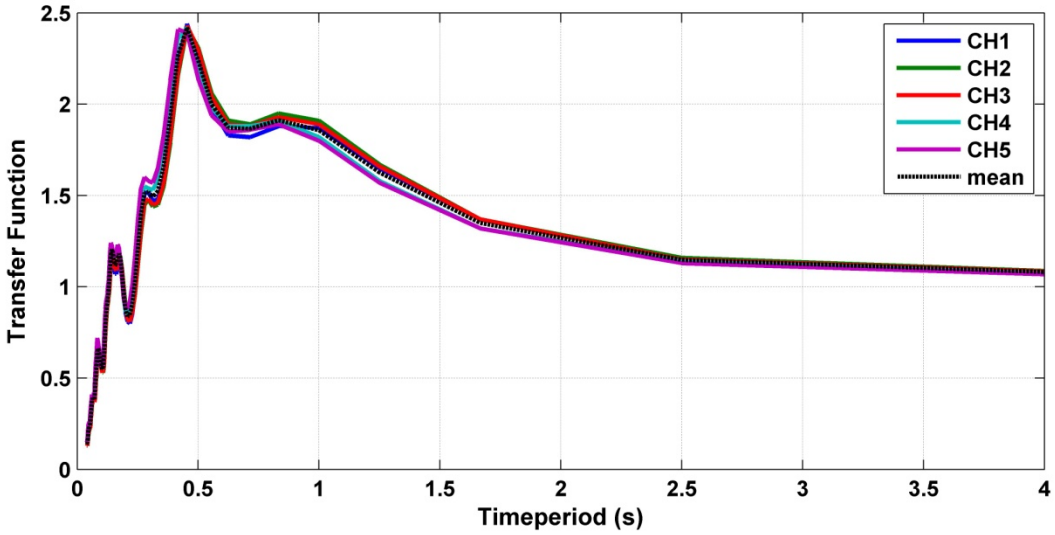

Figure 13. Transfer function with respect to timeperiod

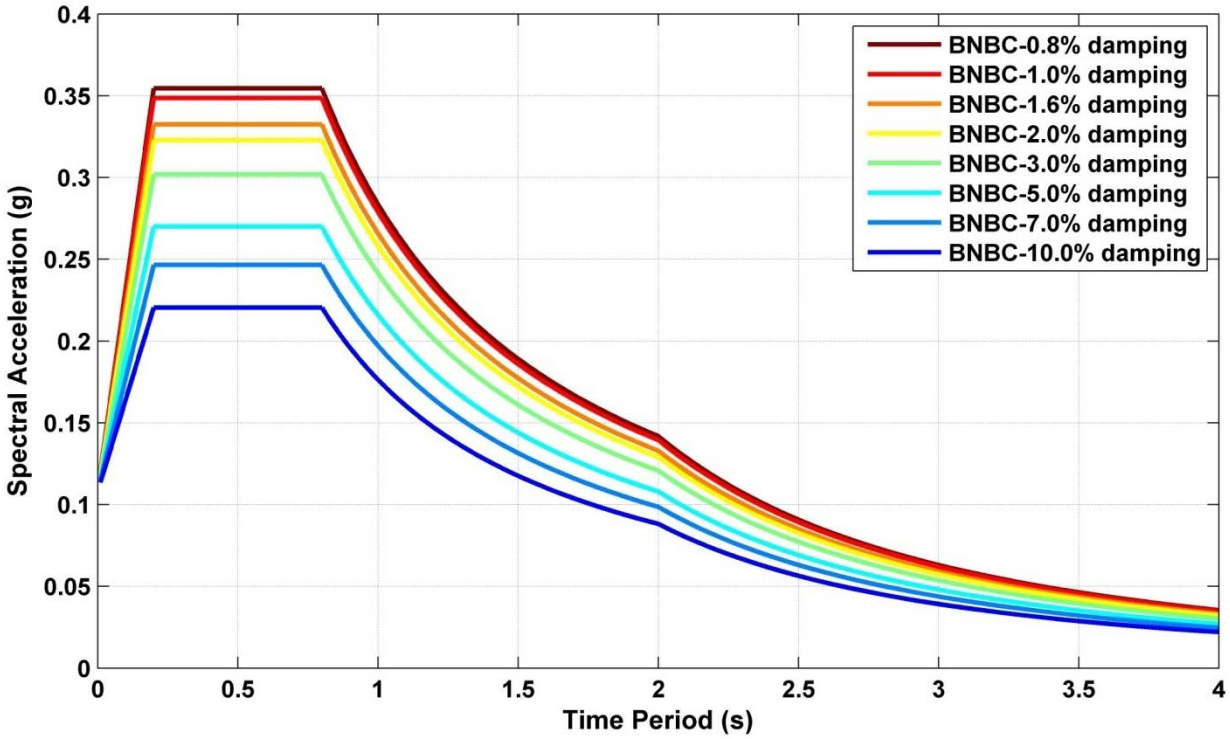

Figure 14. Response spectra according to Bangladesh National Building code (BNBC) for different damping, with Z=0.12, 'SD' type soil class and I and R considered as 1, at BIFPCL, Maitree site, Bagerhat, Bangladesh

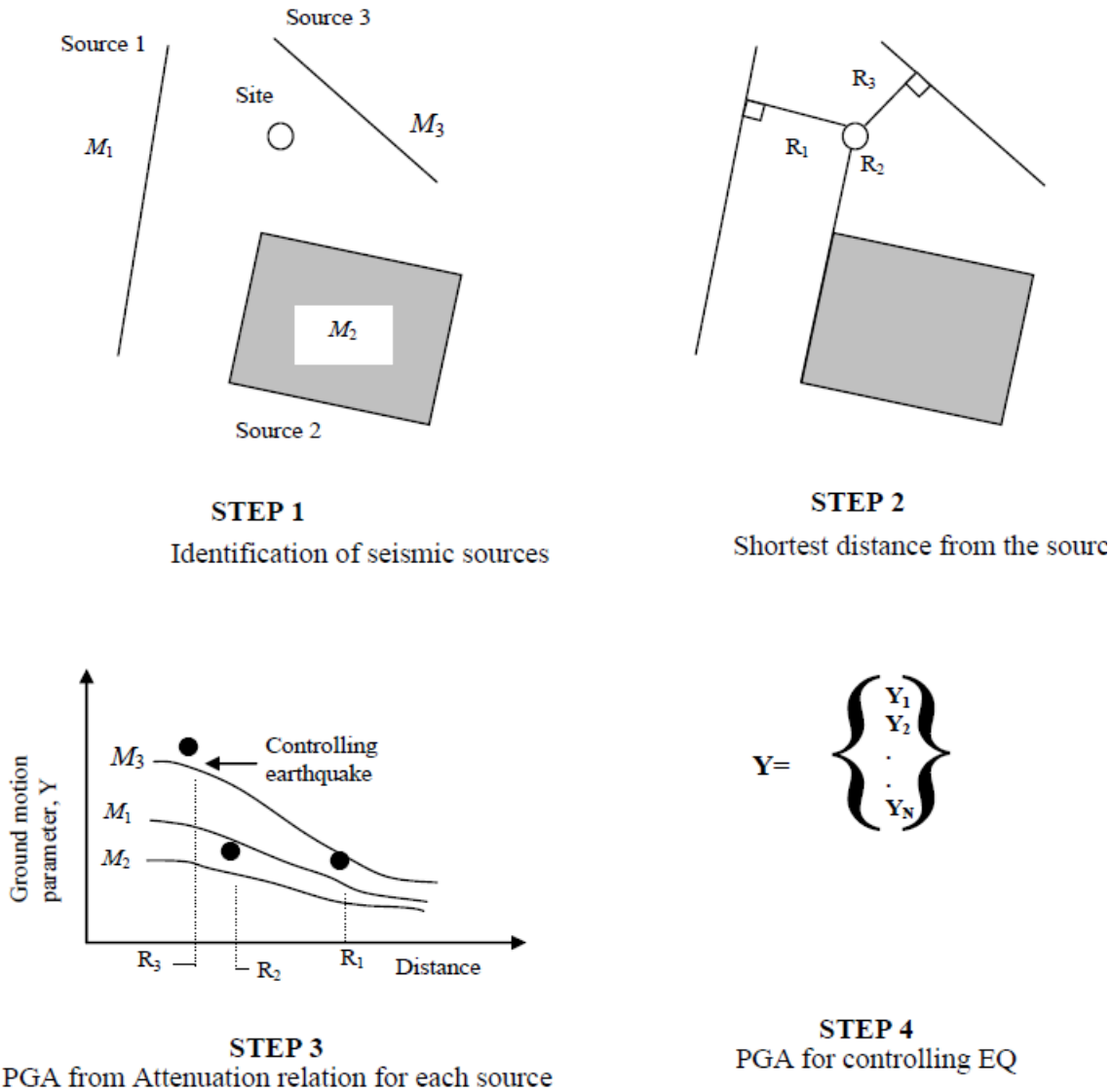

Figure 15. The steps to determine the Deterministic Seismic Hazard.

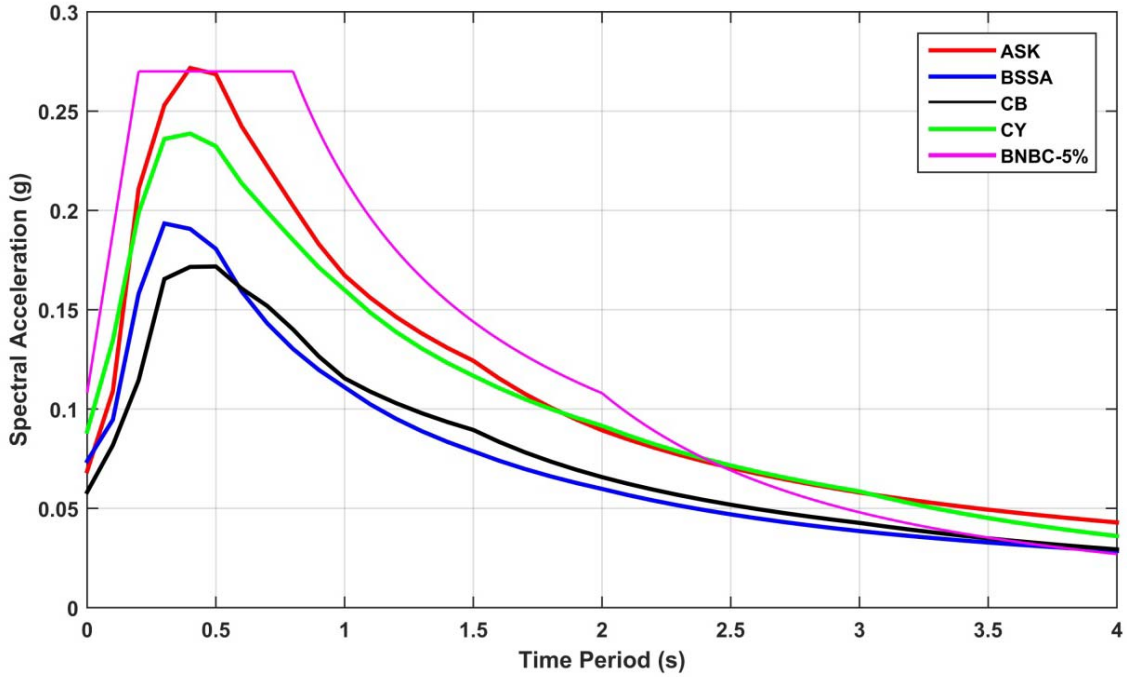

(b)

Figure 16. The response spectra according to deterministic seismic hazard analysis for different attenuation relationships with M_w (7.5) (corresponding to 2500yrs RP) along with that according to Bangladesh National Building code (BNBC) for 5% damping, with Z=0.12, 'SD' type soil class and I and R considered as 1, at BIFPCL, Maitree site, Bagerhat, Bangladesh

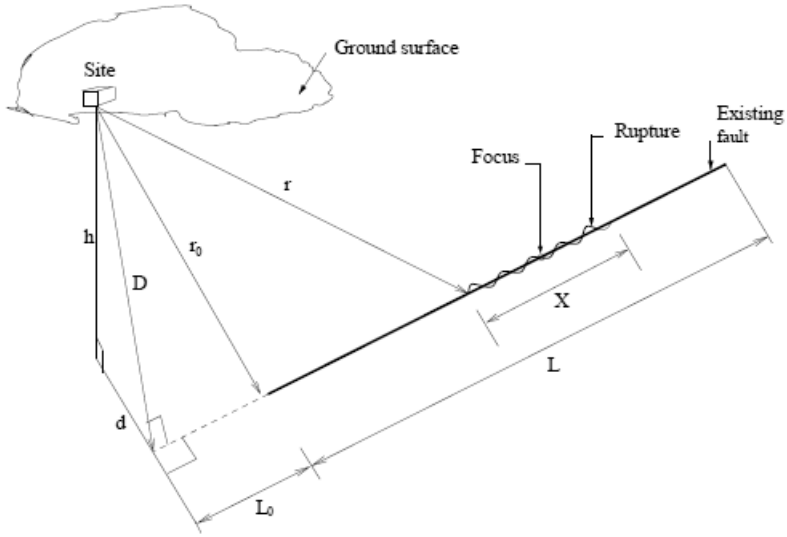

Figure 17. Source, Site and Path for PSHA , Where L is the length of fault, X is the rupture length for a particular magnitude of earthquake, h is the focal depth, r is the minimum distance from site to the region of rupture, r_o is the minimum distance of the site from the fault, D is the perpendicular distance from site to the projection of fault line, L_o is the projected length of the fault line from the end of the fault till the perpendicular from the site(Source: Der Kiureghian and Ang (1977))

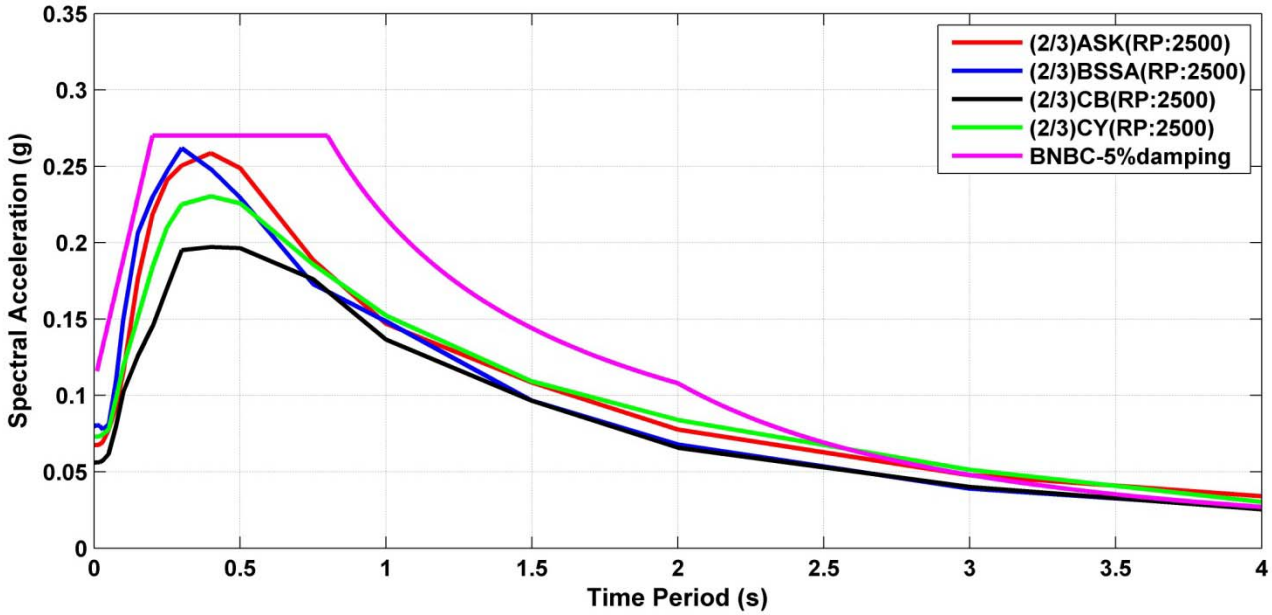

Figure 18. UHRS using different atteneuation relations along with Response spectra according to Bangladesh National Building code (BNBC (2012)) for 5% damping, with Z=0.12, 'SD' type soil class and I and R considered as 1, at BIFPCL, Maitree site, Bagerhat, Bangladesh

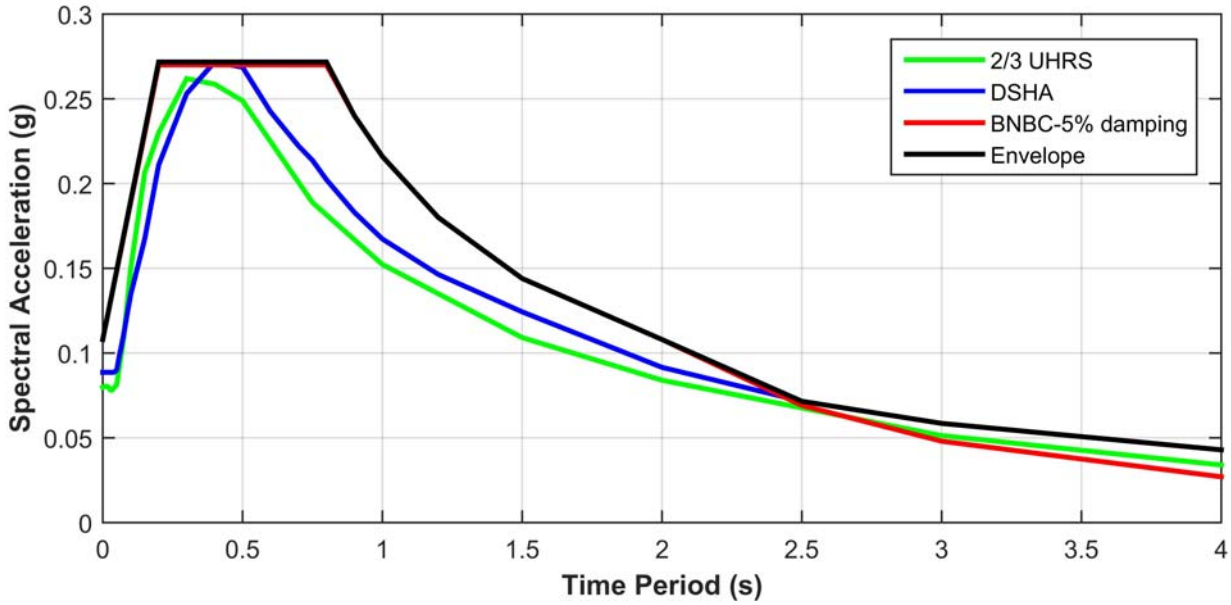

Figure 19. Comparison of response spectra according to Bangladesh National Building code (BNBC) for 5% damping, with Z=0.12, 'SD' type soil class and I and R considered as 1, with maximum values obtained from DSHA and (2/3) of UHRS (PSHA analysis) corresponding to 2500yrs RP at BIFPCL, Maitree site, Bagerhat

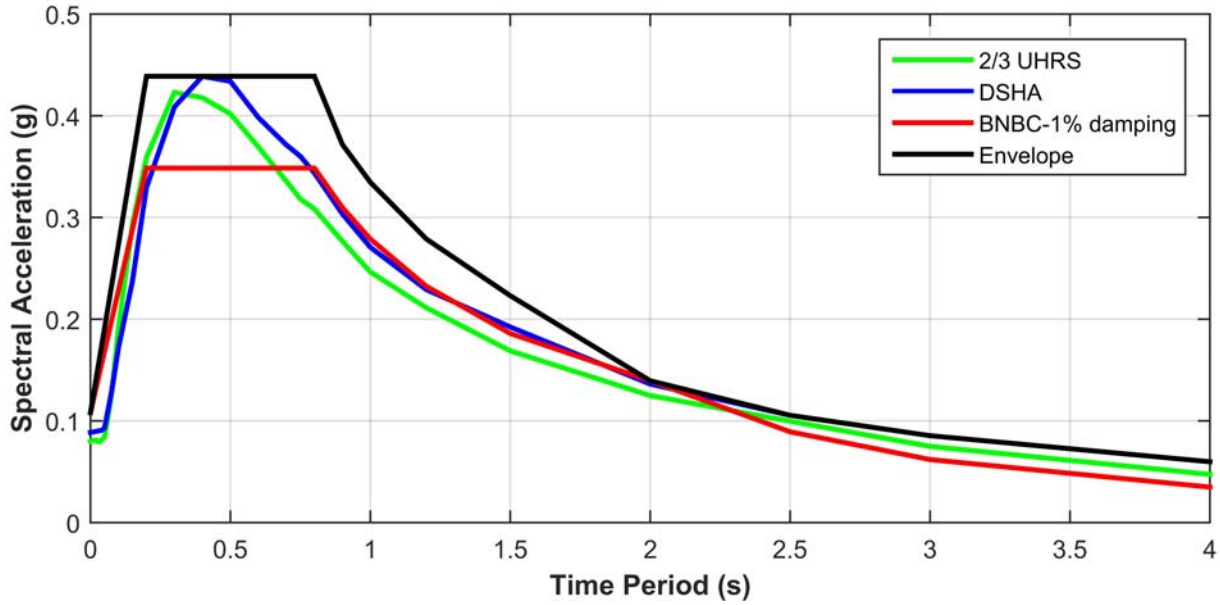

(a)

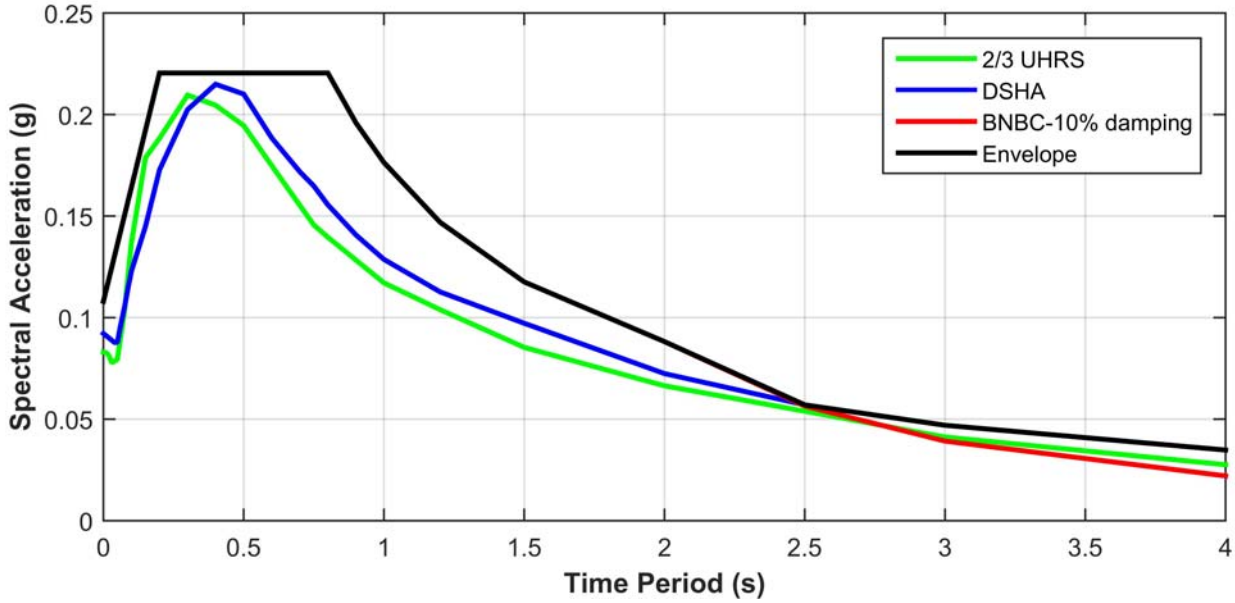

(b)

Figure 20. Comparison of response spectra at BIFPCL, Maitree site, Bagerhat

(a) Bangladesh National Building code (BNBC) for 1% damping, with Z=0.12, 'SD' type soil class and I and R considered as 1, with DSHA and (2/3) of UHRS (PSHA analysis) corresponding to 2500yrs multiplied by damping correction factors for 1%damping

(b) Bangladesh National Building code (BNBC) for 10% damping, with Z=0.12, 'SD' type soil class and I and R considered as 1, with DSHA and (2/3) of UHRS (PSHA analysis) corresponding to 2500yrs multiplied by damping correction factors for 10%damping

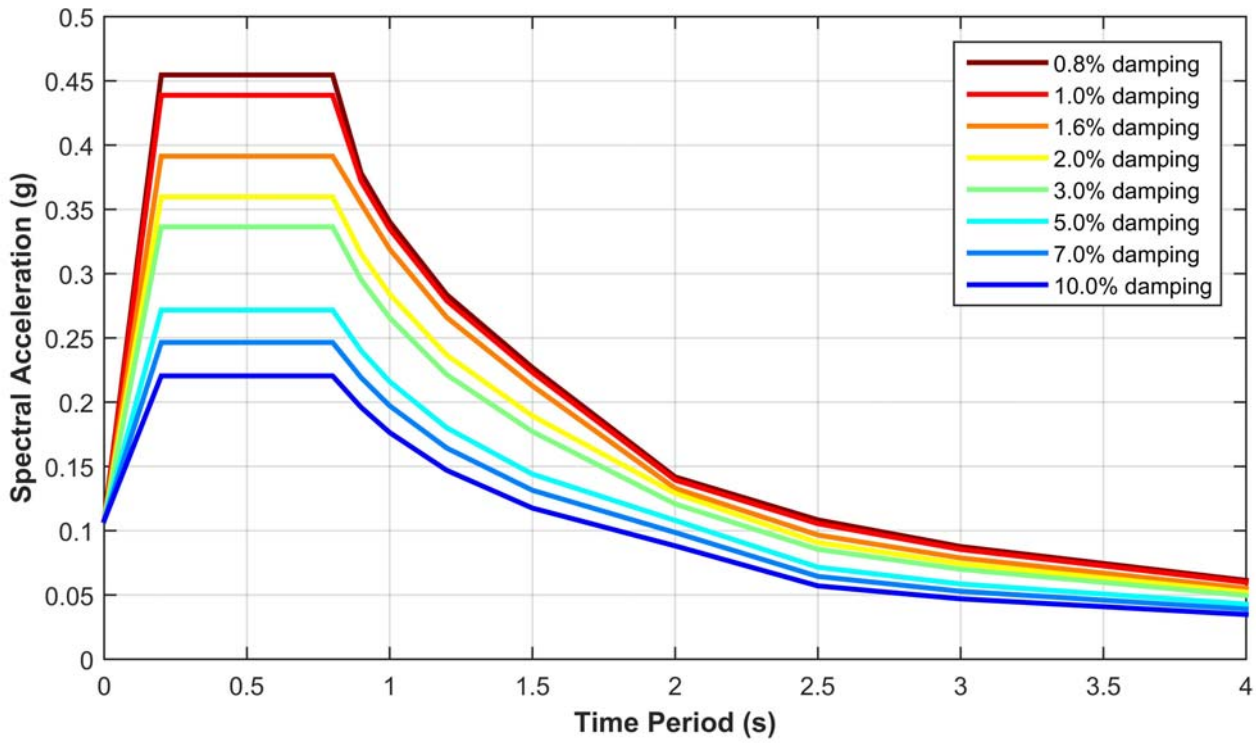

Figure 21. Recomended response spectras for different percentage of damping at BIFPCL, Maitree site, Bagerhat, Bangladesh

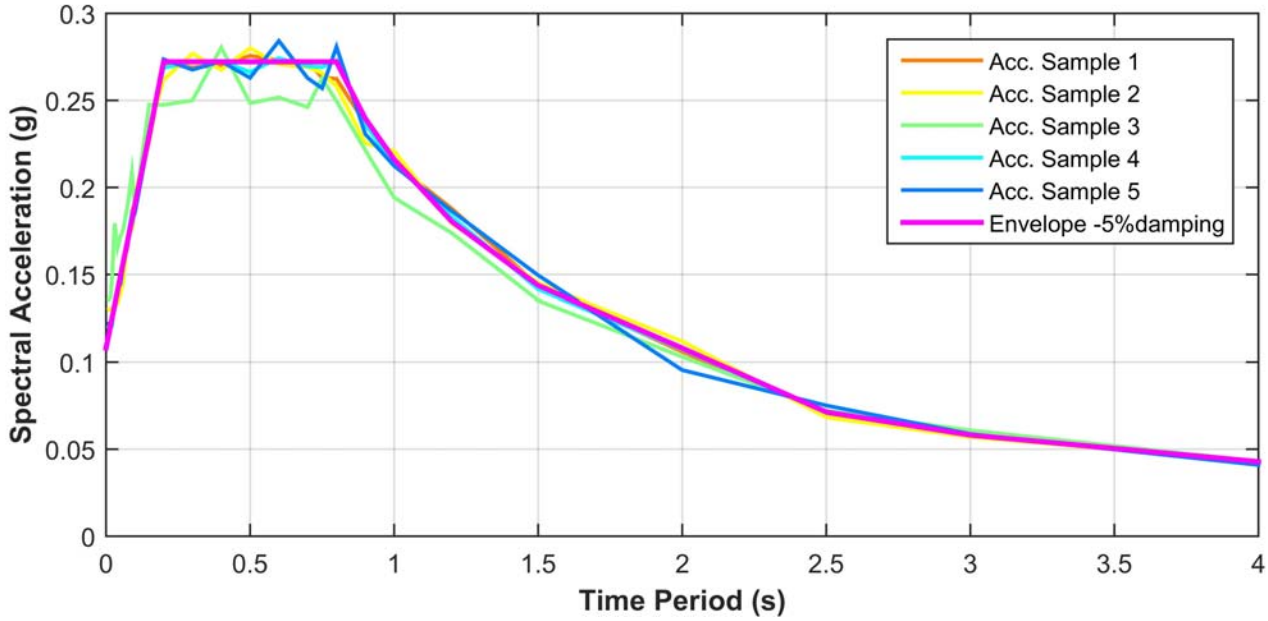

Figure 22. Comparison of response spectra of the 5 sample acceleration time histories with the recommended response spectra for 5% damping, at BIFPCL, Maitree site, Bagerhat, Bangladesh

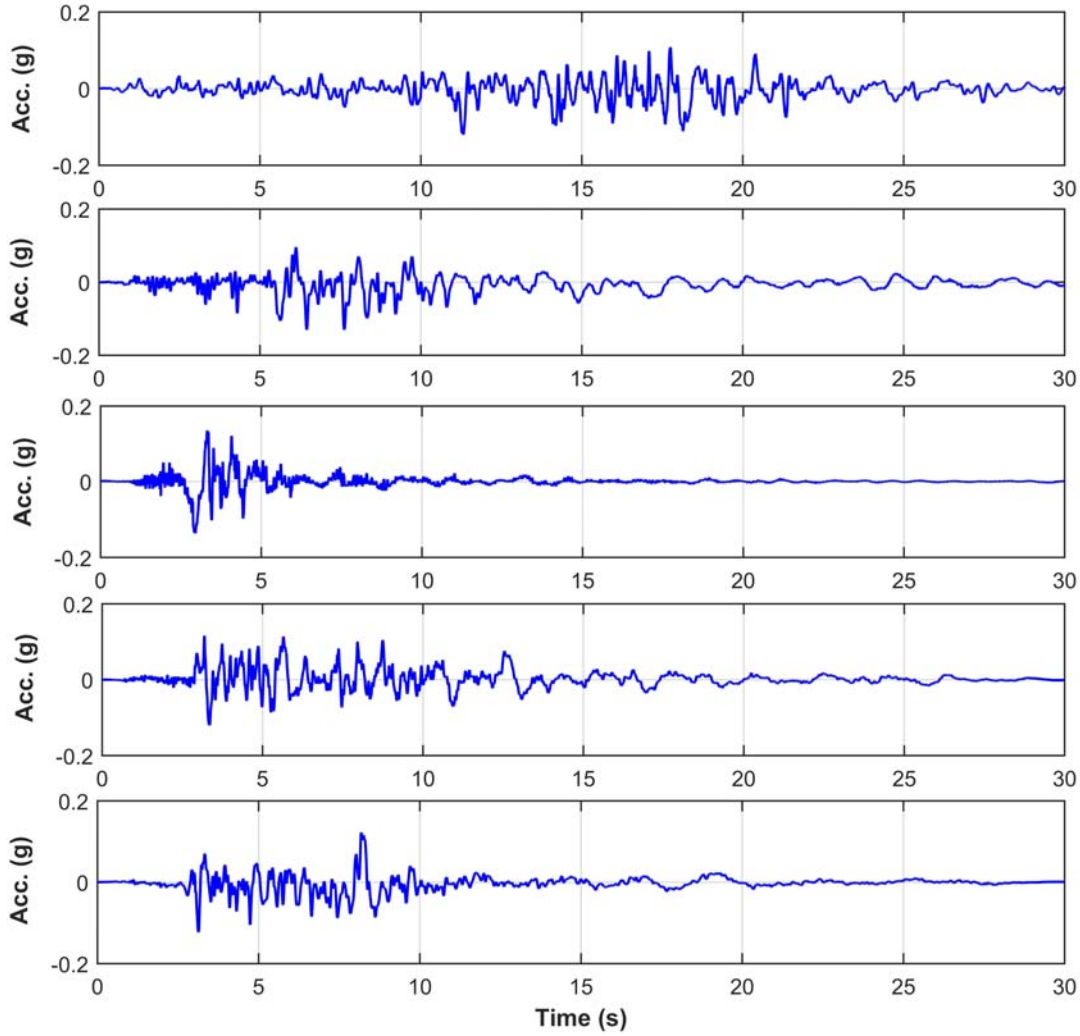

Figure 23. Spectrum compatible acceleration time history samples corresponding to 5% damping for BIFPCL, Maitree site, Bagerhat, Bangladesh